PREDICTING WATER CONSTRAINTS TO PRODUCTIVITY OF CORN USING PLANT-ENVIRONMENTAL SIMULATION MODELS

A Dissertation

Presented to the Faculty of the Graduate School

of Cornell University

In Partial Fulfillment of the Requirements for the Degree of

Doctor of Philosophy

by

Imo Werner Buttler

January 1989

ACKNOWLEDGEMENTS

I would like to express my sincere appreciation to the many people who have contributed to this research. It was a privilege and a real pleasure to have worked under the direction of Dr. Susan J. Riha. Her enthusiasm for science and sincere commitment to teaching and learning were a great source of inspiration for me. I am grateful to Drs. Dave Pimentel, Gary W. Fick, and R. Jeff Wagenet for serving as members of my Special Committee and for providing support and encouragement throughout the course of my studies at Cornell.

My appreciation is also expressed to Dr. John L. Hutson, who provided invaluable advice at numerous occasions and with whom I could always share the highs and lows of modeling work. I wish to thank Dr. Armand van Wambeke for giving me the opportunity to serve as a teaching assistant in his course.

I am very thankful for the friendship and help received from my fellow graduate students, whose support was very much appreciated during the last couple of months of writing the dissertation.

While conducting the field experiment in Brazil, excellent support was provided by the CPAC scientists and staff, to whom I will always be very grateful. Allert R. Suhet and Dr. Elias de Freitas provided invaluable support

as collaborators on the project. Dr. Eric Stoner provided help whenever needed and was an excellent interpreter of Brazilian culture.

I feel very fortunate to have enjoyed the friendship and collaboration of Gustavo C. Rodrigues, who became interested in the experiment and opened up additional dimensions to the research by conducting a large plant sampling effort. Many other researchers at the CPAC contributed greatly through discussions and support in various form.

The experiment would have been impossible without the experienced support of Carlao and the hard work of the TropSoils field team under the direction of Afonso Rodrigues Boaventura. I want to thank Jose Amauri de Carvalho 'Zecao' for help in the field, Emival de Matos Pereira 'Pesquisa' for help with nitrogen analyses, Jatoba for support with the irrigation system, and the staff of the meteorological station under the direction of Balbino for their help with data collection and processing.

I am grateful to Oner Bicakci, who played an instrumental role in designing the user interface of GAPS, particularily the screen menus. James Altucher helped trouble-shoot later version of the program and developed much of the current version of the plotter.

This project was primarily funded by subgrant SM-CRSP-012 of the TropSoils program funded by USAID.

TABLE OF CONTENTS

LIST OF TABLES

LIST OF FIGURES

Chapter I

INTRODUCTION

The Cerrado (Savanna) region of Brazil is an area of considerable agricultural potential (Abelson and Rowe, 1987; Goedert, 1983). The climate is tropical continental with rainy summers and dry winters. Annual precipitation varies with geographical location from 1300 to 1800 mm, of which 95 % is concentrated in the wet season (September to April). Climatic conditions are very conducive to the production of almost any crop. Worldwide, savanna regions occupy more than twice the surface area as the humid tropics, and thus represent an enormous resource for increasing agricultural production.

Initial limitations for agricultural development in the Cerrado were due to the inherent low fertility and acidity of the Oxisols and Ultisols, which together constitute more than 70 percent of the 140 million ha region. Soil research conducted primarily during the last 20 years has improved understanding of the chemistry and fertility of these soils and resulted in the establishment of recommended management practices to alleviate their inherent soil fertility restrictions (Goedert, 1985). According to recent estimates, only about five to ten percent of the estimated 50 million ha of potentially arable land in the Cerrado is under cultivation (Goedert, 1983) and further development of the region is one of the

highest national priorities of the Brazilian government.

With the major soil fertility limitations successfully identified and correctable by soil amendments, increased attention is being focussed on the management of other limiting factors to agricultural production on these soils, including water and nitrogen.

The foundation for sound management of soils and development of successful agronomic systems is a thorough understanding of the physical, chemical and biological processes that occur in them. While the processes themselves are not principally different from the processes studied longer and more intensively in temperate agriculture, environmental conditions, crops and specific soil characteristics can differ. Thus empirical knowledge gained from agricultural research in the temperate regions can not always be successfully transferred to the conditions of the Cerrado. However, knowledge of these processes should, in theory, be applicable to and lead to further understanding of agriculture in the Cerrado.

Mechanistic simulation models representing and integrating knowledge about soil-plant-atmosphere processes are a valuable tool for the transfer of this knowledge. They can provide a rational framework in which to design, analyze and evaluate field experiments and increase our insight into system dynamics. Application of these models, that have been developed primarily in the temperate regions, provides the opportunity to discover if

there are inherent assumptions that do not fit tropical conditions and thus limit their general applicability. Such application could lead to improvement in the model and to a more comprehensive understanding of the important differences in the properties and dynamics of temperate and tropical plant-environmental systems.

The specific objective of this research was the quantitative description of water fluxes in Cerrado soils in simulation model form. The model was applied to Cerrado conditions in order to attempt identify the most important factors determining water fluxes in acid savanna soils. Furthermore, effects of water stress or surplus on corn growth and yield were evaluated with the simulation model. Chapter II describes the software program GAPS that was developed during the course of this research and that served to implement the simulation models used in this work. GAPS was developed with particular emphasis on flexibility, transparency and user-friendliness. It is intended to be usable for a variety of purposes ranging from research applications to use in supporting conceptually oriented teaching. The simulation model components contained in GAPS are fully documented in the GAPS User's Manual, version 1.1 of which is contained in Appendix A.

In chapter III water fluxes in cropped and fallow soils of the Cerrado are predicted. Two main representations of soil water flow are compared. They are

tested against measured data of soil water status obtained from a line-source sprinkler experiment. The sensitivity of the model predictions to various important input parameters is discussed, as well as the implications of specific soil physical properties of tropical soils with respect to modeling water flow.

Chapter IV deals with the response of corn growth and yield to water stress. Predictions of dry matter accumulation and leaf area development over a wide range of irrigation water input are compared to data obtained from a field experiment.

REFERENCES

Abelson, P. H., and J. W. Rowe. 1987. A new agricultural frontier. Science 235:1450-1451.

Goedert, W. J. 1983. Management of the Cerrado soils of Brazil: a review. Journal of Soil Sci. 34:405-428.

Goedert, W. J. 1985. (in portuguese) Solos dos Cerrados. Ministerio da Agricultura / EMBRAPA.

Chapter II

GENERAL PURPOSE SIMULATION MODEL OF WATER FLOW IN THE SOIL-PLANT-ATMOSPHERE SYSTEM

2.1 INTRODUCTION

Understanding of water movement in the soil-plant-atmosphere continuum (SPAC) has been greatly advanced by the ability to develop dynamic simulation models that use numerical techniques to solve equations, based on a mechanistic view of the system. Such models are essential to reasonably evaluate how changes in any one component of the system, such as root depth and density, soil hydraulic properties, leaf area index, or frequency of rainfall or irrigation, will affect the water budget of the soil-plant system. Over the past 15 years many simulation models of water movement in the soil-plant-atmosphere system have been developed, as either independent models (Federer, 1978; Goldstein, et al., 1974; Nimah and Hanks, 1973; Norman and Campbell, 1983). or sub components of larger models (Davidson et al., 1978; Tillotson et al., 1980). These models have most often been developed for fairly specific purposes, such as predicting evapotranspiration for a particular crop (Campbell et al., 1976; Childs et al., 1977; Denmead et al., 1976; Running et al., 1975) or for predicting leaching of solutes in a particular system (Iskandar and Selim, 1981; Robbins et al., 1980; Wagenet and Hutson, 1986).

Although a particular modeling effort should have a well-defined purpose, the computer program supporting this modeling effort need not be written explicitly for this purpose. The high degree of specificity incorporated into the code of simulation models is one major reason use of simulation models by individuals other than those that developed the model has been extremely limited (Addiscott and Wagenet, 1985). It might be argued that simulation models being developed are conceptually very different from one another and the diversity of models represents significant differences in the manner in which different researchers conceive of water movement in SPAC. However, we would suggest that important conceptual differences in deterministic models of water movement in SPAC are relatively few. We believe that development of more general, flexible simulation models of SPAC will lead to increased use of these models by those who are not currently involved in developing them. This, in turn, will increase the rate of progress in our understanding of water movement in the soil-plant-atmosphere system.

2.2 APPROACH

The approach we used was to first consider major reasons that simulation models are not more widely used. Three reasons appeared most important: 1. most programs are not flexible enough to accommodate relatively easily a variety of objectives, 2. most programs are not well

documented, 3. most programs contain little, if any, "user-friendly" interfacing. Our objective, therefore, was to develop a software package for simulating water movement in SPAC that addresses these problems.

There are several aspects of existing simulation models that make them inflexible. Some require a rigid set of input data to run; these inputs may not be available to the user. This, in turn, is due to a lack of alternative representations of various components of the model. For example, some SPAC simulation models require pan evaporation rates as input for calculating evapotranspiration. The user may not have these data, but may have other data that could be used for predicting evapotranspiration. In addition, most SPAC simulation models do not give the user the option to simulate easily only parts of the system, such as evapotranspiration or water flow without evapotranspiration. Our approach was to create a program that would supply the user with more than one option to simulate a particular process, the choice being dependent on available input data, desired level of complexity, and objectives. GAPS (GenerAl Purpose Simulation Model of the Soil-Plant-Atmosphere System) allows the user to construct a situation-specific simulation model from existing components. Furthermore, the program allows users with some programming experience to add their own components, either to substitute for existing components or in addition to them, and to link

them to the existing routines relatively easily.

Clear programming and documentation also support flexibility and encourage use in several ways. These features of GAPS allow users with some programming experience to make changes and add procedures easily. Good documentation helps the user make educated choices regarding the selection of model components. Additionally, such documentation is useful in quickly and easily determining precisely how the model simulates various components.

Providing a user-friendly interface between the simulation model and the user is perhaps scientifically the least necessary component of GAPS. User-friendly interfaces can require large amounts of programming in comparison to the simulation program itself. However, lack of such an interface could be a major deterrent in the use of simulation models by a wider group of people. Our general purpose simulation model is interfaced with user-friendly menus.

2.3 PROGRAM STRUCTURE

GAPS is divided into three major components: the editor, simulator, and plotter (Fig. 2.1). The editor allows the user to create or edit all files that are necessary input to the simulator. The plotter can be used to graph or print selected variables from output files after completion of a simulation run, as well as to print

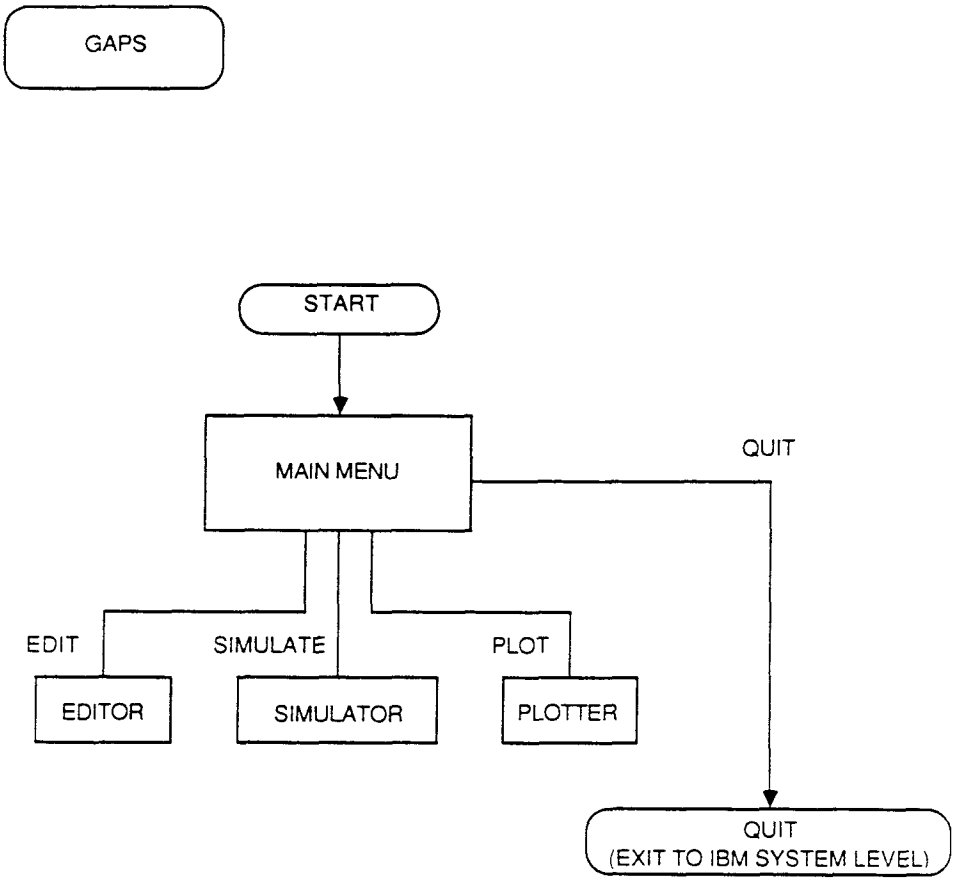

Fig. 2.1 GAPS Structure

input data files. Variables printed can be selected by the user. The simulator contains the library of procedures from which users can select and design their own systems (Fig. 2.2).

The GAPS documentation is organized so that every subroutine/procedure is documented in detail in a separate chapter. Each chapter includes presentation and explanation of all equations, using the same symbols as

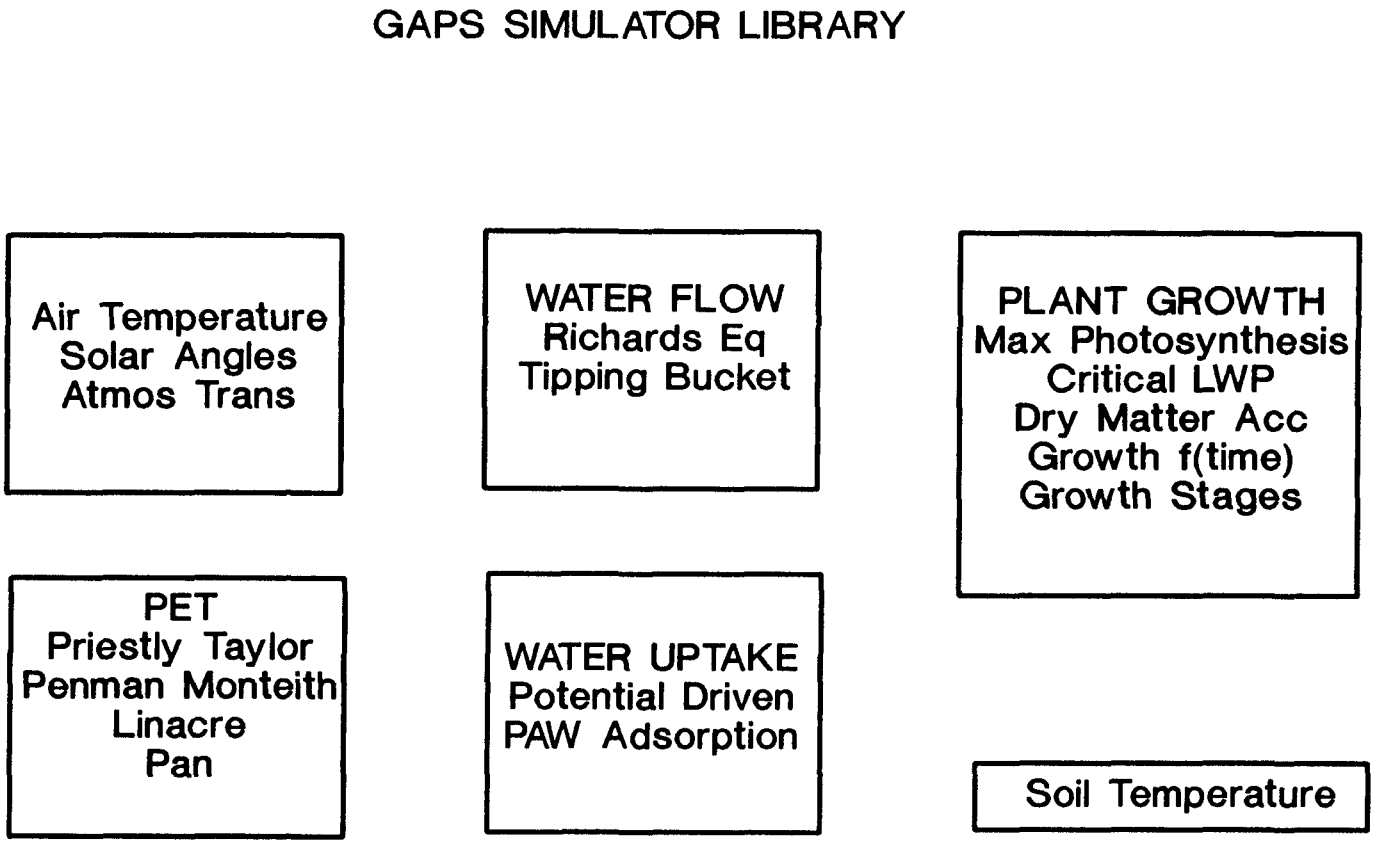

Fig. 2.2 Currently included simulator modules

those used in the code, definition of all symbols as they are presented, explanation of numerical techniques used where necessary, references to relevant publications, the procedural code, a dependency diagram where necessary to illustrate how the procedure is linked to other procedures and internal flow (Fig. 2.3), and a summary list of all symbols used in the procedure along with their definition. In addition to documentation of the procedures currently contained in the simulator, the GAPS User's Manual includes instructions on how to change existing procedures and how to add procedures to the simulator library.

GAPS contains several user-friendly features. First, the simulator routines in GAPS (the simulator) are linked to input (the editor) and output (the plotter) routines. The editor, simulator, and plotter all interface with the user through a series of menus. The menus have a similar design (Fig. 2.4) which facilitates a clear presentation of the options available to the user at any point within the program. A title section in the upper left-hand corner of the screen informs the user of the current location in the program. A menu in the center displays the options available to the user, for example, to load, save, edit, or delete a data file while in the editor. Function keys are utilized for user input. Abbreviated versions of the options are repeated in the function keys window. The user has the option to respond by hitting either the appropriate function key or the first

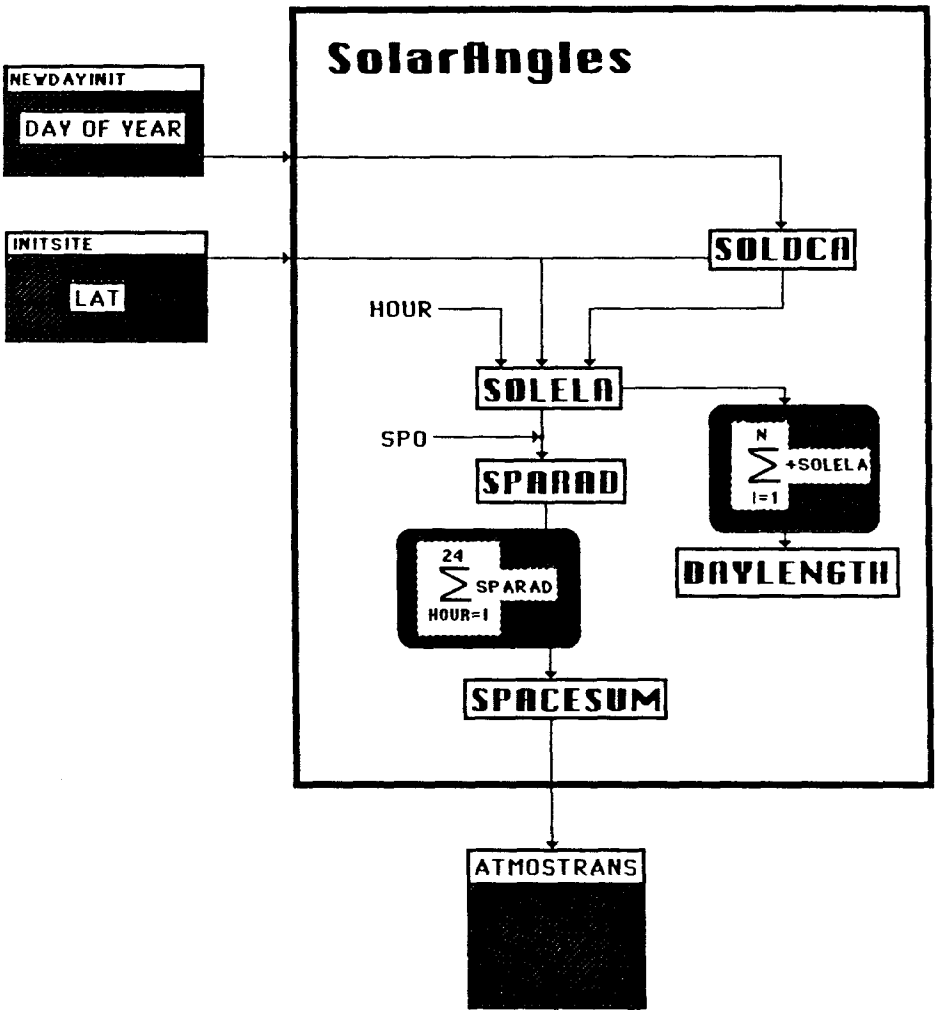

Fig. 2.3 Example of Dependency Diagram (Solar_Angles)

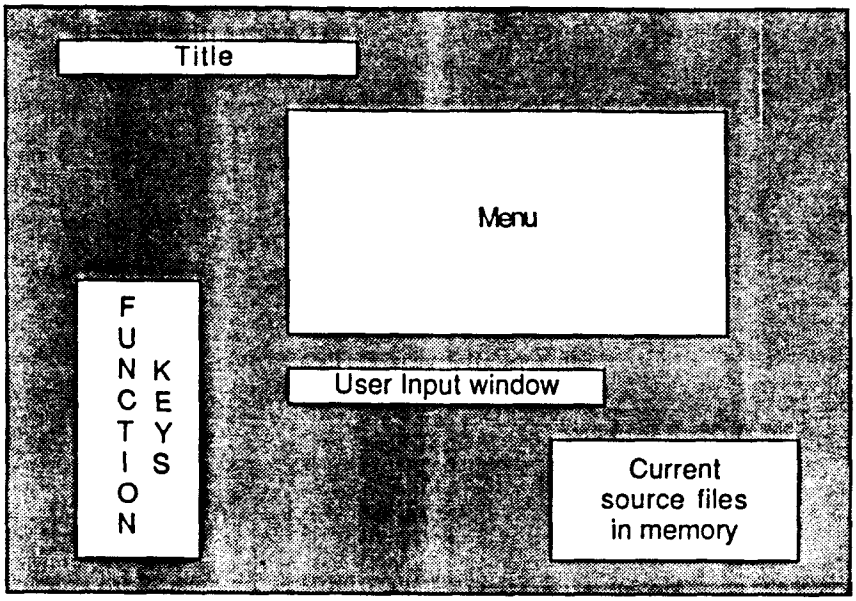

Fig. 2.4 GAPS Screen Menu Format

(highlighted) letter of the respective choice. If there is user input of text or numbers, the user can enter those into the user input window. Names of date files that are currently in memory are displayed in the small window in the lower right-hand corner of the screen. In addition, strings used in the GAPS menus were defined in a manner that involves only minor editing to change them from English to another language or to change statements in the menus.

The editor is structured to allow users to create and edit quickly input files necessary to run the various

procedures in the GAPS simulator. There is a run-time plotter associated with the simulator that the user can use to view simulator results instantly. The user can choose to view up to four graphs simultaneously.

The user can choose to save simulated output to a file before running a simulation. The plotter can then be used after the simulation to plot selected variables from specified output or input files. If desired, GAPS produces a summary output table containing the names of input data files, simulation procedures used in the particular simulation run, and summary water budget information (Table 2.1). For examples of input data files, please refer to the GAPS User's Manual (Appendix A).

2.4 APPLICATIONS

GAPS can be used for a number of different purposes. As a research tool, GAPS can be used most easily to build a simulation model for interpreting and analyzing field experiments. In addition, users can use GAPS as a water flow shell to which they can add components, such as root growth models or solute flow models, of major interest to them. They can also compare different mathematical representation of the same processes, such as ETP or water flow, under a particular set of conditions. This can produce insight into when it is or is not appropriate to

TABLE 2.1

Example of GAPS Summary information table

Simulation started on 8/6/1988 at 11:41

Site File Name	:	CPAC
Soil File Name	:	Oxisol
Climate File Name	:	Brasilia 1987
Plant File Name	:	Corn
Output File Name	:	Testrun

*** Procedures used in simulation ***

Soil_Temperature
Priestley_Taylor_ETP
Max_Photosynthesis
Critical_Leaf_Water_Potential
Dry_Matter_Accumulation
Growth_Stages
Water_Uptake
Richards_Equation

*** Summary data for simulation run ***

Starting day	:	96
Last day	:	252
Total water input (mm)	:	327
Total potential ET (mm)	:	641
Total potential transpiration (mm)	:	353
Total actual transpiration (mm)	:	250
Total potential soil evaporation (mm)	:	288
Total actual soil evaporation (mm)	:	171
Total deep drainage (mm)	:	4
Initially in profile (mm)	:	492
Finally in profile (mm)	:	394
Change in Storage (mm)	:	-98

Simulation stopped on 8/6/1988 at 12:52

use certain representations of a process.

GAPS can be used as a teaching tool to introduce students to simulation modeling. Students have the opportunity to work with individual components of the system as well as linking components together. They can explore the effect of changing specific parameter values, such as saturated hydraulic conductivity, or changing input data, such as climate files, to see how various aspects of the water budget, such as evaporation from the soil surface and movement of water below the root zone, are changed.

2.5 FUTURE DEVELOPMENT

The core of GAPS is the simulator, which contains the library of procedures available to construct simulation models. In this version only procedures relating to water flow in the SPAC and crop growth procedures have been included. Work is currently being conducted on simulation models of nitrogen transformation and transport and reaction routines that will be incorporated into GAPS. We envision that those who use GAPS will add or modify procedures and make these available to other GAPS users.

Some aspects of the current version have been identified as needing improvement in the future. For example, using a spreadsheet format in the editor that will not scroll horizontally limits the number of variables that can be included in one input data file.

The plotter is still in the early stage of development. Currently, the editor and plotter, and the global routines they access, represent the bulk of the GAPS program. In the future we may consider interfacing the simulator of GAPS with commonly available database management software and graphics software.

There appears to be an increasing demand for simulation modeling of soil-plant-atmosphere systems. Additionally, development of these models will become increasingly a multi-disciplinary effort. Such effort requires clear, fully documented programming and a programming style as independent as possible to the author's disciplinary affiliation. A modular structure to simulation models, such as that represented by GAPS, will also facilitate multi-disciplinary development and use.

2.6 SOFTWARE AND HARDWARE REQUIREMENTS

GAPS is entirely written in TURBO PASCAL 4.0 and can be implemented on an IBM PC or PC compatible system with a graphics adapter, DOS 3.0 or higher and 256K of memory.

REFERENCES

Addiscott, T.M. and R.J. Wagenet. 1985. Concepts of solute leaching in soils: A review of modeling approaches. J. Soil Sci. 36:411-424.

Campbell, M.D., Campbell, G.S., Kunkel, R., and R.I. Papendick. 1976. A model describing soil-plant-water relations for potatoes. Am. Potato J. 53:431-441.

Childs, S.W., Gilley, F.R., and W.E. Splinter. 1977. A simplified model for corn growth under moisture stress. Trans. ASAE 20:858-865.

Davidson, J.M., Graetz, D.A., Rao, S.P.C., and H.M. Selim. 1978. Simulations of nitrogen movement, transformation, and uptake in plant root zone. EPA 600/3-78-029.

Denmead, O.T., and B.D. Miller. 1978. Water transport in wheat plants in the field. Agron. J. 68:297-303.

Federer, C.A. 1978. A soil-plant-atmosphere model for transpiration and availability of soil water. Water Resour. Res. 15:555-562.

Goldstein, R.A., Mankin, J.B., and R.J. Luxmoore. 1974. Documentation of PROSPER. A model of atmosphere-soil-plant-water flow. EDFB-IBP-73-9, Oak Ridge National Laboratory, Oak Ridge, TN.

Iskandar, I, and H.M. Selim. 1981. Modeling nitrogen transport and transformation in soils. 1. Theoretical considerations. Soil Sci. 131:233-241.

Nimah, M.N., and R.J. Hanks. 1973. Model for estimating soil water, plant and atmosphere interrelations. Description and sensitivity. Soil Sci Soc. Am. Proc.37:522-527.

Norman, J.N., and G.S. Campbell. 1983. Application of a plant-environmental model to problems in irrigation. Adv. Irrig. 2:155-188.

Robbins, C.W., Wagenet, R.J., and J.J. Jurinak. 1980. A combined salt transport-chemical equilibrium model for calcareous and gypsiferous soils. Soil Sci. Soc. Am. J. 44:1191-1194.

Running, S.W., Waring, R.H., and R.A. Rydell. 1975. Physiological control of water flux in conifers: a computer simulation model. Oecologia 18:1-16.

Tillotson, W.R., Robbins, C.W., and R.J. Hanks. 1980. Soil water, solute, and plant growth simulation. Utah Agricultural Experiment Station Bull. 502.

Wagenet, R.J. and J.L. Hutson. 1986. Predicting the fate of nonvolatile pesticides in the unsaturated zone. J. Environ. Qual. 15:315-322.

Chapter III

WATER FLUXES IN ACID SAVANNA SOILS: A COMPARISON OF APPROACHES

3.1 INTRODUCTION

The ability to quantitatively describe field soil water fluxes is an important aspect of a wide range of agricultural and environmental research. Soil water simulation models have been used to estimate crop irrigation water requirements (Norman and Campbell, 1983), to assess the environmental fate of agricultural chemicals (Wagenet and Hutson, 1986), and for soil classification (Van Wambeke, 1985), amongst other purposes. The extent that simulation models correctly represent the most important processes and interactions effecting soil water fluxes in the soil-plant-atmosphere system will determine their ability to be extrapolated to previously unstudied locations and conditions.

The ability to extrapolate knowledge across a range of environmental conditions is particularly important in the transfer of agricultural technology. While empirical knowledge is essential in that it provides a valuable body of information, empirical relationships derived from it are often site-specific and frequently do not apply across a range of soils or climates. Mechanistic simulation models such as the plant-environmental models used in this research can fill an important role in providing the

conceptual framework in which to extrapolate research results to broad regions as well as aide in the design and interpretation of agronomic experiments.

The Cerrado region in Brazil is a good example of the great need to extrapolate agricultural knowledge acquired in a short time to a large region, in which climatic conditions and soil properties vary considerably. Most of the existing understanding of soil and crop management under Cerrado conditions has been acquired within the last 15 years, when the large-scale agricultural development of this region was first conceived. Only a few experimental research sites exist in an area larger than the corn and wheat belt of the United States.

Furthermore, there are several features of acid savanna systems that make proper evaluation of water fluxes critical to sound management. The most unusual features of highly weathered acid savanna soils in terms of water movement are their moisture release characteristics. Although they often exhibit high clay contents in the order of 50 to 70 % and even higher (EMBRAPA, 1981) their high degree of aggregation due to iron and aluminum oxides gives them the drainage characteristics of sands in the wet range. They are often referred to as 'pseudo-sands'. At 'permanent wilting point' (-1500 J kg^{-1}), these soils typically hold between 18 and 22 vol % of water due to their high clay content. Rapid initial drainage possibly via macropores resulting

in low water contents at field capacity and high water contents at 'permanent wilting point' result in very low amounts of plant available water stored in the soil profile (Goedert, 1983; Wolf, 1975). Under these conditions crop rooting depths determine the likelihood of crop survival during the frequently occurring 'veranicos' or drought periods that occur in the wet season. When crop rooting depths are restricted by 'chemical boundaries' such as Al-toxicity or severe Ca deficiency (Richtey, 1982), not only are the plants more likely to be subjected to water stress in case of a drought, but nutrients stored at greater depth are unavailable to the crop. Yields of corn were shown to be positively related to the depth of lime incorporation into the soil (Gonzales-Erico, et al., 1979; Lobato and Ritchey, 1979). Dry season survival of different legumes species that might serve to protect the otherwise unused soil surface against erosion and contribute symbiotically fixed nitrogen to a succeeding crop appears to be related to their rooting depths (Bowen, personal communication). If the roots of acid-tolerant legume species could explore a deep enough soil profile, chances for surviving the dry season and resuming growth at the onset of the first rains would be greatly increased.

Due to the high amounts of rainfall, low cation exchange capacities and rapid drainage of these soils, downward movement of Ca within a relatively short period

of time (several years) has been observed (EMBRAPA, 1978). The application of gypsum is currently the recommended method to amend the acid subsoils of the Cerrado. While the leaching of Ca into the subsoil might well be a desirable effect, leaching losses of nitrate, potassium and other cations can be substantial under Cerrado conditions (Grove, 1979; Richtey, 1979). A better understanding of the water movement and the leaching process in these soils is needed (Goedert, 1983) and a resulting ability to better manage water fluxes will provide the basis for improved management of soil amendments and plant nutrients.

Estimates made for the Federal District on the basis of available water resources predict a potential for irrigation of five to ten percent of the total land area (Pruntel, 1975). Quantification of water fluxes in Cerrado soils is an essential prerequisite for irrigation project planning and management. Studies have been conducted to quantify irrigation water requirements of Cerrado crops (Luchiari, 1988). This information should be in a form that can be extrapolated from research station experiments to other acid savanna soils and climatic conditions within the Cerrado or elsewhere (Goedert, 1983). Simulation models will provide a valuable tool to increase understanding of the interactions between soil physical properties, water dynamics and crop growth under Cerrado conditions.

This research had as it's major objective the quantitative description of water fluxes in Cerrado soils under cropped and fallow conditions. A field experiment was conducted at the Centro de Pesquisa Agropecuaria dos Cerrados (CPAC) near Planaltina, Brazil from April to September 1987 to collect data on the water budget of acid savanna soils under a wide range of irrigation water inputs. Data obtained from this field experiment was compared to simulated data using two soil water simulation models. The General Purpose Simulation Model GAPS (Buttler and Riha, 1987, 1988) was used to implement alternative simulation model representations and to compare the effect of their respective assumptions and limitations on model performance. Two major alternative approaches to model soil water flow, the Richards equation (Campbell, 1985) and the Tipping Bucket method (Jones and Kiniry, 1986; Ritchie et al., 1986), were compared in their ability to predict measured soil water contents and soil water potentials (for Richards equation only). Specific objectives were to test the hypotheses and assumptions contained in two alternative representations of water flow in the soil and their resulting ability to predict within reasonable range of error soil water contents in cropped and fallow soils subjected to a wide range of water inputs.

3.2 MATERIALS AND METHODS

3.2.1 Line Source Irrigation Experiment

The experimental site was located on the EMBRAPA-CPAC (Cerrado Agricultural Research Center) research station in the Federal District of Brazil, latitude of 15.5 degrees south and longitude of 27.5 degrees west, at an altitude of 1000 m. The soil is classified as an Oxisol (Typic Haplustox, isohyperthermic, fine, kaolinitic) or a Dark-red Latosol in the Brazilian classification system (Macedo and Bryant, 1987). Corn (Zea mays L., 'Cargill 111 S') was planted on 21 April 87 in 80 cm wide rows at a final population density of 62,500 plants/ha. The crop was grown during the dry season in order to have optimal control of irrigation water treatments.

A line-source sprinkler irrigation system (Hanks et al., 1976) was used to establish a gradient of irrigation water application across a plot perpendicular to the irrigation line. Irrigation water was applied at the same frequency to all plots, but at rates ranging from approximately 3 to 25 mm $hour^{-1}$. Quantities of applied water were measured after each irrigation event with catch cans located between the corn rows just above the crop canopy. Three rows of 40 catch cans each spaced approximately 15 meters apart were used to collect the irrigation water. Uniformity along the irrigation line was relatively good, with coefficients of variation generally around five percent. This allowed the mean of

the three sampling locations to be used to represent amounts of irrigation water applied as a function of distance from the line source. Wind conditions led to a consistently different distribution of water between the two halves of the experimental field, prohibiting treating plots on opposite sides of the irrigation line as replicates.

Irrigation water was applied every three to five days for two to three hours after dusk, when wind speed was low. Accumulated irrigation water application for all eight soil sampling locations is presented in Fig. 3.1a. The total amount of irrigation water received at the two extreme sampling locations during the experimental period (including 104 mm natural precipitation) was 105 mm (S-16) and 1020 mm (N-01) (Fig. 3.1b). Comparisons between measured and predicted data will be discussed for four irrigation treatments (N-01, N-11, N-16, and S-16), representing approximately 1.6, 1.0, 0.6, and 0.3 of potential evapotranspiration (PET), respectively, when averaged over the whole growing season.

Treatments perpendicular to the irrigation line consisted of three different nitrogen (N) fertilizer application rates (0, 100, and 200 kg N/ha) planted to corn and replicated twice on each side of the sprinkler line and two non-replicated fallow plots. Only the results from the cropped treatment receiving 200 kg N/ha nitrogen fertilizer and the fallow treatments are reported

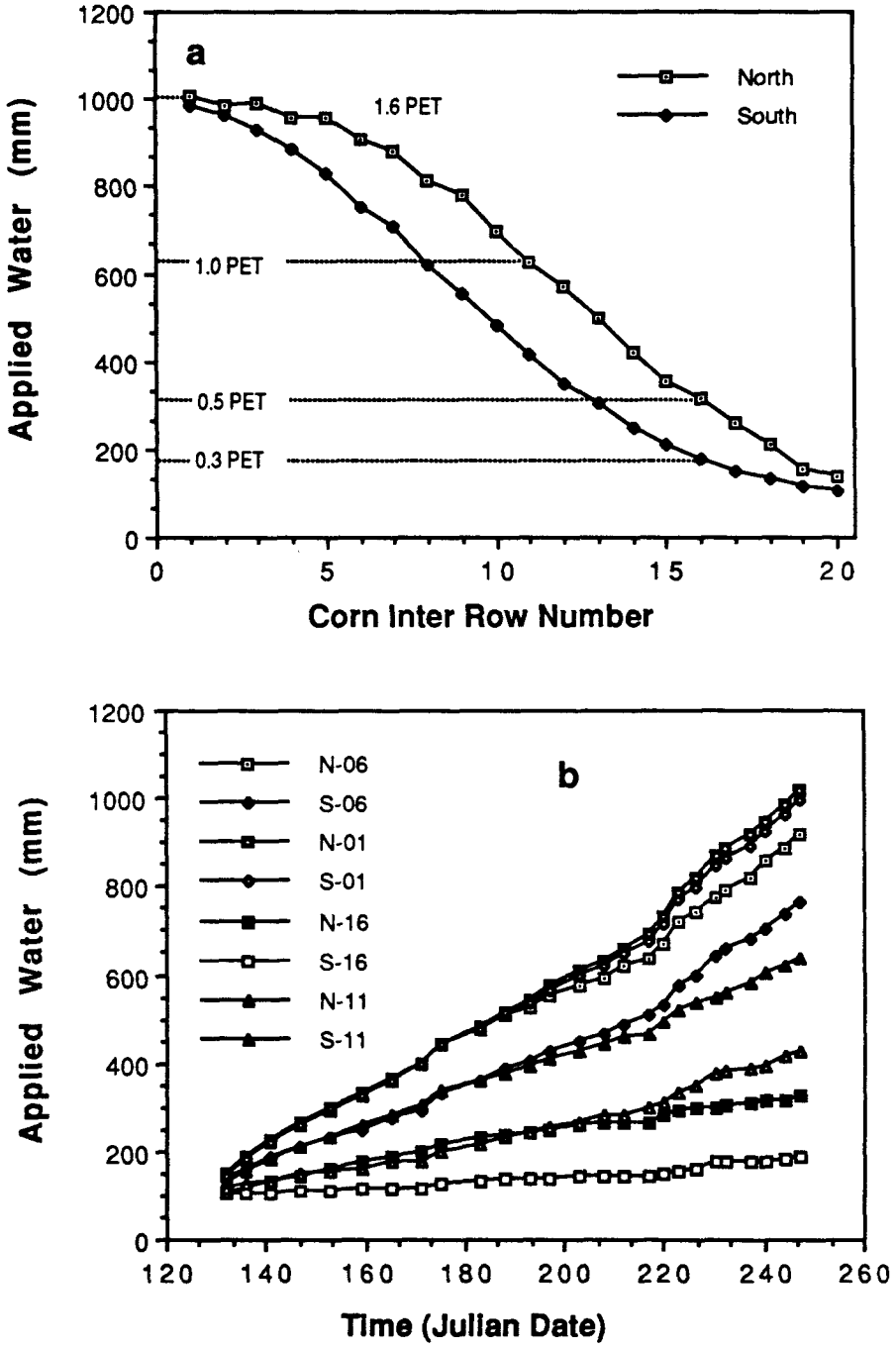

Figure 3.1 Total amounts of irrigation water received for soil and plant sampling location. a) as a function of distance from the line source b) cumulative amounts as a function of time.

in this chapter.

3.2.2 Soil and Plant Sampling

Soil samples were collected every two weeks between specified corn rows. Of the twenty rows of corn on each side of the sprinkler line (numbered 1 to 20 starting at the irrigation line) rows 1/2, 6/7, 11/12, and 16/17 were designated as soil sampling locations to represent different water regimes along the continuous gradient of water application across the plot. The sampling locations will be referred to as N-01, N-06, N-11, and N-16 for the northern side of the experimental field and as S-01, S-06, S-11, and S-16 for the southern side. Soils were sampled a total of nine times during the experimental period and the water content determined gravimetrically. Additionally, a neutron probe was used during the later part of the season to support the gravimetric sampling scheme. 48 mercury tensiometers were installed in two blocks (blocks 4 and 14) in three maize rows (rows 3, 8, and 13) at depths of 0.30, 0.45, 0.75, and 1.05 m in replicates of two and were read daily to obtain measurements of soil water potential.

Sequential harvests of the above-ground part of the maize plants were made weekly for the first five weeks starting 30 days after emergence and then biweekly on the same days as the soil was sampled. Leaf area was measured using a leaf area meter.

3.2.3 Simulation Procedures

Two different soil water transport models were used to simulate soil water content distributions over time and as a function of depth under the different irrigation treatments. The GenerAl Purpose Simulation Model (GAPS) (Buttler and Riha, 1987, 1988) was used to compare two main approaches to the simulation of soil water movement: a numerical solution to the Richards equation (Campbell, 1985) and a capacity-type water budgeting routine adapted from the CERES Maize model water flow routine (Jones and Kiniry, 1986; Ritchie, et al., 1985) and incorporated into GAPS as the 'Tipping Bucket' water flow procedure. Detailed documentation of the two water flow procedures with explanations of governing equations and their solutions is contained in the GAPS User's Manual (Buttler and Riha, 1988, Appendix A).

The Priestley-Taylor equation (alpha = 1.26) was used to estimate potential evapotranspiration (Priestley and Taylor, 1972), which was partitioned into potential soil evaporation and potential transpiration using an equation presented for corn by Stockle and Campbell (1985). For simulating plant water uptake, two different water uptake procedures compatible with the water flow simulation procedures were used. In the case of the Richards equation, which predicts hourly changes in soil water potentials, a potential-driven plant water uptake procedures was used to estimate root water uptake and

actual transpiration (Riha and Campbell, 1986). Actual transpiration is determined by the response of stomatal resistance to leaf water potential (Fisher et al., 1981), assuming a critical leaf water potential of -1400 J kg^{-1}. Water flow into roots was assumed to be inversely dependent on the resistance to water flow in the soil and in the root (Gardner and Ehlig, 1962). Water flow from the bulk soil to the root is directly dependent on the gradient between roots and soil water potentials (Gardner, 1960). The root water potential was not allowed to drop below -1500 J kg^{-1}. Soil evaporation is incorporated into the Richards equation as proposed by Campbell (1985), with actual soil evaporation being controlled by the humidity at the evaporating surface during first stage drying and by the liquid flux to the evaporating surface during second- and third-stage drying.

The Tipping Bucket procedure was combined with a plant water uptake routine based on the concept of plant-available water. Plant water uptake from any layer in the soil containing roots is allowed to proceed until a lower limit of plant-extractable water (permanent wilting point) is reached. The root density distribution in the soil profile is used to partition the transpirational demand between soil layers. Demand not met in any one layer is transferred to other layers as an additional demand. Root densities thus do not limit root water uptake in this simple representation, but serve solely to partition

transpiration in the soil profile. Soil evaporation was included in the Tipping Bucket water flow procedure as simple first-stage evaporation, which was allowed to proceed until the soil water content reached 50 % of its value at permanent wilting point. Soil evaporation occurred only from the surface soil node. No upward water flow was simulated in the Tipping Bucket water flow routine. An hourly time step was used for both water flow models. Simulations were conducted from 06 April 87 (Day 96), starting with a measured water content distribution, to 09 September 87 (Day 252).

3.2.4 Simulation Input Data

3.2.4.1 Climate and Location Data

Daily climatic data for the experimental site was obtained from CPAC's main meteorological station located approximately 50 m away from the experimental location. Climatic data include daily precipitation (mm), Class 'A' pan evaporation (mm), solar radiation (cal m^{-2} day^{-1}), daily average wind speed (m s^{-1}), maximum and minimum air temperature (°C), maximum and minimum relative humidity. The climate file for the experimental period containing the above variables is included as Appendix B. Daily minimum and maximum air temperatures and daily total solar radiation were transformed into hourly values (see GAPS Manual, Appendix A).

3.2.4.2 Soil Parameter Estimation

Soil physical properties were characterized to the extent that they were needed as inputs to the water flow routines. Soil particle density and texture was determined on soil samples collected from three randomly chosen locations in the experimental field in 0.15 m depth intervals to a depth of 1.80 m (Gee and Bauder, 1985). Mean soil clay, silt, and sand percentages were 58.7 (1.8), 6.0 (1.1), and 35.3 (1.3) percent, with the numbers in parenthesis being the standard deviations. The mean particle density was 2.66 Mg m^{-3} (0.02 Mg m^{-3}). Differences in soil texture and particle density were not significant between depths.

Dry bulk density and hydraulic parameters were measured on undisturbed soil cores. A pit (2 m by 1.5 m) was excavated in the border area of the experimental field to a depth of 1.85 m. Twelve soil cores per depth (depth increments corresponding to later soil sampling depths) were collected along the 2 m face of the pit. A total of 110 core samples was collected. An additional 80 core samples were collected to a depth of 0.65 m at four other sites randomly chosen within the experimental field, to test for within field variability. Bulk densities and hydraulic conductivities measured on the latter 80 samples did not differ from the samples collected in the deep pit, and are not reported.

Soil saturated hydraulic conductivity was determined on the cores using the constant head method (Klute and Dirksen, 1985). The weight of the soil cores was determined immediately after each conductivity measurement to obtain an estimate of the relative saturation of the sample during the determination of saturated hydraulic conductivity. The degree of saturation during the determination of saturated hydraulic conductivity on the 50 core samples, for which soil moisture release parameters were later measured, ranged from 89% to 101% of calculated total porosity (Table 3.1). Soil bulk densities showed increased values at the 0.15 to 0.45 m depths probably due to compaction. The higher soil bulk densities were highly negatively correlated with measured saturated conductivities (Fig. 3.2).

Saturated hydraulic conductivities measured in the laboratory compare well with values reported by others for the same soil under field conditions (EMBRAPA-CPAC, 1981). A value of 125 cm day^{-1} (0.00148 kg s m^{-3}) was a field-measured value for satiated hydraulic conductivity reported by Luchiari (1988) and is well in the range of the conductivity measured in the soil layer with the highest bulk density (0.0016 kg s m^{-3}). Bouldin (1979) reported infiltration rates between 17 and 22 cm $hour^{-1}$ (0.004 and 0.006 kg s m^{-3}, respectively), which is also in agreement with the laboratory measurements.

TABLE 3.1

Soil physical parameters (mean, standard deviation, maximum and minimum values for 50 soil cores from 9 depths (0.07 - 1.85 m).

Parameter		Ú	Min	Max
Bulk density ($Mg\ m^{-3}$)	1.051	0.084	0.932	1.295
Total porosity ($m^3\ m^{-3}$)	0.605	0.032	0.513	0.649
Sat. hydr. conductivity ($kg\ s\ m^{-3}$)	0.00424	0.00178	0.000369	0.00723
Water content ($m^3\ m^{-3}$)	0.567	0.030	0.485	0.618
Degree of saturation (%)	0.938	0.031	0.891	1.01

Moisture characteristic curves were determined on 60 of the above 110 core samples using pressure plates (Klute, 1985 c) (Fig. 3.3). Soil water potentials below the air entry potential are described as a function of soil water content using an equation proposed by Campbell (1974,1985): $WP = AE\ (WC/WS)^{-b}$, where WP is the soil water potential ($J\ kg^{-1}$), WC is the soil water content ($m^3\ m^{-3}$), WS is the saturation water content ($m^3\ m^{-3}$), AE is the air entry potential ($J\ kg^{-1}$) and b is the soil-B value. AE and B can be determined from moisture release data by plotting log(WP) against log(WC/WS) and fitting a best fit line to the data. One set of soil b-values and air-entry potentials was calculated using only the

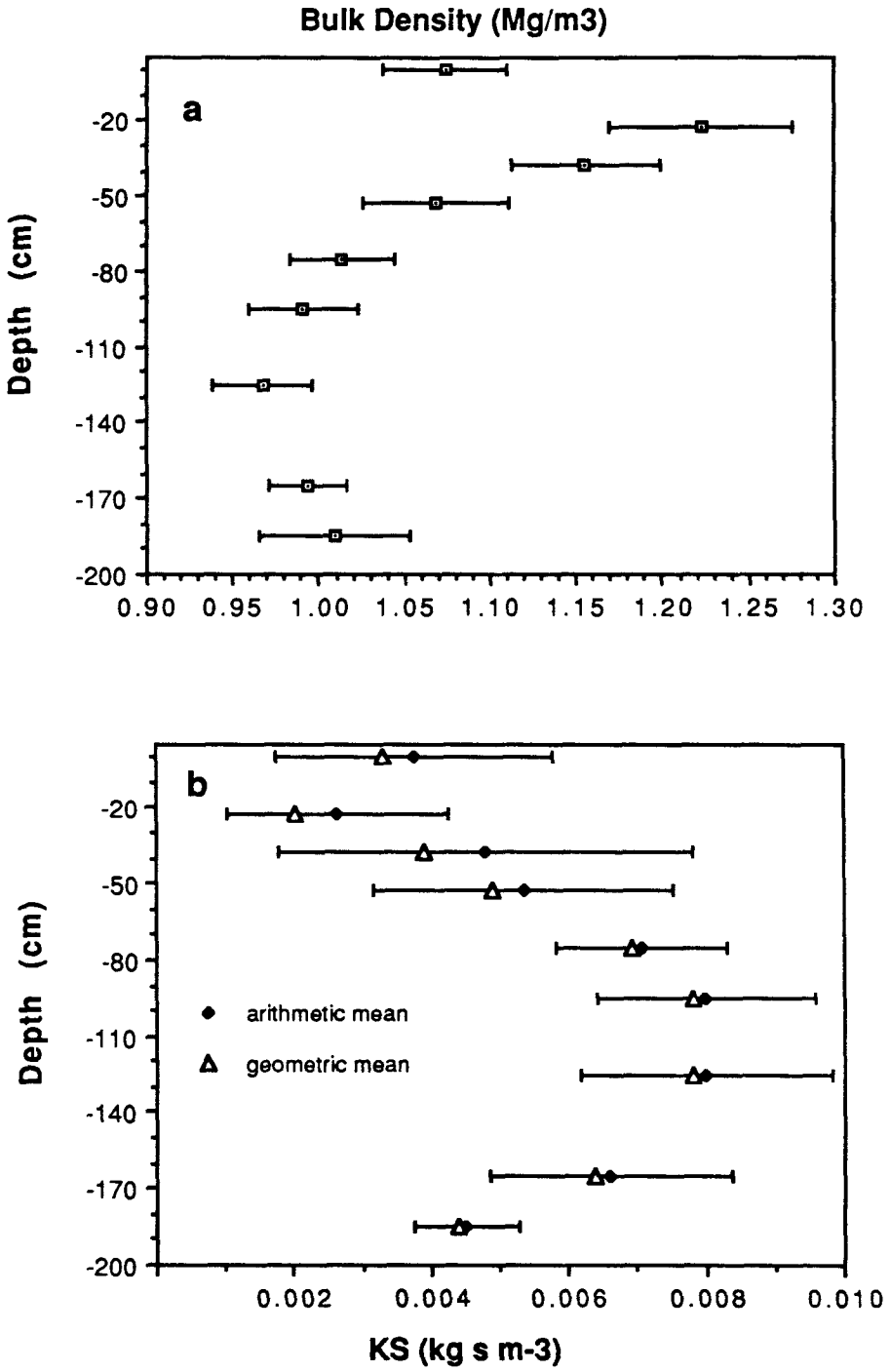

Figure 3.2 Soil physical properties measured on 110 undisturbed soil cores. a) bulk densities b) laboratory measured saturated hydraulic conductivities.

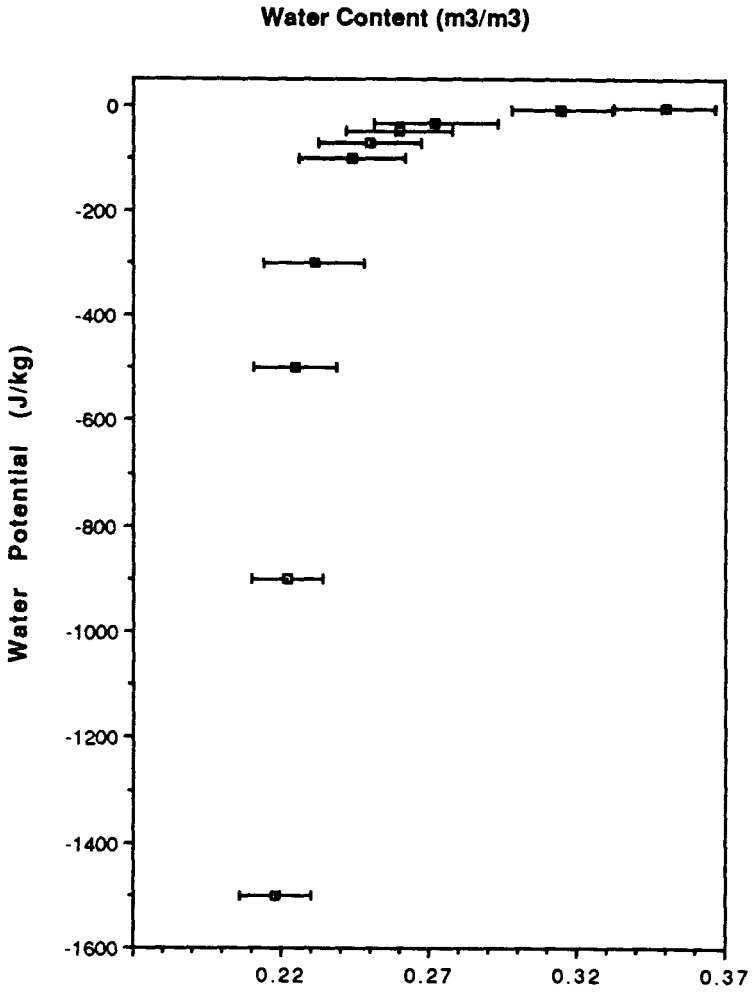

Figure 3.3 Soil moisture release curve. Data points represent means of 60 sample ± 1 Ú taken to a depth of 1.85 m.

water content/water potential data for the wet range (-6 to -100 J kg^{-1}) (Fig. 3.4a), and a second set of parameters was obtained from fitting the equation over the whole range from -6 to -1500 J kg^{-1} (Fig. 3.4b), using mean water contents and potentials over all depths.

Input data for the Tipping Bucket water flow routine were calculated from moisture release data. The volumetric water content at -33 J kg^{-1} (0.272 m^3 m^{-3}) was used as the Drained Upper Limit (DUL) or 'field capacity' and the volumetric water content at -1500 J kg^{-1} (0.20 m^3 m^{-3}) as the Lower Limit (LL). The Profile Drainage Constant and other parameters used in the Tipping Bucket procedure were calculated according to the equations given by Ritchie et al. (1986). The soil input data file used for the simulations is presented in Table 3.2.

3.2.4.3 Plant Input Data

For the purpose of the water budget simulations presented in this chapter, plant growth was treated as an input to the model rather than being simulated. Second-order polynomial exponentials were fit to the measured leaf area data obtained from the sequential harvests (Fig. 3.5). For this purpose the eight sampling points (N-01 to S-16) were grouped into 4 classes according to the amounts of irrigation water they received. Empirical equations were then used in the model to estimate leaf area index as

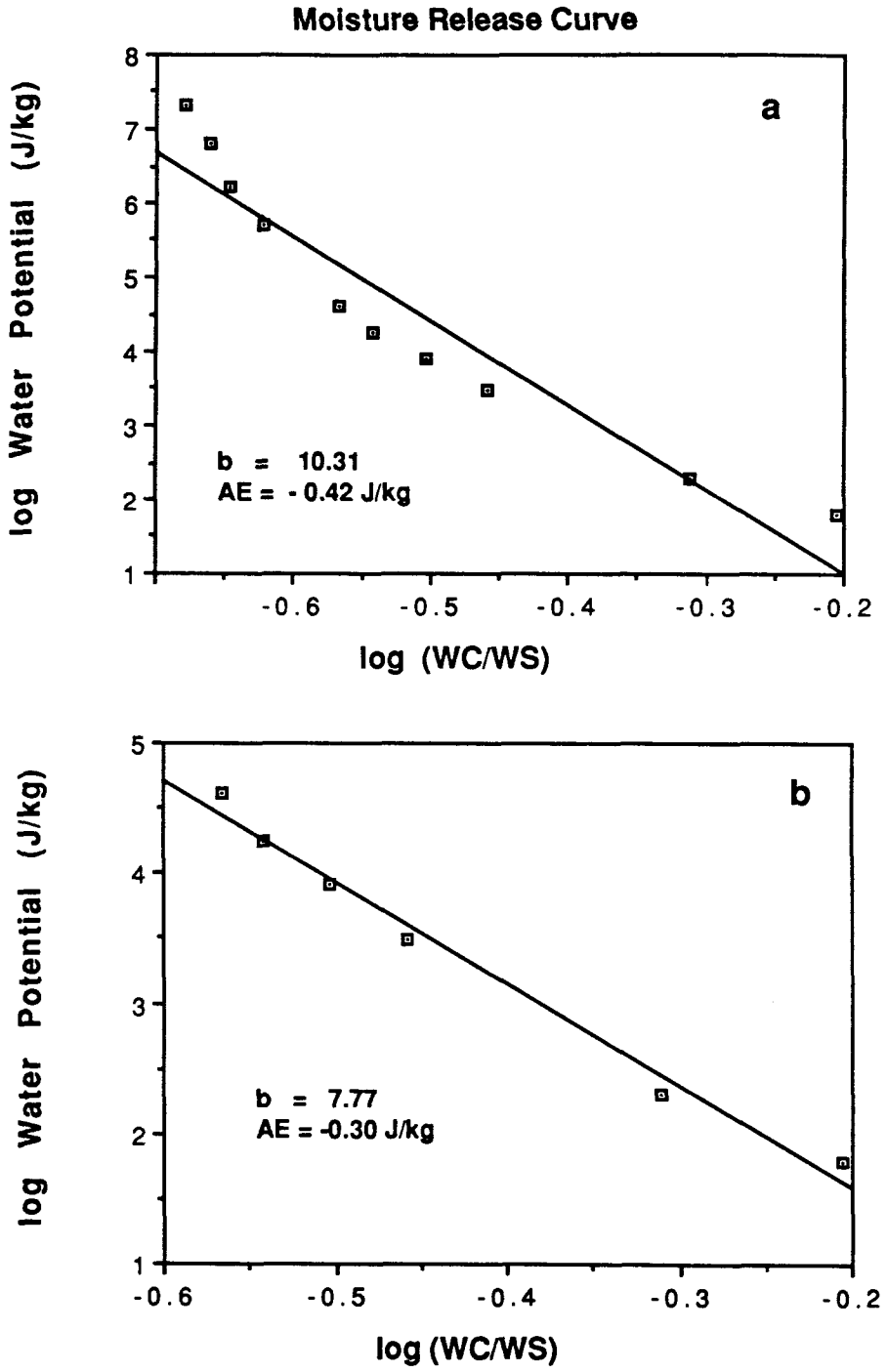

Figure 3.4 Soil moisture release parameters for the Campbell equation. Fit to a) the whole range (-6 to -1500 J/kg) of water potentials b) to the wet range only (-6 to -100 J/kg).

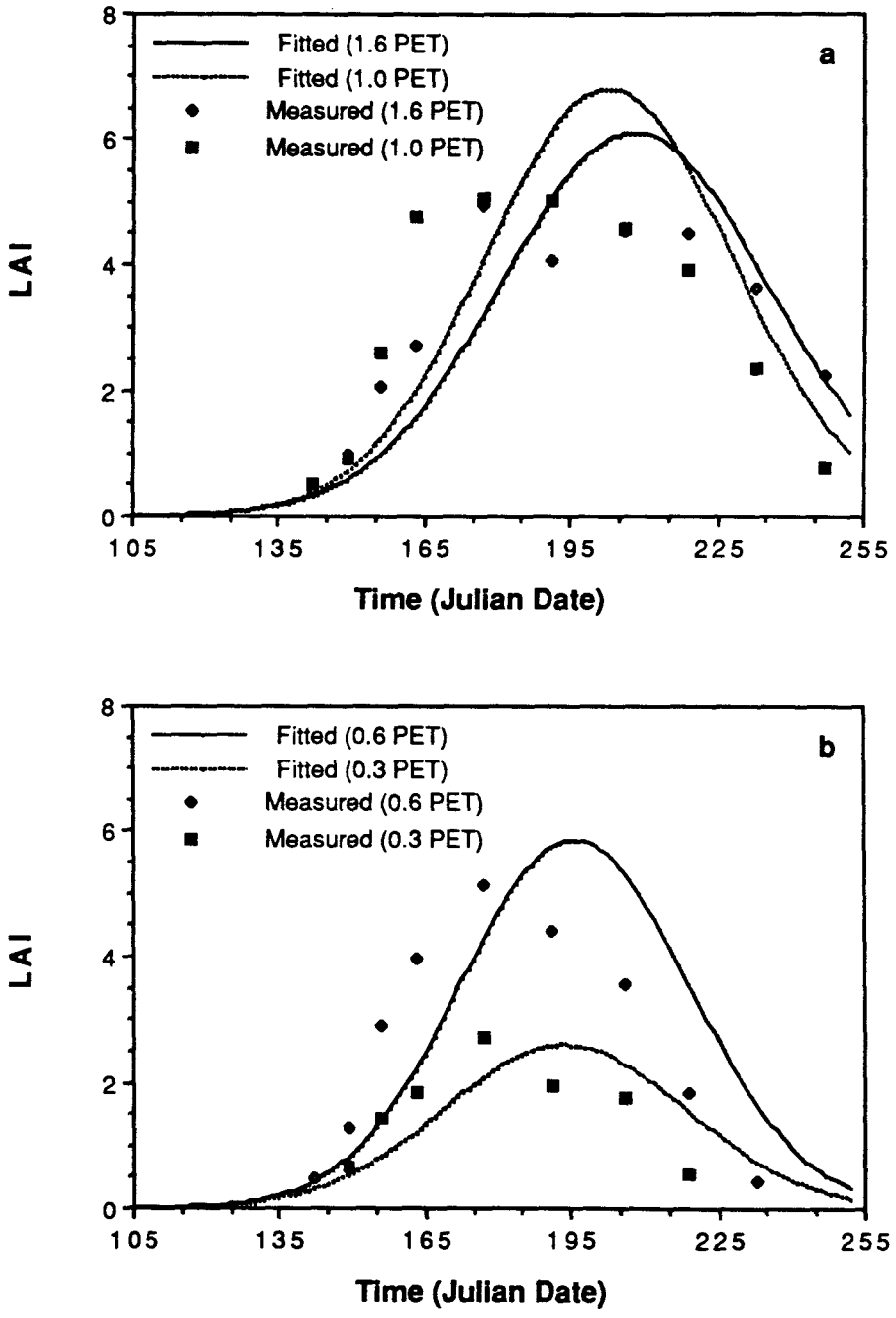

Figure 3.5 Measured leaf area index developement over time and the second-order polynomial exponentials that best fit the data. a) irrigation treatments 1.6 PET and 1.0 PET b) irrigation treatments 0.6 PET and 0.3 PET.

TABLE 3.2

Soil input data file

Soil File Name	:	Oxisol
Soil Name	:	Dark Red Latosol
Clay	:	60 %
Particle Density	:	2.66 Mg m^{-3}
Soil b-value	:	10.31
Air Entry Pot.	:	-0.42 J kg^{-1}
Drained Upper Limit	:	0.30 m^3 m^{-3}
Lower Limit	:	0.20 m^3 m^{-3}

Node	Depth (m)	BD (Mg m^{-3})	KS (kg s m^{-3})	Initial WC (m^3 m^{-3})
1	0.01	1.07	0.0026	0.32
2	0.08	1.07	0.0026	0.32
3	0.23	1.22	0.0016	0.31
4	0.38	1.15	0.0031	0.31
5	0.53	1.07	0.0039	0.28
6	0.75	1.00	0.0054	0.27
7	1.05	1.00	0.0061	0.27
8	1.35	1.00	0.0061	0.27
9	1.65	1.00	0.0050	0.27
10	1.85	1.00	0.0035	0.27

the sample was used to determine relative root density distributions in the soil profile. The maximum rooting depth observed in the high water/high nitrogen treatments was 1.20 m. More than half of the total root weight in the 90 cm soil profile was concentrated in the uppermost 15 cm. Root densities reported by Gonzales-Erico (1979) for the same location and corn variety were 4.6 to 5.1 cm cm^3 under limed conditions and consequently, a root length value of 5.0 cm cm^3 was assumed for the 0 to 15 cm depth increment. Root densities were than reduced with depth using the measured relative root distribution. To

simulate root growth, the crop growth components included in GAPS and based on a simulation model developed by Stockle and Campbell (1985) were used. They are described in greater detail in chapter IV and fully documented in the GAPS user's manual (Appendix A). Rooting depth was simulated on the basis of simulated daily dry matter partitioned to roots (Foth, 1962). Instead of changing root densities in each layer over time, a static root density distribution was used and additional layers were activated as the season progressed in accordance with the simulated rooting depth. The plant input data used is presented in Table 3.3.

3.2.5 Statistical Analysis

Statistical analysis of the experimental data was performed using the Statistical Analysis System (SAS User's Guide, 1985). The main objective of the statistical analysis of the measured water content data was to obtain a mean and standard deviation of soil water content as functions of applied irrigation water and as a function of time and depth. These measurements were than compared to data obtained from the simulation model.

Multivariate analysis of the soil water content data was performed using the REPEATED MEASURE OPTION in PROC ANOVA, treating measurements over depth as repeated measures and performing the analysis for each sampling

TABLE 3.3

Plant input data

Plant File Name	:	Corn
Plant Name	:	Cargill 111 S
Emergence date	:	117 (Julian date)
Initial LAI	:	0.07
Minimum root water potential	:	-1500 J kg^{-1}
Root radius	:	0.002 m
Root resistance	:	2.5E+10 kg s m^{-4}
Initial canopy height	:	0.10 m
Aerodynamic resistance (RA)	:	40.0 s m^{-1}
Short-wave absorptivity (AS)	:	0.70
Critical leaf water potential	:	-1400 J kg^{-1}

Soil profile node	Root Density ($m\ m^{-3}$)
1	1.0 E+04
2	5.0 E+04
3	3.0 E+04
4	1.0 E+04
5	0.6 E+04
6	0.4 E+04
7	0.2 E+04

date. IRRIGATION was treated as nested within SIDE due to the differences in irrigation water application rate between sides. To test for the effect of IRRIGATION (SIDE), p-values were hand-calculated using the appropriate mean square error for the overall model.

Expecting the water contents over depths of sampling to be correlated, Wilk's criterion was used to test for differences among treatments. The advantage of employing a multivariate technique is that a statement can be made about the correlation of a number of variables that are

studied simultaneously. The 'within subject effects' thus relate to the changes in water contents with depth. The 'between subjects effects' test the hypothesis that the between subject factors (e.g. irrigation treatment, nitrogen treatment) have no effect on the dependent variables ignoring the within subject effect in the design. The test sums over the dependent variables, in this case it sums the water contents over all sampling depths and tests hypotheses relating to the effect of a treatment for water content on the average.

3.3 RESULTS AND DISCUSSION

3.3.1 Water Content Distribution in the Soil Profile over Time under Various Irrigation Treatments

The initial soil sampling on 06 April showed very little variability in soil water content distribution in the field with coefficients of variation ranging from one to two percent. This sampling occurred 20 days after the grass sod previously covering the experimental area had been broken and 15 days before planting. By May 07, 16 days after planting, but before the first irrigation water application, water contents still varied very little. Rainfall and one uniform application of irrigation water were sufficient to provide adequate moisture for germination.

3.3.1.1 Fallow Treatments

Fig. 3.6 depicts the progression of measured soil water contents and their profile distribution with time under the four representative irrigation treatments, corresponding to approximately 1.6 (N-01), 1.0 (N-11), 0.6 (N-16) and 0.3 (S-16) potential evapotranspiration. The difference in amounts of irrigation water applied led to a clear separation of water contents which became more pronounced with time. Since the fallow plots were not replicated, no statistics are presented.

3.3.1.2 Cropped Treatments

On Day 141, nine days after the first and four days after the second irrigation water application, irrigation water treatment (IRRIG) already showed a significant effect on water contents in the profile. Throughout the soil profile to a depth of 1.80 m, IRRIG (SIDE) was significant at $p=0.0001$ and remained significant throughout the soil profile for water contents throughout the season (Fig. 3.7).

These results show that the experimental design and data collection scheme was able to provide statistically significant differences in measured soil water contents between the sampling locations selected along the continuous gradient of irrigation water application. This is an important prerequisite for a meaningful comparison of these measured data with simulation model output.

Figure 3.6 Measured soil water contents in fallow plots under four irrigation treatments on days a) 141 b) 169 c) 197 and d) 225.

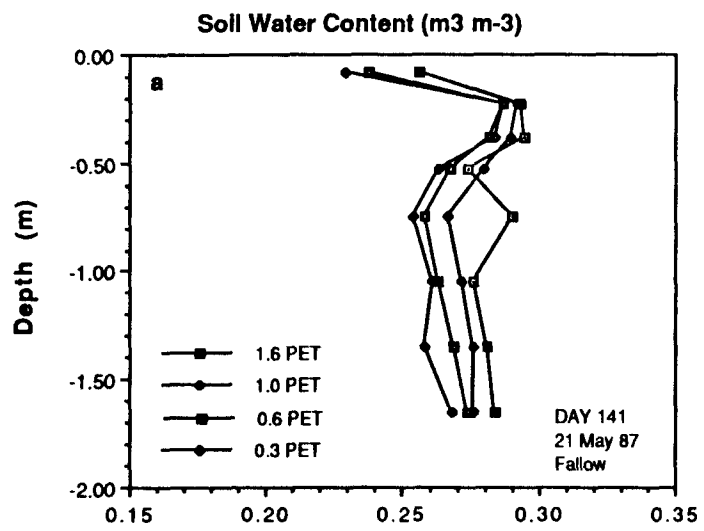
Soil Water Content (m3 m-3)
a
Depth (m)
0.00
-0.50
-1.00
-1.50
-2.00
0.15
0.20
0.25
0.30
0.35
1.6 PET
1.0 PET
0.6 PET
0.3 PET
DAY 141
21 May 87
Fallow

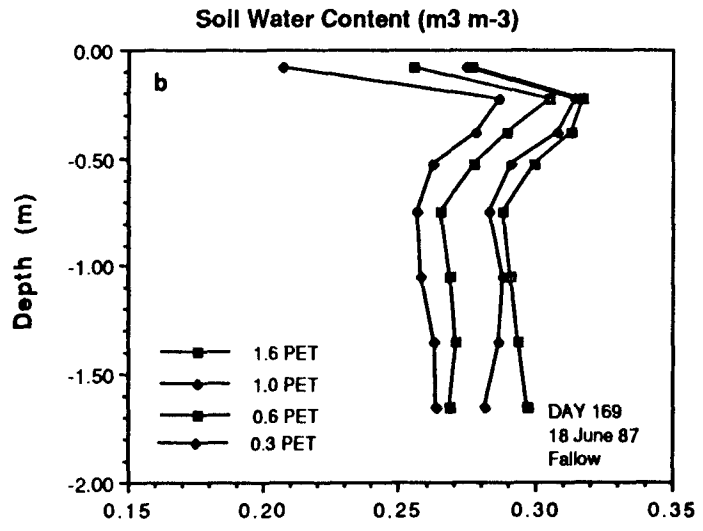
Soil Water Content (m3 m-3)
b
Depth (m)
0.00
-0.50
-1.00
-1.50
-2.00
0.15
0.20
0.25
0.30
0.35
1.6 PET
1.0 PET
0.6 PET
0.3 PET
DAY 169
18 June 87
Fallow

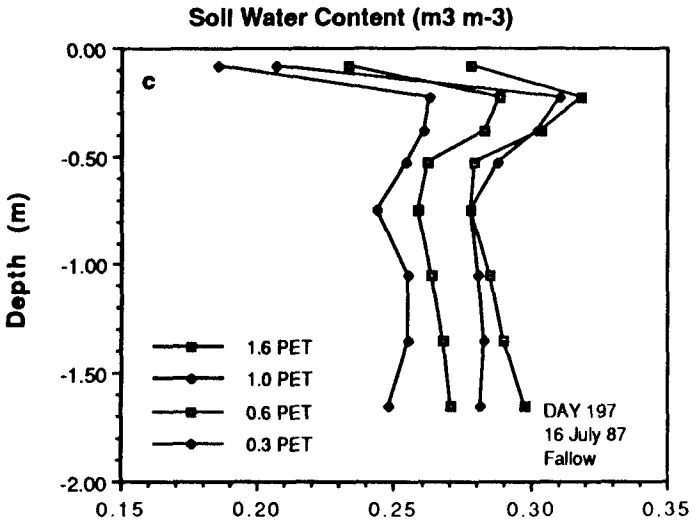
Soil Water Content (m3 m-3)
c
Depth (m)
0.00
-0.50
-1.00
-1.50
-2.00
0.15
0.20
0.25
0.30
0.35
1.6 PET
1.0 PET
0.6 PET
0.3 PET
DAY 197
16 July 87
Fallow

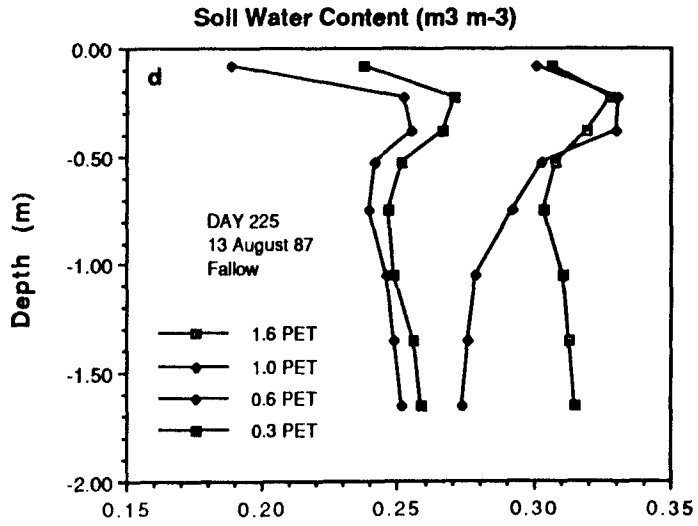
Soil Water Content (m3 m-3)
d
Depth (m)
0.00
-0.50
-1.00
-1.50
-2.00
0.15
0.20
0.25
0.30
0.35
DAY 225
13 August 87
Fallow
1.6 PET
1.0 PET
0.6 PET
0.3 PET

Figure 3.7 Measured soil water content distributions in plots planted to corn under four irrigation treatments on days a) 141 b) 169 c) 197 and d) 225.

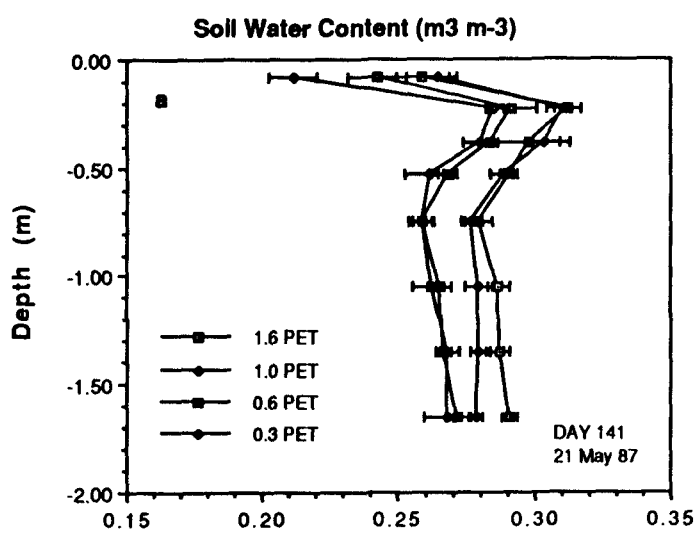
Soil Water Content (m3 m-3)
Depth (m)
a
1.6 PET
1.0 PET
0.6 PET
0.3 PET
DAY 141
21 May 87
0.00
-0.50
-1.00
-1.50
-2.00
0.15
0.20
0.25
0.30
0.35

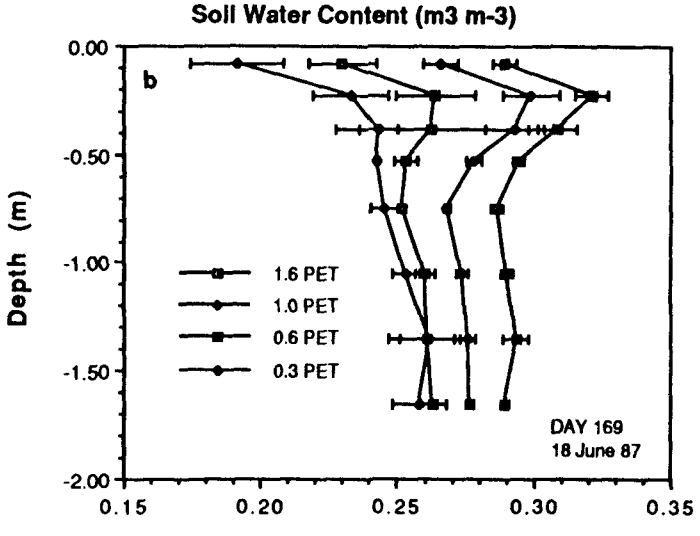
Soil Water Content (m3 m-3)
Depth (m)
b
1.6 PET
1.0 PET
0.6 PET
0.3 PET
DAY 169
18 June 87
0.00
-0.50
-1.00
-1.50
-2.00
0.15
0.20
0.25
0.30
0.35

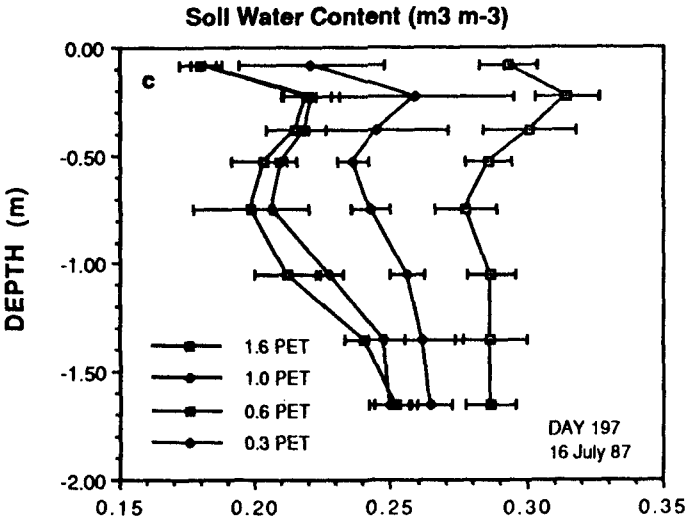
Soil Water Content (m3 m-3)
DEPTH (m)
c
1.6 PET
1.0 PET
0.6 PET
0.3 PET
DAY 197
16 July 87
0.00
-0.50
-1.00
-1.50
-2.00
0.15
0.20
0.25
0.30
0.35

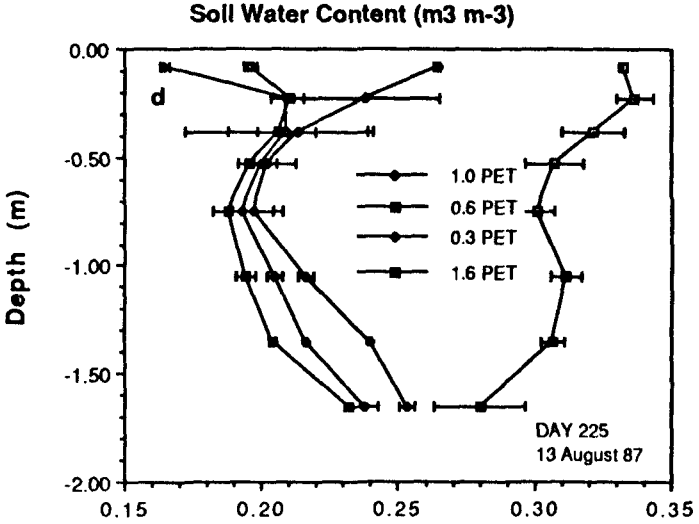
Soil Water Content (m3 m-3)
Depth (m)
d
1.0 PET
0.6 PET
0.3 PET
1.6 PET
DAY 225
13 August 87
0.00
-0.50
-1.00
-1.50
-2.00
0.15
0.20
0.25
0.30
0.35

3.2.2 Comparison of Predicted and Measured Soil Water Contents and Potentials

3.2.2.1 Fallow Treatments

Initial model execution using the Richards equation indicated that simulated soil water contents were consistently higher then field-measured values. It was concluded that the assumption that field saturated water content is equal to total porosity was not valid for this soil, which has bulk densities around 1.00 Mg m^{-3} and approximately 15% of total porosity is macroporosity (Luchiari, 1988). Although saturation percentages of about 95 % (85-100) were obtained during measurements of saturated hydraulic conductivity on undisturbed soil cores in the laboratory (see Table 3.1), the soil does not reach these high values under field conditions. Luchiari (1988) reported field saturated or 'satiated' water contents of about 0.47 m^3 m^{-3} measured on the same soil in close proximity to this experiment's location. This would correspond to a saturation percentage of 75 % of total porosity at a bulk density of 1.00 Mg m^{-3}. The highest volumetric water contents ever measured in the field during this experiment were in the range of 0.35 to 0.37 m^3 m^{-3}.

Using 70 % of total porosity as a saturation water content yielded satisfactory results for most of the profile layers, except for those layers that exhibited increased bulk densities due to compaction. Increasing

bulk density leads to lower predicted water contents at the same soil water potential when all other soil parameters are held constant. This is due to the decrease in soil pore volume, calculated from measured bulk and particle densities. In reality, measured soil water contents at the 15-30 and 30-45 cm depth increments were consistently higher during the entire season than water contents below and above these layers (see Fig. 3.7). It was hypothesized that the process of compaction leads first to a loss of macroporosity. A loss of 10 to 20 percent of macroporosity might not lead to a proportional decrease in saturation water content, which is implicit in using a fraction of total porosity as the field saturation water content. It was decided to use 70 % of total porosity (0.43 m^3 m^{-3}) throughout the soil profile, except for the layers exhibiting higher bulk densities, for which a fraction of total porosity equivalent to a field saturated water content of 0.43 m^3 m^{-3} was calculated. It was assumed that the loss of macroporosity reflected in increased bulk densities did not result in an equivalent decrease in field saturated water content. This adjustment of the field saturation water content was performed using a subset of the experimental data, namely the highest irrigation treatment of the fallow plot. The air entry potential was recalculated assuming the field saturated water content WS in equation (1). The relationship of the log of soil water potential to the log

of soil water contents is not linear over the whole range of soil water potentials for this particular soil. When the Campbell equation is fit to the range from -6 to -1500 J kg^{-1}, water contents at the wet end of the moisture release curve will be under predicted, while it provides a reasonable fit at low water potentials. Soil water content predictions can be improved in the high water content range, when using parameters fit to moisture release data to -100 J kg^{-1}, only (see Fig. 3.4). The choice of the range of water potentials to which to fit the parameters has a strong effect on their values, particularly on the value for B (in equation 1).

Results of the comparison between predicted and observed soil water contents for the fallow plots under the four irrigation treatments using the moisture release parameters obtained from fitting equation 1 to the full range of water potentials are shown in Fig. 3.8 (Day 141) and Fig. 3.9 (Day 181) for the fallow soil. Comparisons between the predictions made by the two water flow models used and the measured data are presented for two sampling dates. The two sampling dates on day 141 and 182 occurred 5 and 6 days after the last irrigation treatment, respectively. Agreement between the Richards equation and measured values is generally good with differences between measured and predicted soil water contents generally around 1-3 volume percents for all the sampling dates.

Figure 3.8 Comparison of measured soil water contents in the fallow plots with predictions by the Richards equation (R) and the Tipping Bucket routine (T) for Day 141 under four irrigation treatments corresponding to a) 1.6 b) 1.0 c) 0.6 and d) 0.3 potential evapotranspiration (PET).

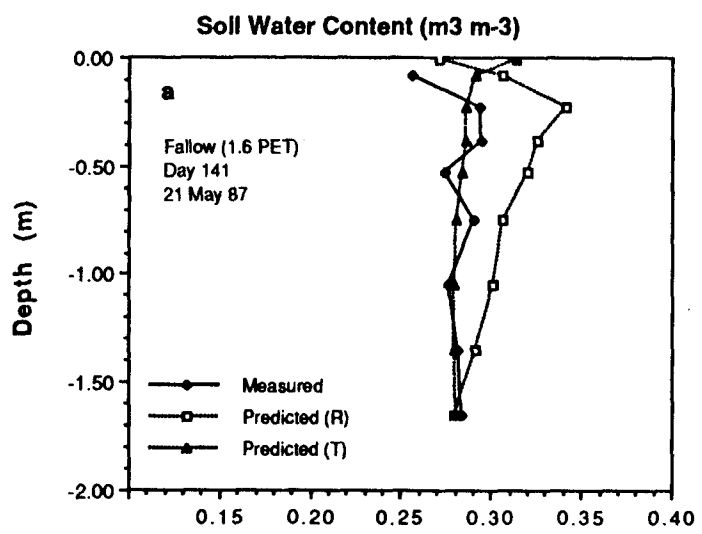
Soil Water Content (m3 m-3)
a
Fallow (1.6 PET)
Day 141
21 May 87
Measured
Predicted (R)
Predicted (T)
Depth (m)
0.00
-0.50
-1.00
-1.50
-2.00
0.15
0.20
0.25
0.30
0.35
0.40

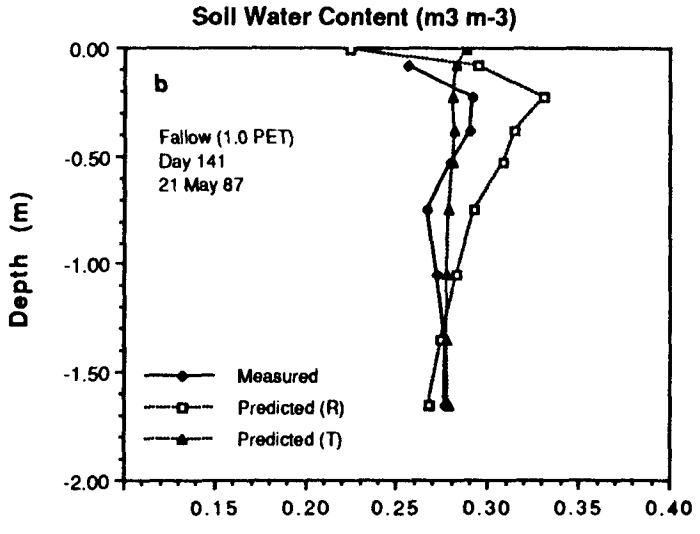
Soil Water Content (m3 m-3)
b
Fallow (1.0 PET)
Day 141
21 May 87
Measured
Predicted (R)
Predicted (T)
Depth (m)
0.00
-0.50
-1.00
-1.50
-2.00
0.15
0.20
0.25
0.30
0.35
0.40

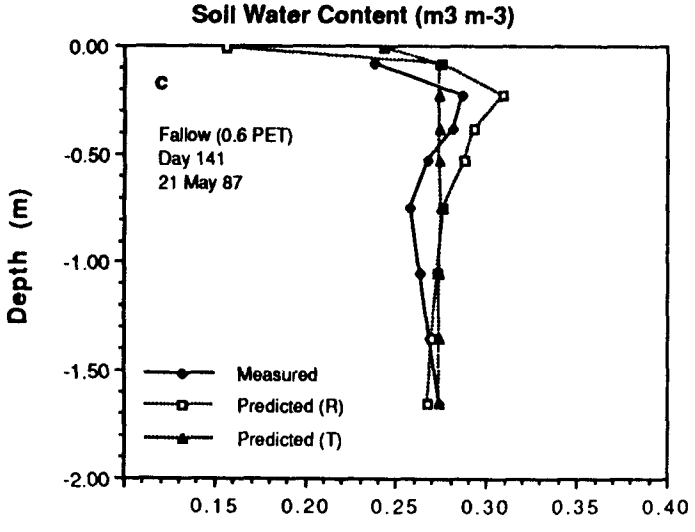
Soil Water Content (m3 m-3)
c
Fallow (0.6 PET)
Day 141
21 May 87
Measured
Predicted (R)
Predicted (T)
Depth (m)
0.00
-0.50
-1.00
-1.50
-2.00
0.15
0.20
0.25
0.30
0.35
0.40

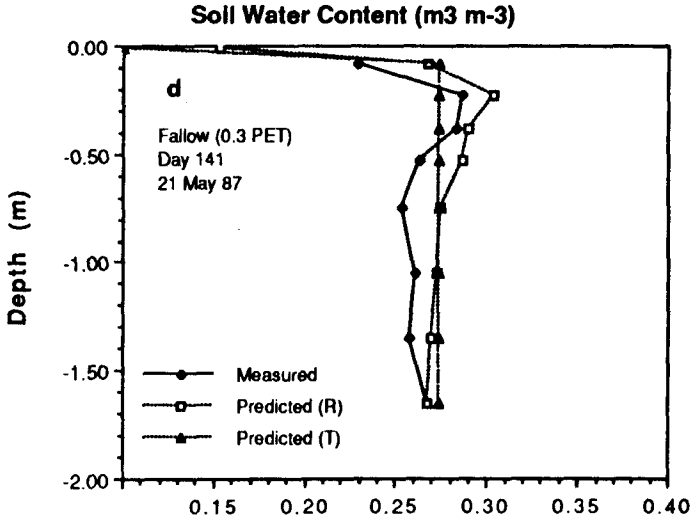
Soil Water Content (m3 m-3)
d
Fallow (0.3 PET)
Day 141
21 May 87
Measured
Predicted (R)
Predicted (T)
Depth (m)
0.00
-0.50
-1.00
-1.50
-2.00
0.15
0.20
0.25
0.30
0.35
0.40

Figure 3.9 Comparison of measured soil water contents in the fallow plots with predictions by the Richards equation (R) and the Tipping Bucket (T) routine for Day 182 under four irrigation treatments corresponding to a) 1.6 b) 1.0 c) 0.6 and d) 0.3 potential evapotranspiration (PET).

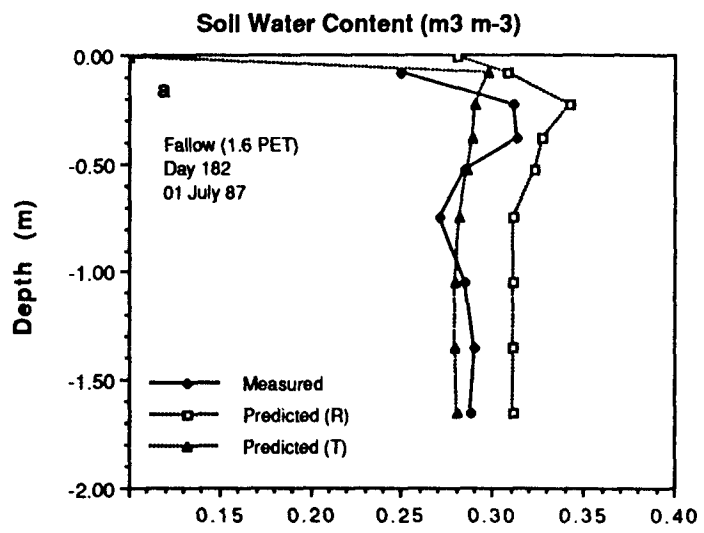
Soil Water Content (m3 m-3)
a
Fallow (1.6 PET)
Day 182
01 July 87
Measured
Predicted (R)
Predicted (T)
Depth (m)
0.00
-0.50
-1.00
-1.50
-2.00
0.15
0.20
0.25
0.30
0.35
0.40

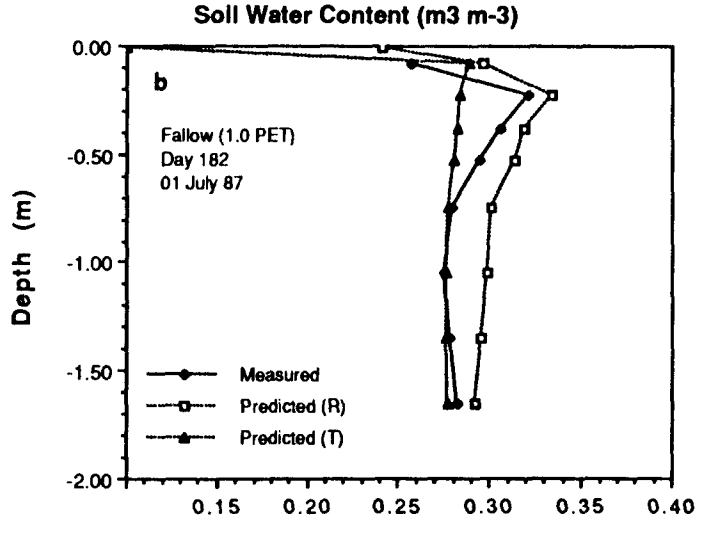
Soil Water Content (m3 m-3)
b
Fallow (1.0 PET)
Day 182
01 July 87
Measured
Predicted (R)
Predicted (T)
Depth (m)
0.00
-0.50
-1.00
-1.50
-2.00
0.15
0.20
0.25
0.30
0.35
0.40

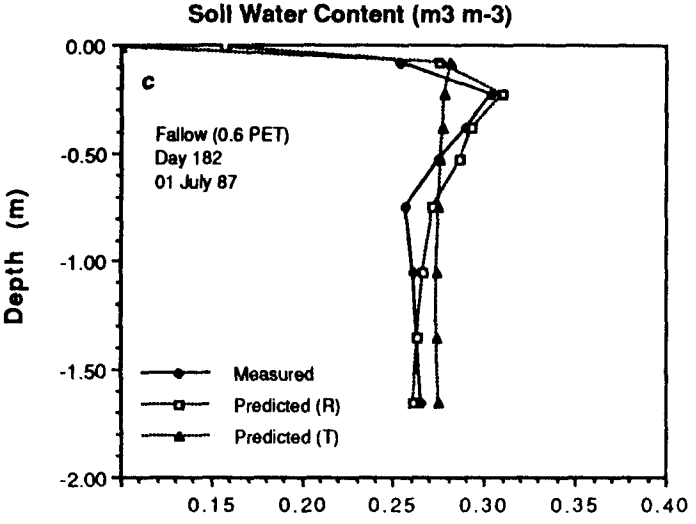
Soil Water Content (m3 m-3)
c
Fallow (0.6 PET)
Day 182
01 July 87
Measured
Predicted (R)
Predicted (T)
Depth (m)
0.00
-0.50
-1.00
-1.50
-2.00
0.15
0.20
0.25
0.30
0.35
0.40

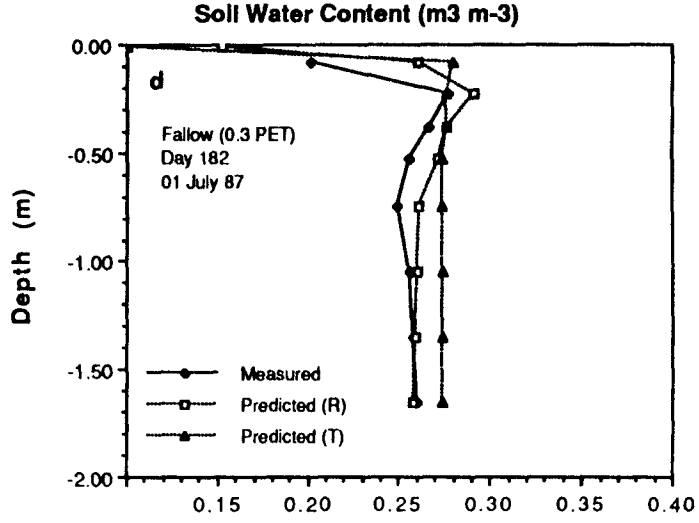
Soil Water Content (m3 m-3)
d
Fallow (0.3 PET)
Day 182
01 July 87
Measured
Predicted (R)
Predicted (T)
Depth (m)
0.00
-0.50
-1.00
-1.50
-2.00
0.15
0.20
0.25
0.30
0.35
0.40

Note that the most shallow depth collected in the field was an integrated value for the 0-15 cm depth, whereas model predictions are for 1 and 8 cm nodes and should be weighted when being compared to measured values. Because of the lack of fit at the wet end of the moisture release curve, when using parameters fit to the whole range of water potentials, the Richards equation overpredicts soil water contents, especially in the excess irrigation treatment (1.6 PET). Predictions for the deficit treatments are much better.

The Tipping Bucket routine is extremely sensitive to the value chosen for field capacity, since it will (under fallow conditions) not decrease water contents below this value. The value used for field capacity was based on the water content at - 33.0 J kg^{-1}, although using - 33 J kg^{-1} is typically thought to underestimate the amount of available water in these soils (Wolf, 1975). The Tipping Bucket routine predicts soil water contents rather well, although soil water content distribution in the soil profile are not as well predicted, but could probably be improved by using different values for LL and DUL for each soil layer.

Evaporation in these simulations was restricted to the upper soil node for the Tipping Bucket routine. The Richards equation, on the other hand, can and does predict a decrease in soil water content as the surface of the soil profile is approached, as in fact was measured in

the field.

Comparisons between predicted and measured soil water potentials are shown in Fig. 3.10 for the fallow plot (S-03) for a period of 60 days (from day 190 to 250). Agreements in absolute values are reasonable, and the effect of the increase in irrigation rate after Day 220 (see Fig. 3.1b) is well reflected in the predictions.

3.2.2.2 Cropped Treatments

For the purpose of predicting the soil water budget, measured leaf area indices over time were used in the model to partition potential evapotranspiration. The same four representative sampling locations were used to generate the simulated data. Simulated and predicted soil water contents for two sampling dates are shown in Fig. 3.11 and 3.12. Day 182 (Fig. 3.11) corresponds approximately to tasseling stage (65 days after emergence). As in the fallow plots, the Richards equation again predicts water contents and their distribution with depth reasonably well, except in the wet treatments, where the misfit of the moisture release curve causes predicted water contents to be to high. The effect of the two sets of soil moisture parameters on the soil water content predictions is shown in Fig. 3.13 for Day 182. In the wet treatment (1.6 PET), the set of parameters fit to the range between -6 and -100 J kg^{-1} predicts measured water contents better than the set derived from the whole range

Figure 3.10 Soil water potentials in the fallow plot under irrigation treatment S-03. Comparison of predictions by the Richards equation and measurements by duplicate tensiometers at a) 0.30 m b) 0.45 m c) 0.75 m d) 1.05 m depth.

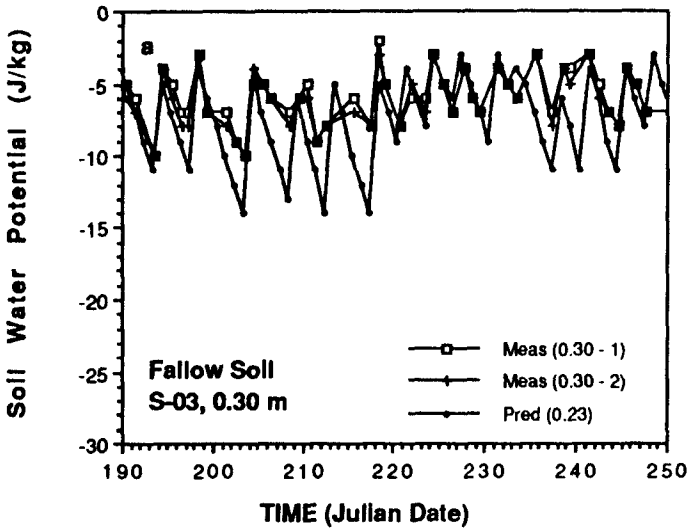
a
Soil Water Potential (J/kg)
0
-5
-10
-15
-20
-25
-30
190
200
210
220
230
240
250
TIME (Julian Date)
Fallow Soil
S-03, 0.30 m
Meas (0.30 - 1)
Meas (0.30 - 2)
Pred (0.23)

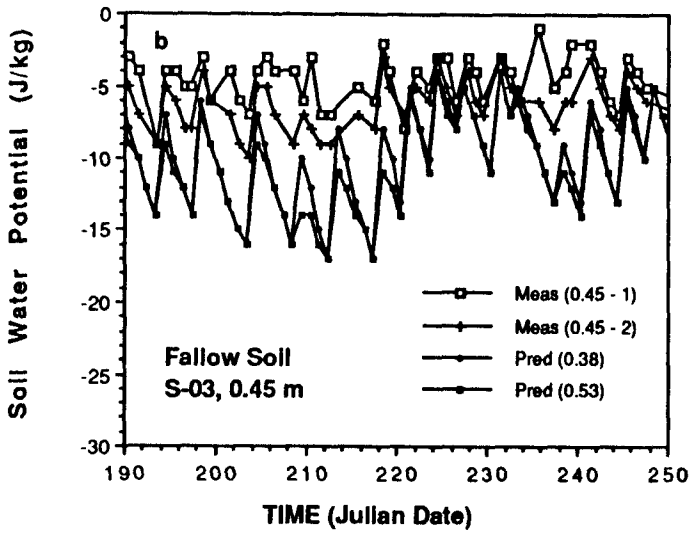
b
Soil Water Potential (J/kg)
0
-5
-10
-15
-20
-25
-30
190
200
210
220
230
240
250
TIME (Julian Date)
Fallow Soil
S-03, 0.45 m
Meas (0.45 - 1)
Meas (0.45 - 2)
Pred (0.38)
Pred (0.53)

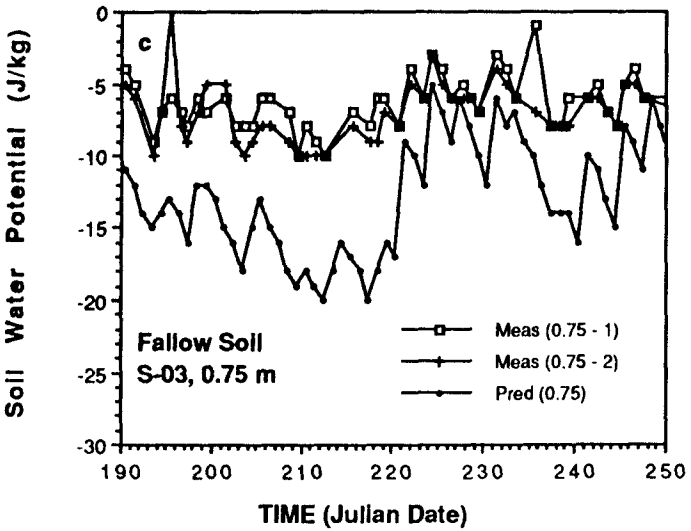
c
Soil Water Potential (J/kg)
0
-5
-10
-15
-20
-25
-30
190
200
210
220
230
240
250
TIME (Julian Date)
Fallow Soil
S-03, 0.75 m
Meas (0.75 - 1)
Meas (0.75 - 2)
Pred (0.75)

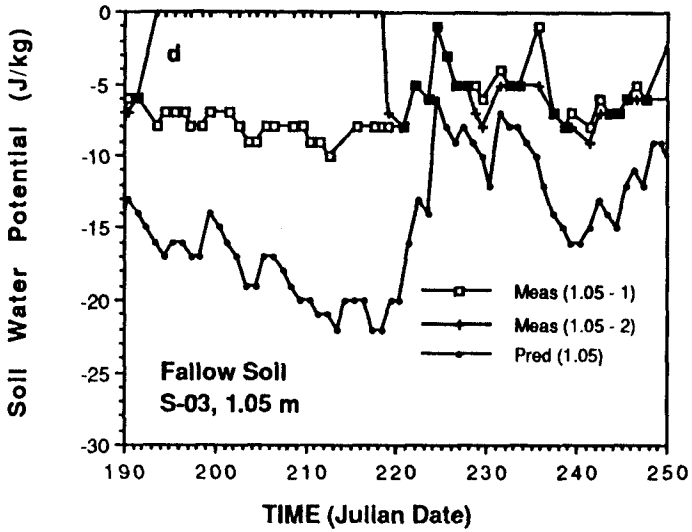
d
Soil Water Potential (J/kg)
0
-5
-10
-15
-20
-25
-30
190
200
210
220
230
240
250
TIME (Julian Date)
Fallow Soil
S-03, 1.05 m
Meas (1.05 - 1)
Meas (1.05 - 2)
Pred (1.05)

Figure 3.11 Comparison of measured soil water contents in the plots planted to corn with predictions by the Richards equation (R) and the Tipping Bucket routine (T) for Day 182 under four irrigation treatments corresponding to a) 1.6 b) 1.0 c) 0.6 and d) 0.3 potential evapotranspiration (PET).

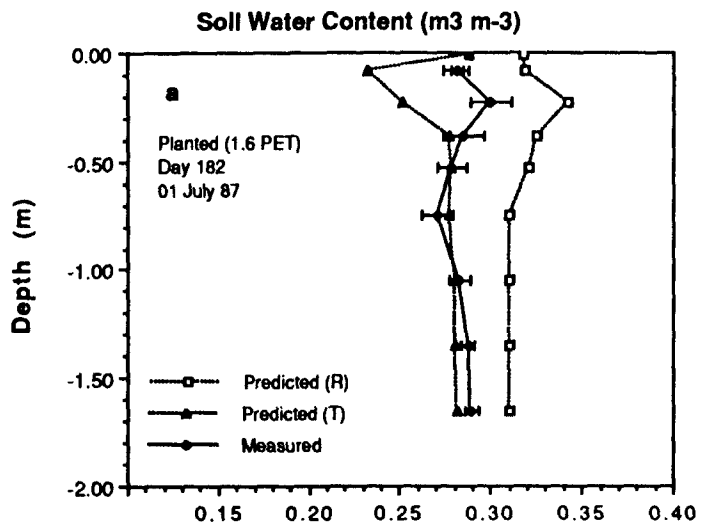
Soil Water Content (m3 m-3)
a
Planted (1.6 PET)
Day 182
01 July 87
Predicted (R)
Predicted (T)
Measured
Depth (m)
0.00
-0.50
-1.00
-1.50
-2.00
0.15
0.20
0.25
0.30
0.35
0.40

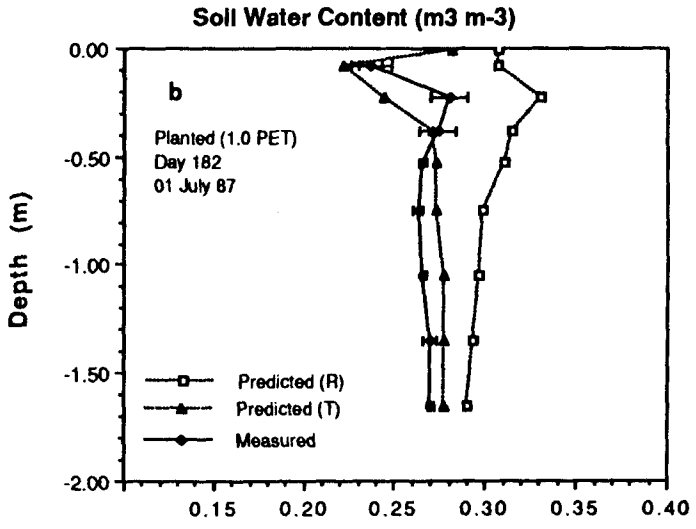
Soil Water Content (m3 m-3)
b
Planted (1.0 PET)
Day 182
01 July 87
Predicted (R)
Predicted (T)
Measured
Depth (m)
0.00
-0.50
-1.00
-1.50
-2.00
0.15
0.20
0.25
0.30
0.35
0.40

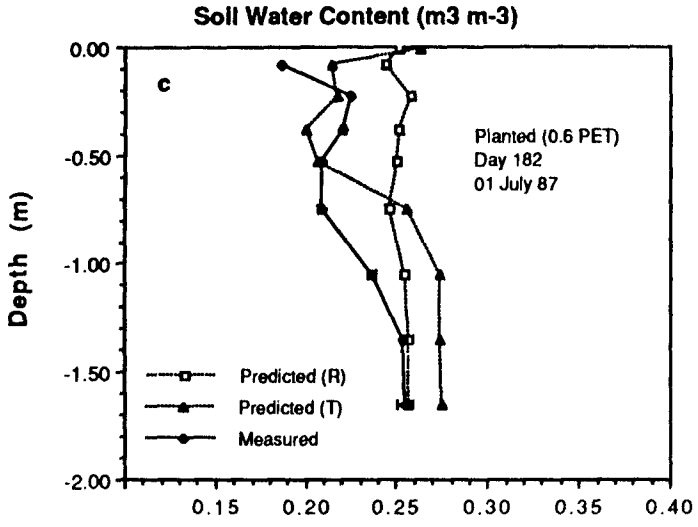
Soil Water Content (m3 m-3)
c
Planted (0.6 PET)
Day 182
01 July 87
Predicted (R)
Predicted (T)
Measured
Depth (m)
0.00
-0.50
-1.00
-1.50
-2.00
0.15
0.20
0.25
0.30
0.35
0.40

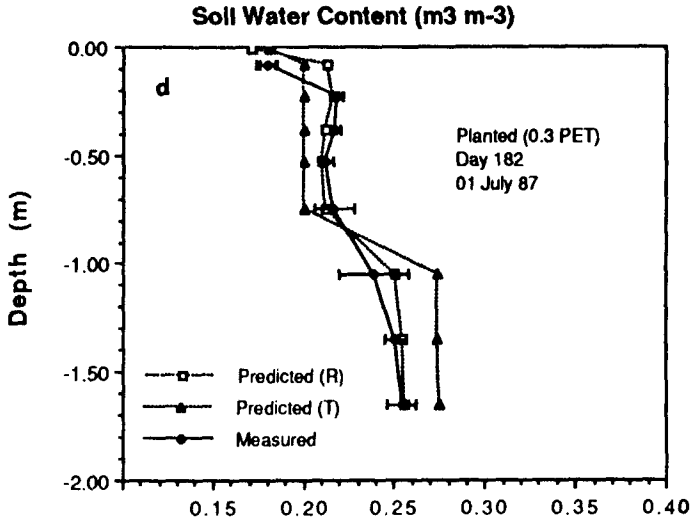
Soil Water Content (m3 m-3)
d
Planted (0.3 PET)
Day 182
01 July 87
Predicted (R)
Predicted (T)
Measured
Depth (m)
0.00
-0.50
-1.00
-1.50
-2.00
0.15
0.20
0.25
0.30
0.35
0.40

Figure 3.12 Comparison of measured soil water contents in the plots planted to corn with predictions by the Richards equation and the Tipping Bucket routine for Day 225 under four irrigation treatments corresponding to a) 1.6 b) 1.0 c) 0.6 and d) 0.3 potential evapotranspiration (PET).

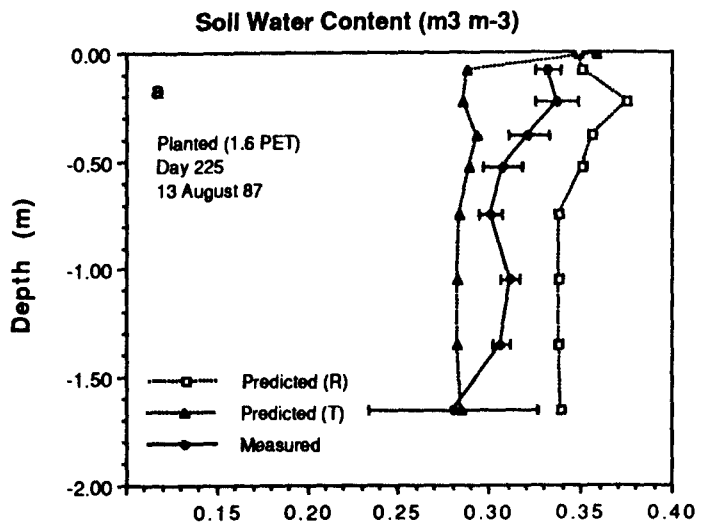
Soil Water Content (m3 m-3)
a
Planted (1.6 PET)
Day 225
13 August 87
Predicted (R)
Predicted (T)
Measured
Depth (m)
0.00
-0.50
-1.00
-1.50
-2.00
0.15
0.20
0.25
0.30
0.35
0.40

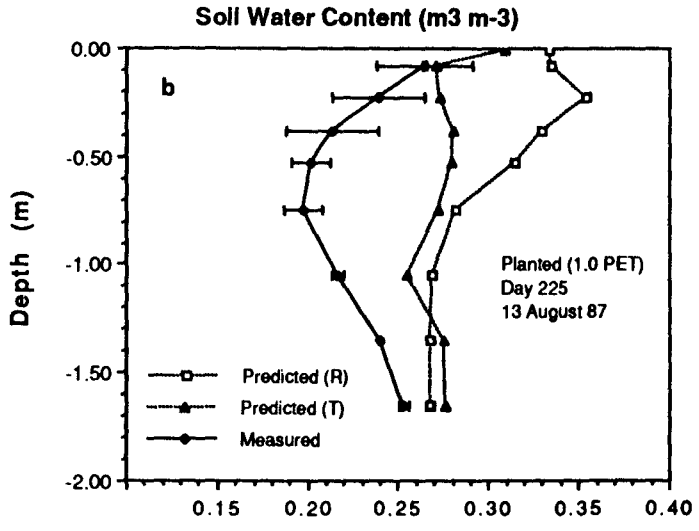
Soil Water Content (m3 m-3)
b
Planted (1.0 PET)
Day 225
13 August 87
Predicted (R)
Predicted (T)
Measured
Depth (m)
0.00
-0.50
-1.00
-1.50
-2.00
0.15
0.20
0.25
0.30
0.35
0.40

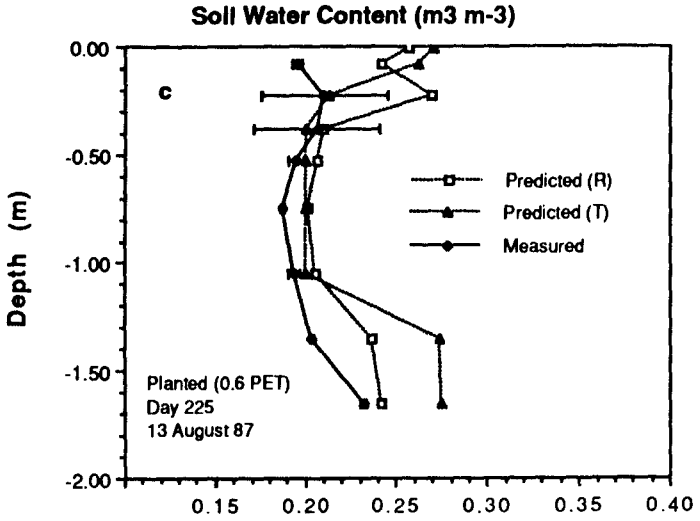
Soil Water Content (m3 m-3)
c
Planted (0.6 PET)
Day 225
13 August 87
Predicted (R)
Predicted (T)
Measured
Depth (m)
0.00
-0.50
-1.00
-1.50
-2.00
0.15
0.20
0.25
0.30
0.35
0.40

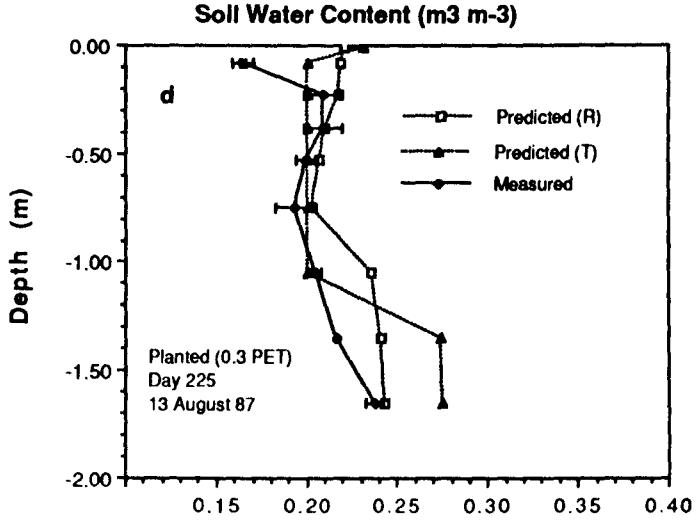
Soil Water Content (m3 m-3)
d
Planted (0.3 PET)
Day 225
13 August 87
Predicted (R)
Predicted (T)
Measured
Depth (m)
0.00
-0.50
-1.00
-1.50
-2.00
0.15
0.20
0.25
0.30
0.35
0.40

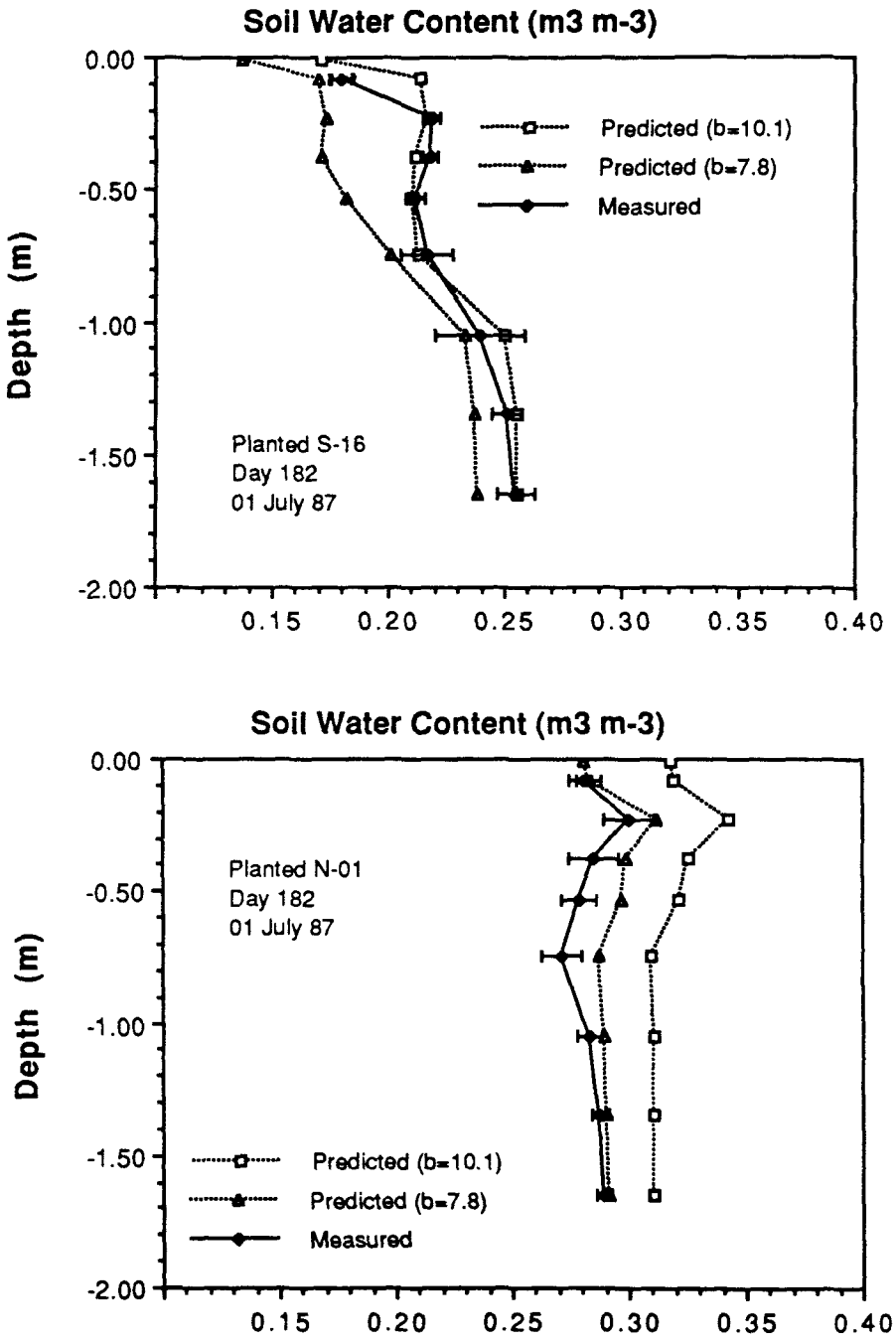

Figure 3.13 Effect of moisture release curve parameters on water content predictions fit to whole water potential range (b=10.1) and fit to wet range only (b=7.8) a) for irrigation treatment 0.3 PET b) 1.6 PET.

down to -1500 J kg^{-1}. The reverse is true for the dry treatment (0.3 PET), where using the wet range parameters leads to a overprediction of plant water uptake and a resulting underprediction of soil water contents. On day 182, predictions by the Richards equation are within 2 - 3 volume percent of the field measured values.

Predictions of soil water potentials coincide reasonably well with the measurements. The drying and rewetting in treatment N-03 (Fig. 3.14) between day 200 and 230 is again reflected in the predictions similar to the fallow case, although measured water potentials drop somewhat faster and to a lower potential than the predictions indicate. In the N-08 treatment (Fig. 3.15), the course of soil water potentials is predicted very well for the 0.75 and 1.05 m depths, but the dry out of the surface soil is not reflected in the predictions. For the driest treatment modelled (N-13) (Fig. 3.16), soil water potentials drop below the tensiometer range about the same time in both the predictions and the measurements. Again, the drying of the surface soil is not modelled well.

The discrepancies in simulated versus measured soil water potentials can be explained by several possible factors. First, predicted soil water potentials are extremely sensitive to the choice of the value for air-entry potential (AE in equation 1). Lowering the air entry potential only slightly will lower predicted soil water potentials. Given the described problems about the

Figure 3.14 Soil water potentials in the cropped plot under irrigation treatment N-03. Comparison of predictions by the Richards equation and measurements by duplicate tensiometers at a) 0.30 m b) 0.45 m c) 0.75 m d) 1.05 m depth.

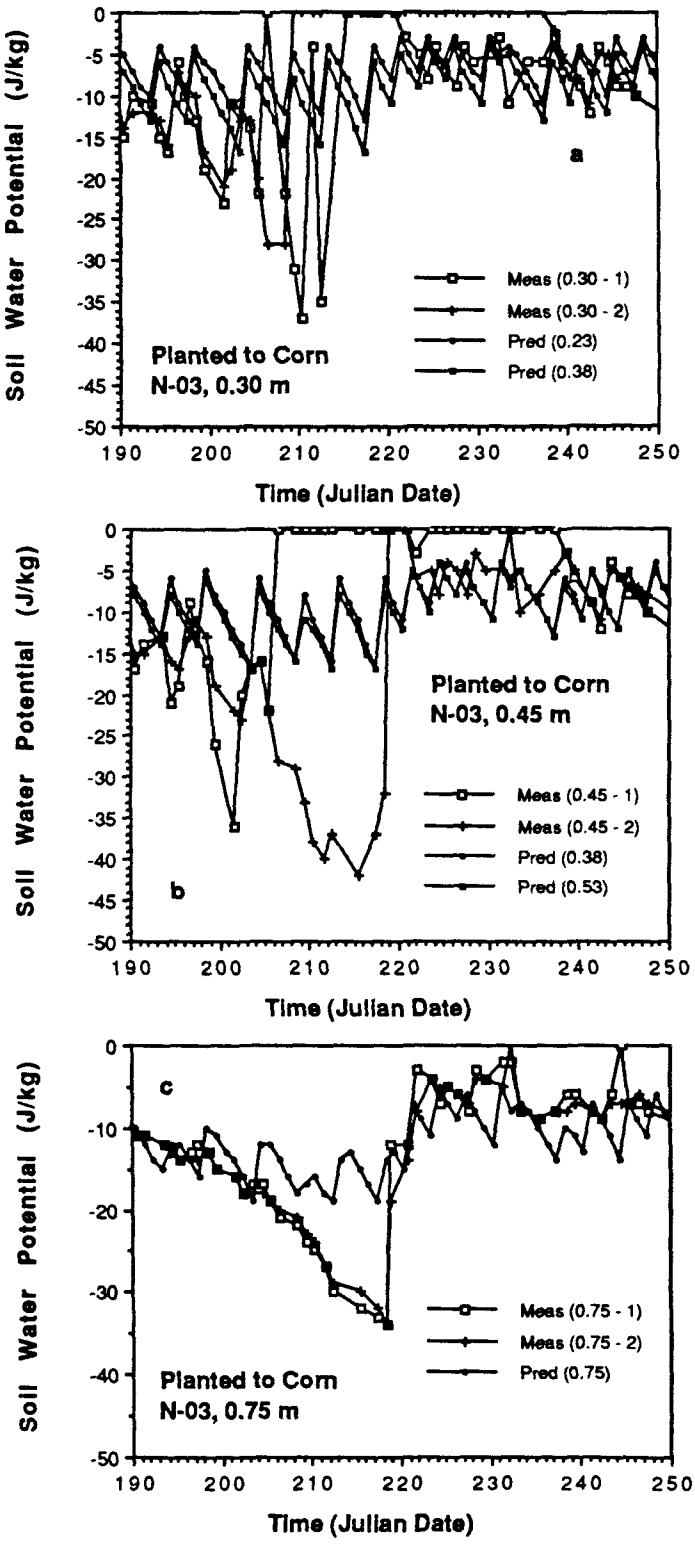
Soil Water Potential (J/kg)
0
-5
-10
-15
-20
-25
-30
-35
-40
-45
-50
190
200
210
220
230
240
250
Time (Julian Date)
a
Planted to Corn
N-03, 0.30 m
Meas (0.30 - 1)
Meas (0.30 - 2)
Pred (0.23)
Pred (0.38)
b
Planted to Corn
N-03, 0.45 m
Meas (0.45 - 1)
Meas (0.45 - 2)
Pred (0.38)
Pred (0.53)
c
Planted to Corn
N-03, 0.75 m
Meas (0.75 - 1)
Meas (0.75 - 2)
Pred (0.75)

Figure 3.15 Soil water potentials in the cropped plot under irrigation treatment N-08. Comparison of predictions by the Richards equation and measurements by duplicate tensiometers at a) 0.30 m b) 0.45 m c) 0.75 m d) 1.05 m depth.

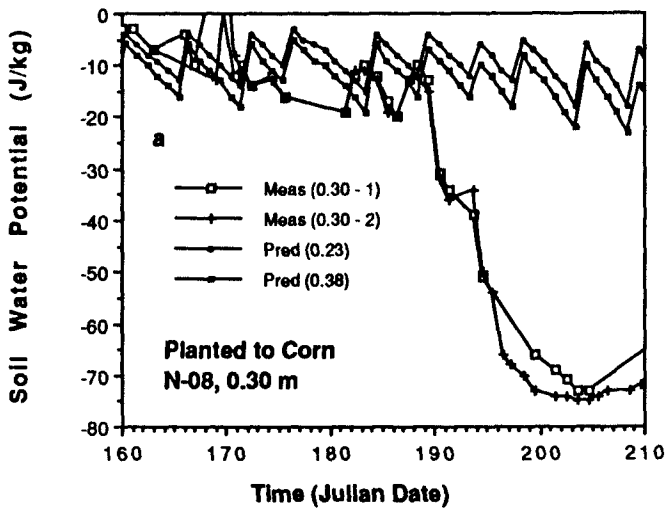
a
Meas (0.30 - 1)
Meas (0.30 - 2)
Pred (0.23)
Pred (0.38)
Planted to Corn
N-08, 0.30 m
Soil Water Potential (J/kg)
Time (Julian Date)

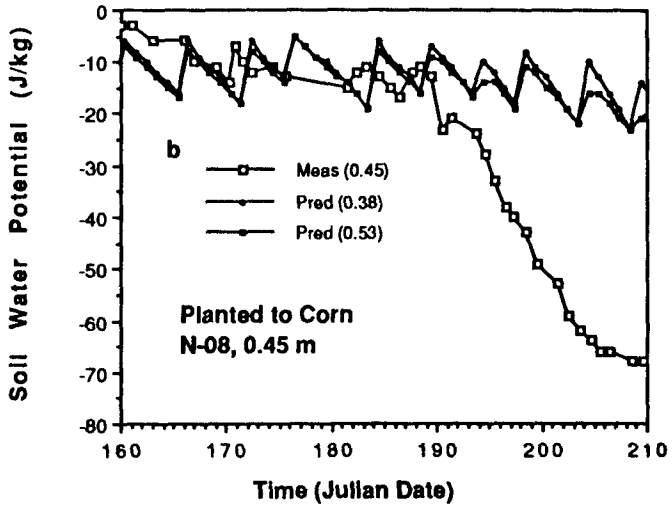
b
Meas (0.45)
Pred (0.38)
Pred (0.53)
Planted to Corn
N-08, 0.45 m
Soil Water Potential (J/kg)
Time (Julian Date)

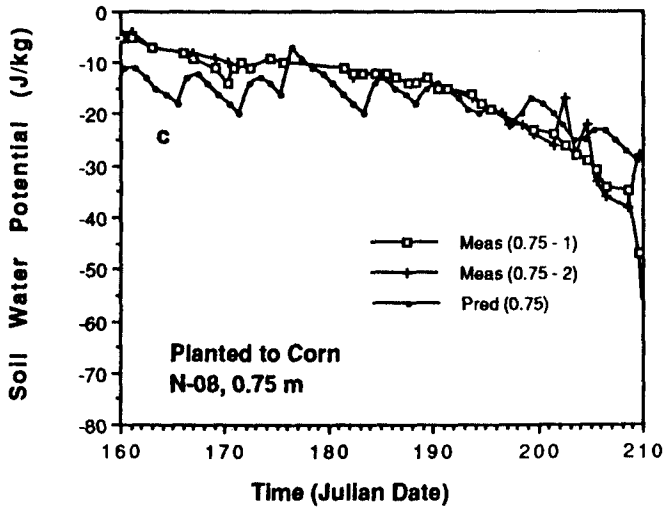
c
Meas (0.75 - 1)
Meas (0.75 - 2)
Pred (0.75)
Planted to Corn
N-08, 0.75 m
Soil Water Potential (J/kg)
Time (Julian Date)

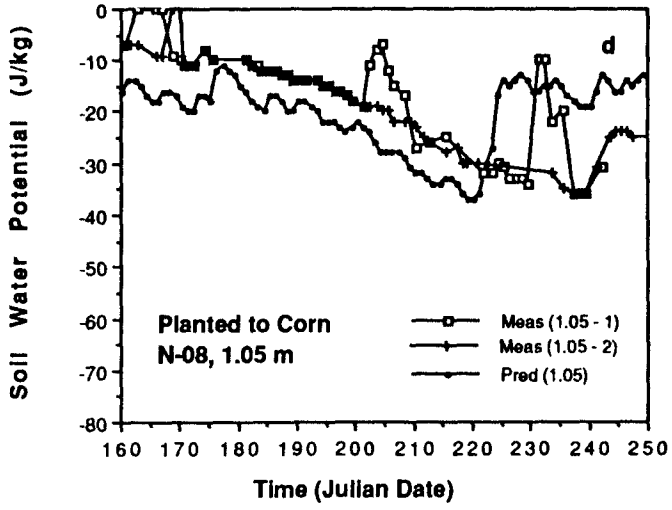
d
Meas (1.05 - 1)
Meas (1.05 - 2)
Pred (1.05)
Planted to Corn
N-08, 1.05 m
Soil Water Potential (J/kg)
Time (Julian Date)

Figure 3.16 Soil water potentials in the cropped plot under irrigation treatment N-03. Comparison of predictions by the Richards equation and measurements by duplicate tensiometers at a) 0.30 m b) 0.45 m c) 0.75 m d) 1.05 m depth.

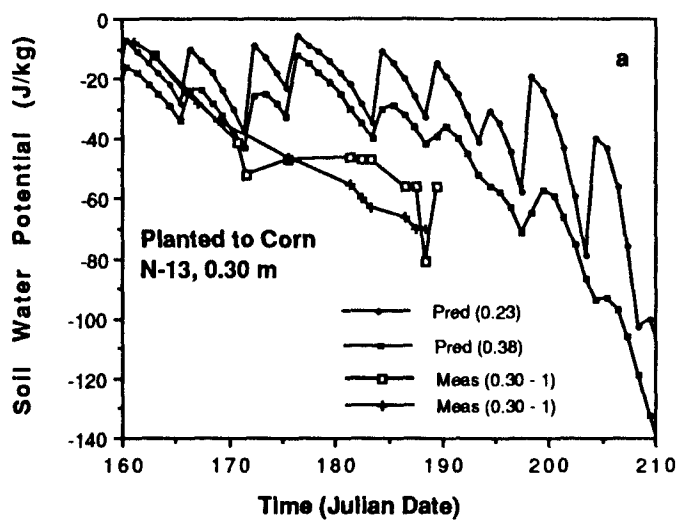
a
Planted to Corn
N-13, 0.30 m
Pred (0.23)
Pred (0.38)
Meas (0.30 - 1)
Meas (0.30 - 1)
Soil Water Potential (J/kg)
Time (Julian Date)

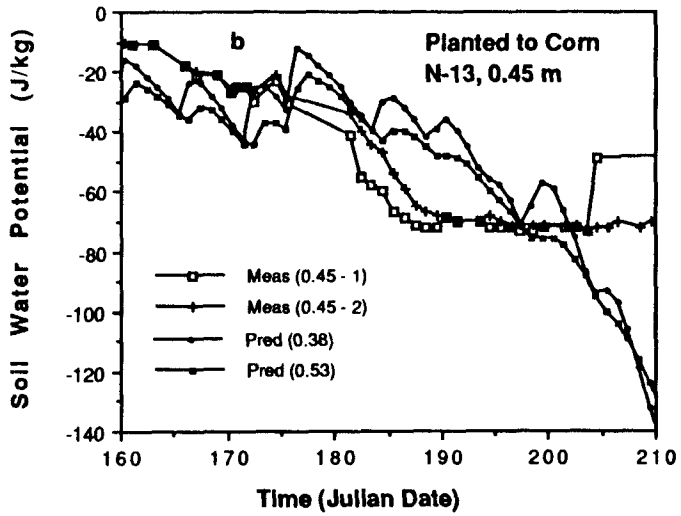
b
Planted to Corn
N-13, 0.45 m
Meas (0.45 - 1)
Meas (0.45 - 2)
Pred (0.38)
Pred (0.53)
Soil Water Potential (J/kg)
Time (Julian Date)

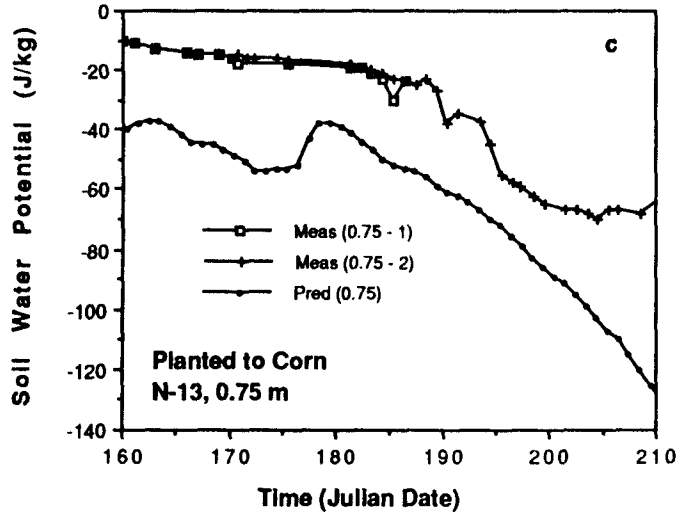
c
Meas (0.75 - 1)
Meas (0.75 - 2)
Pred (0.75)
Planted to Corn
N-13, 0.75 m
Soil Water Potential (J/kg)
Time (Julian Date)

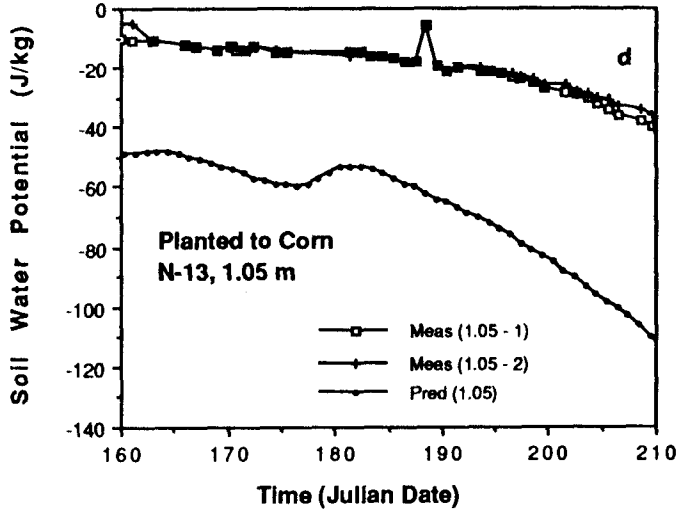
d
Planted to Corn
N-13, 1.05 m
Meas (1.05 - 1)
Meas (1.05 - 2)
Pred (1.05)
Soil Water Potential (J/kg)
Time (Julian Date)

goodness of fit of the moisture release curve, predictions compare well with the measurements. Second, assumptions about rooting depth and densities will effect predicted soil water potentials significantly. The fact, that predictions do not coincide with the observed drying of the soil surface could be the result of an underprediction of roots in the surface soil compared to deeper layers. This is supported by the faster predicted decrease in soil water potentials at the 0.75 and 1.05 m depth, compared to the measurements (Fig. 3.16). The lower than predicted soil water contents in the soil surface could also be due to an underprediction of available energy partitioned to the soil surface for soil evaporation. The radiation partitioning model used only partitions incoming solar radiation. There is recent evidence that additional energy can be available at the soil surface as a result of heat convection within the canopy.

3.3.3 Water Budget Components

3.3.3.1 Fallow Soil

The predicted fluxes of applied water (soil evaporation and drainage) is shown in Fig. 3.17 for the fallow soil. Predictions of actual soil evaporation by the Richards equation were consistently higher across all irrigation treatments than the ones obtain from the Tipping Bucket routine, probably due to the restriction of

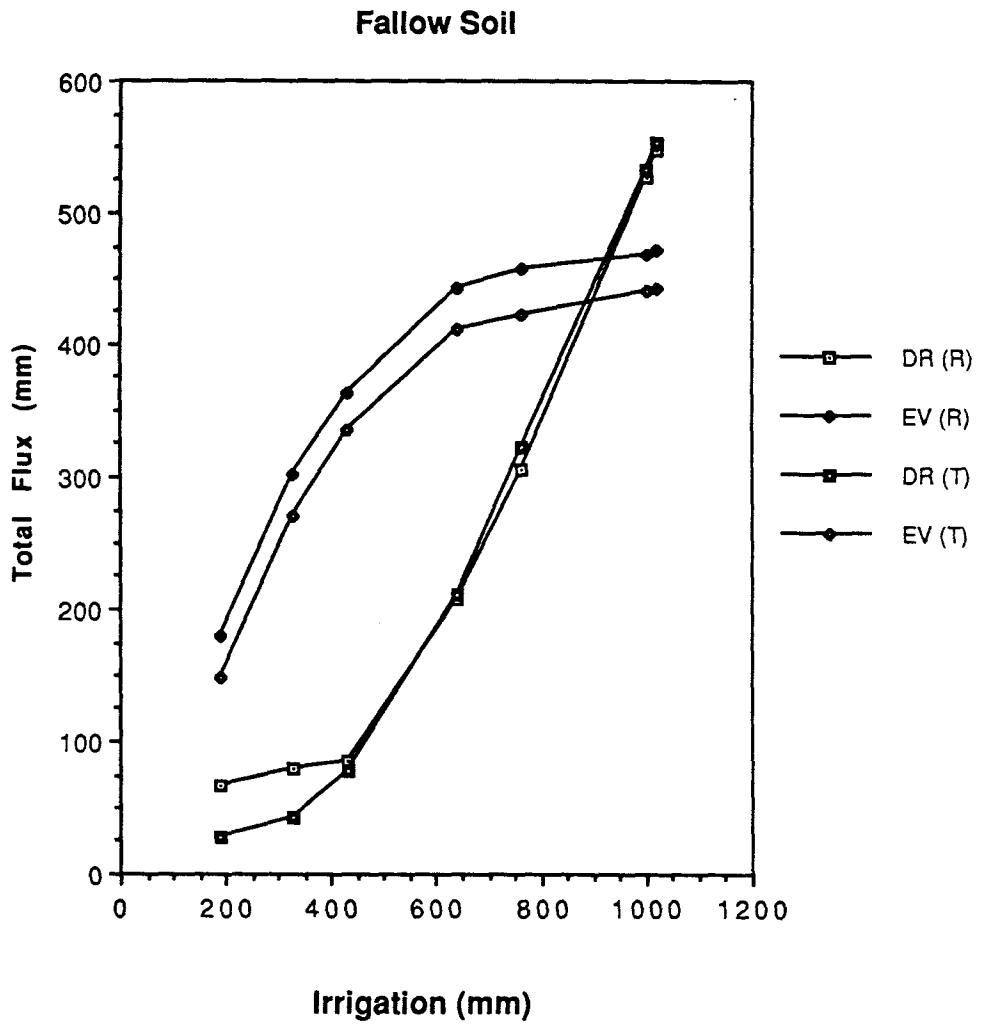

Figure 3.17 Predicted total amounts of drainage below 1.20 m and predicted soil evaporation for fallow soil conditions over a range of irrigation water applications. a) predicted by the Richards equation (R) b) predicted by the Tipping Bucket routine (T).

evaporation to the uppermost layer in the Tipping Bucket routine. Prediction by the Richards equation of soil evaporation is very sensitive to the values chosen for the soil hydraulic parameters affecting unsaturated hydraulic conductivity.

Fig. 3.18 shows comparisons between predicted water flux densities below a depth of 1.20 m, which was the maximum crop rooting depth measured in the field. Because the Tipping Bucket routine redistributes water in the soil profile in discrete increments, predicted soil water fluxes across the 1.20 m depth are not continuous, as are fluxes predicted by the Richards equation. In the Tipping Bucket routine, water movement only occurs when there is water input at the top node, a result of the assumption about field-capacity in conjunction with the normally used daily time step.

Total amounts of predicted drainage are higher using the Tipping Bucket routine, due mainly to the difference in predicted soil evaporation. Predicted soil evaporation was much higher using the Richards equation. Actual soil evaporation is restricted to the uppermost soil layer in the Tipping Bucket procedure with no upward flow of water from lower depths being allowed. This will tend to underpredict soil evaporation under wet conditions in comparison to predictions made using the Richards equation, as is evident from Fig. 3.19. Under dry conditions differences in predicted values between the two

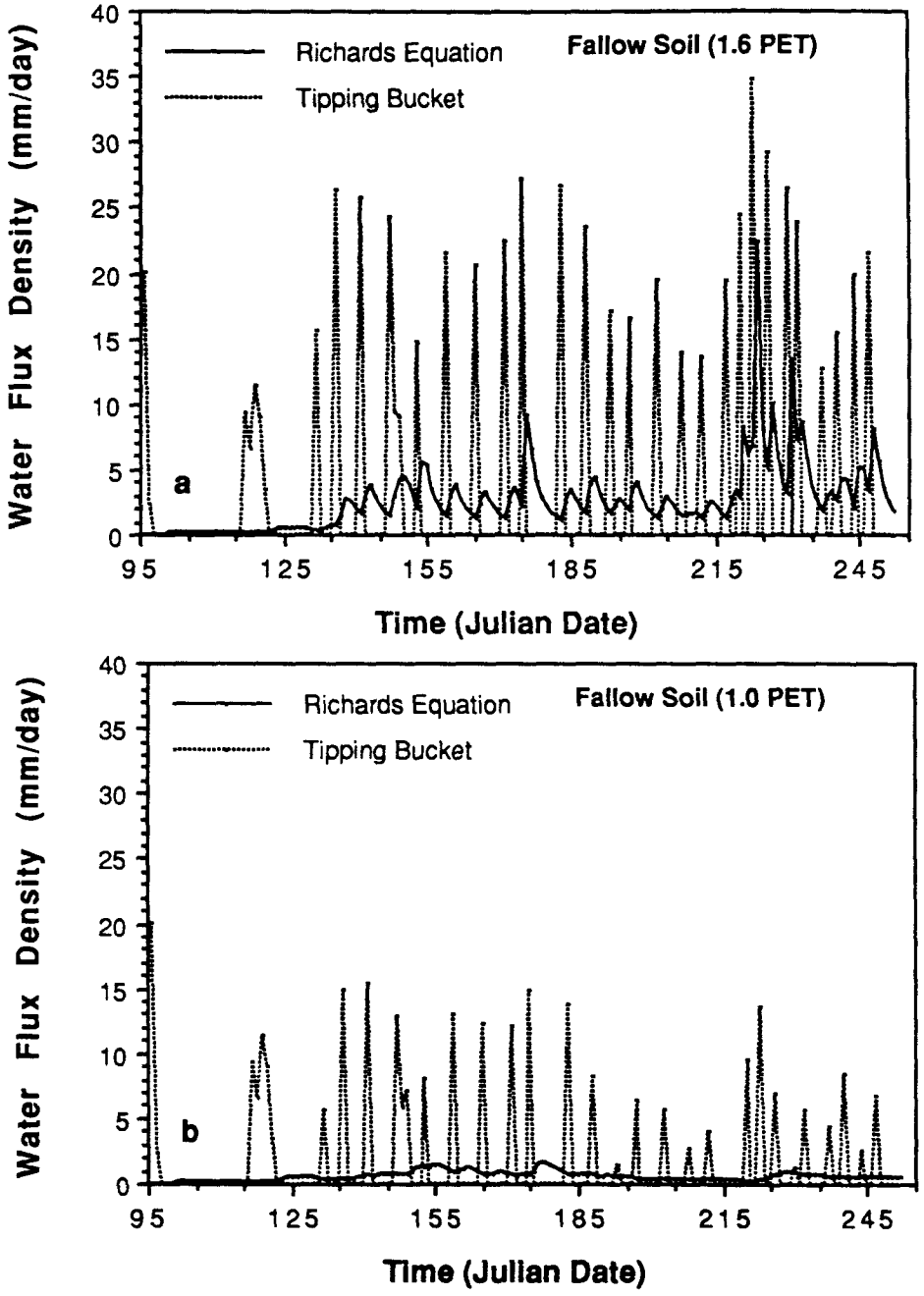

Figure 3.18 Water fluxes below 1.20 m for fallow soil conditions prdicted by the Richards equation (R) and the Tipping Bucket routine (T). a) irrigation treatment 1.6 PET b) irrigation treatment 1.0 PET.

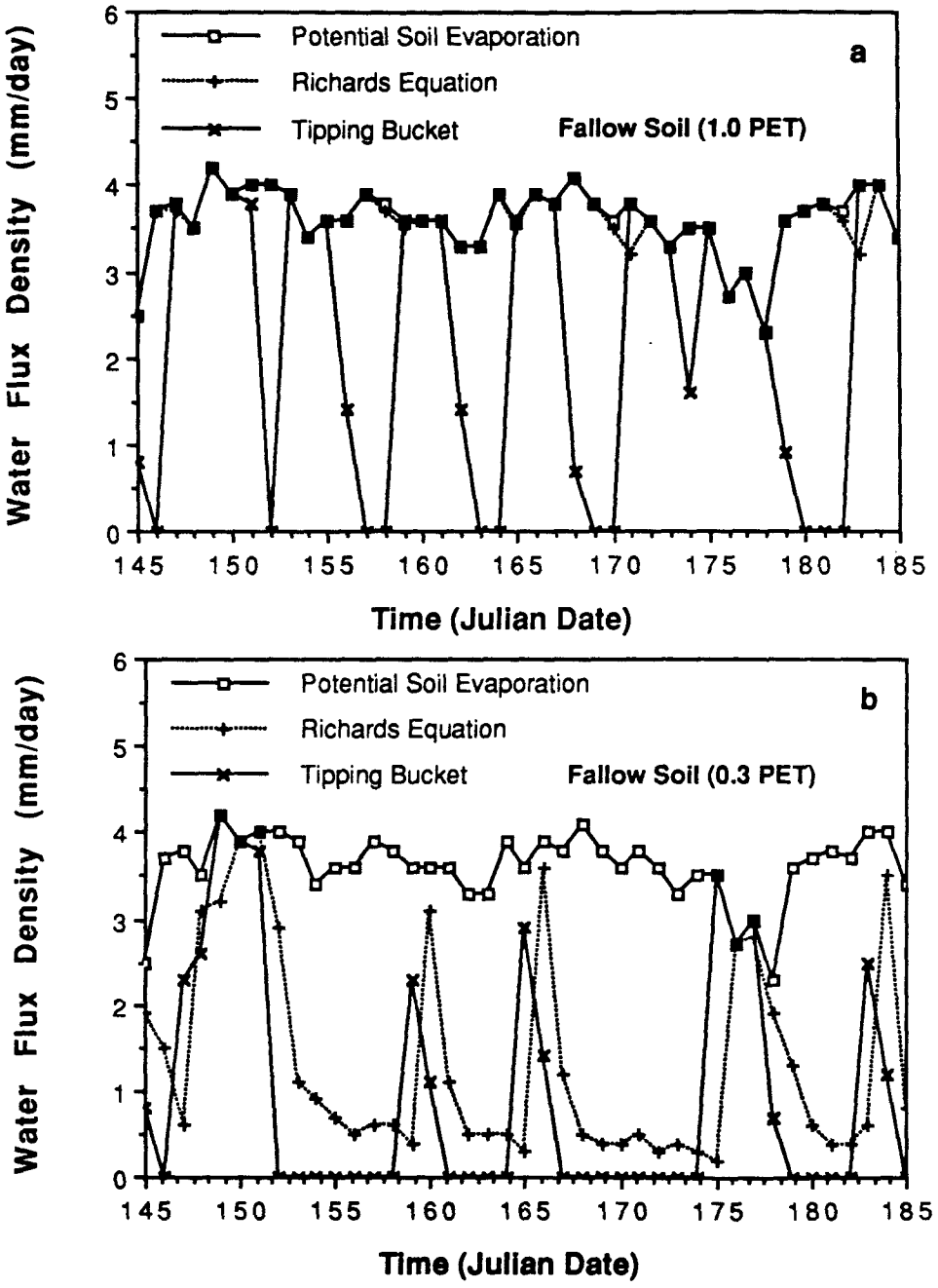

Figure 3.19 Soil evaporation predicted by the Richards equation (R) and the Tipping Bucket routine (T) for fallow soil conditions. a) for irrigation treatments 1.0 PET b) 0.3 PET.

methods become smaller, due to the decrease in unsaturated hydraulic conductivity upon drying and the concomitant reduction of flow to the evaporating surface predicted by the Richards equation. The predictions of actual soil evaporation by the Richards equation are sensitive to changes in air entry potential. A more negative air entry potential will increase unsaturated hydraulic conductivity at a given water potential, thus maintaining first-stage soil evaporation for a longer time.

The predicted total amount of water present in the upper 1.80 m of the soil profile is shown in Fig. 3.20 for the four irrigation treatments in comparison with the measured data. Good agreement is obtained between the Richards equation and measured data for all but the excess water (1.6 PET) treatment. A difference of 20 mm of total water in the soil profile (1.80 m) corresponds to only 0.01 m^3 m^{-3} difference in average water content throughout the profile. The predictions of total profile water by the Tipping Bucket routine oscillate around the value corresponding to field capacity, without reflecting well changes in storage or continued drying as reflected in the predictions by the Richards equation.

3.2.3.2 Cropped Treatments

Total amounts of predicted actual transpiration over the whole range of irrigation water treatments are very similar as predicted by the potential-driven water uptake

Figure 3.20 Total amounts of water contained in the 1.80 m fallow soil profile as measured and as predicted by the Richards equation and the Tipping Bucket procedure. For irrigation treatments a) 1.6 PET b) 1.0 PET c) 0.6 PET and d) 0.3 PET.

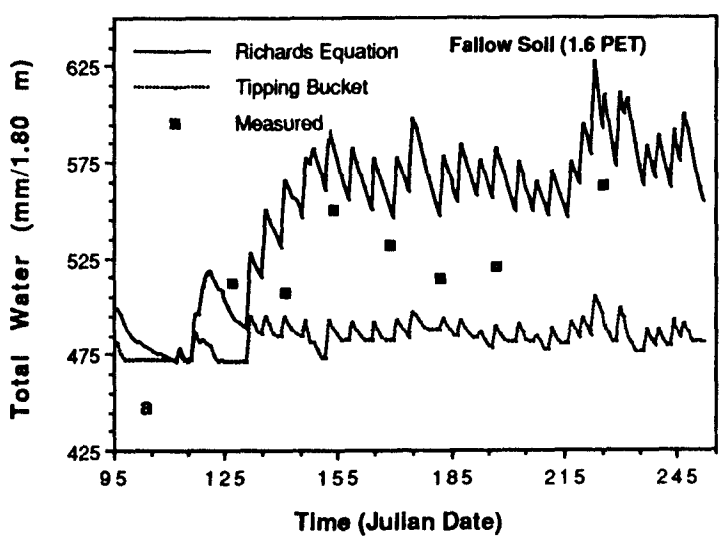
Richards Equation
Tipping Bucket
Measured
Fallow Soil (1.6 PET)
a
Total Water (mm/1.80 m)
625
575
525
475
425
95
125
155
185
215
245
Time (Julian Date)

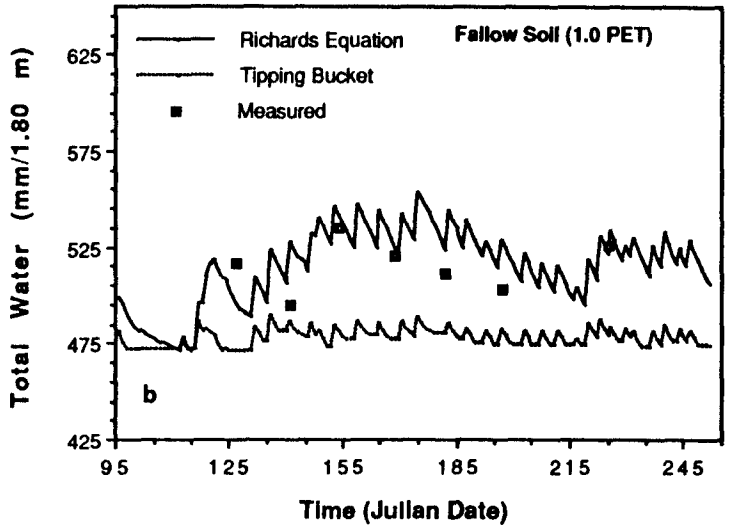
Richards Equation
Tipping Bucket
Measured
Fallow Soil (1.0 PET)
b
Total Water (mm/1.80 m)
625
575
525
475
425
95
125
155
185
215
245
Time (Julian Date)

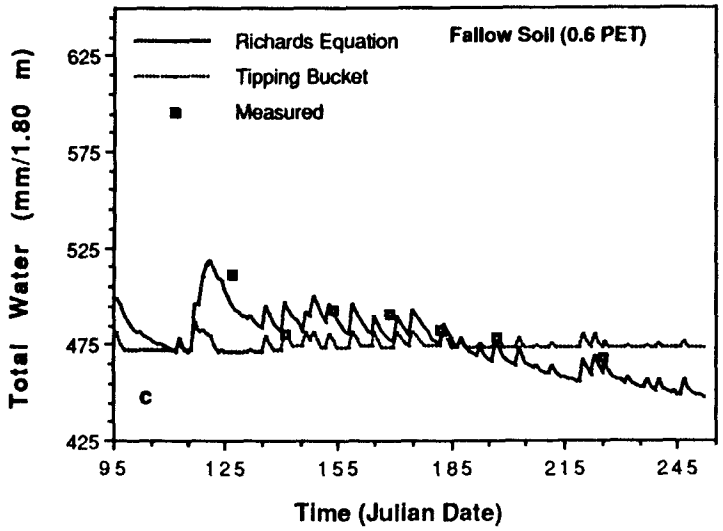
Richards Equation
Tipping Bucket
Measured
Fallow Soil (0.6 PET)
c
Total Water (mm/1.80 m)
625
575
525
475
425
95
125
155
185
215
245
Time (Julian Date)

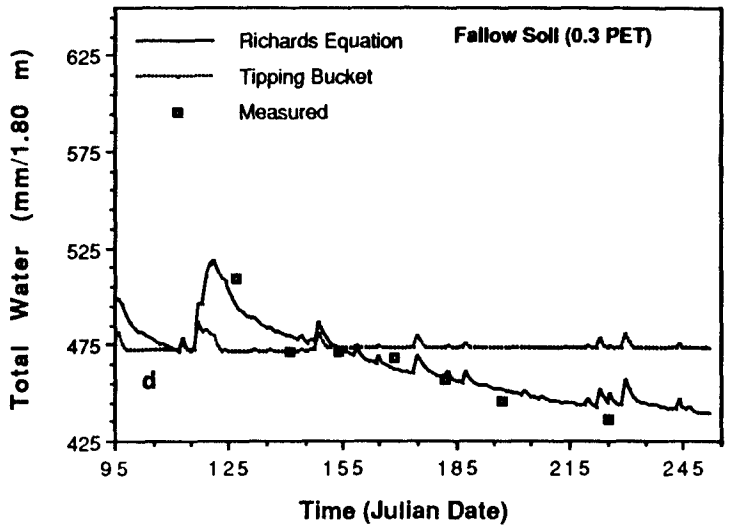
Richards Equation
Tipping Bucket
Measured
Fallow Soil (0.3 PET)
d
Total Water (mm/1.80 m)
625
575
525
475
425
95
125
155
185
215
245
Time (Julian Date)

procedure (in conjunction with the Richards equation) and the Tipping Bucket procedure (Fig. 3.21). The Richards equation predicts higher amounts of soil evaporation, most likely for the reasons discussed above. The differences in predicted drainage and soil evaporation are almost constant across the range of irrigation water amounts, which would suggest that both representations predict about the same relative change in fluxes. Fig. 3.22 shows the predictions (Richards equation) of the partitioning of potential ET between soil evaporation and transpiration and the degree to which this demand can be met under the well-watered (1.0 PET) and a deficit treatments (0.3 PET). Irrigation started on Day 132, after which actual rates of both transpiration and evaporation proceed at potential rates for the well-watered treatment. The much lower LAI developed under irrigation treatment 0.3 PET is an indication of the plant's ability to avoid severe water stress through an early reduction in leaf area. However, starting 45 days after emergence, water stress in terms of transpiration deficit is indicated.

Under cropped conditions, predictions of actual transpiration increase with increasing amounts of water applied up to an amount equivalent to potential transpiration, but predictions by either method are very similar over a range of irrigation water treatments. Predictions of drainage below 1.20 m are very similar to the predictions for the fallow soil.

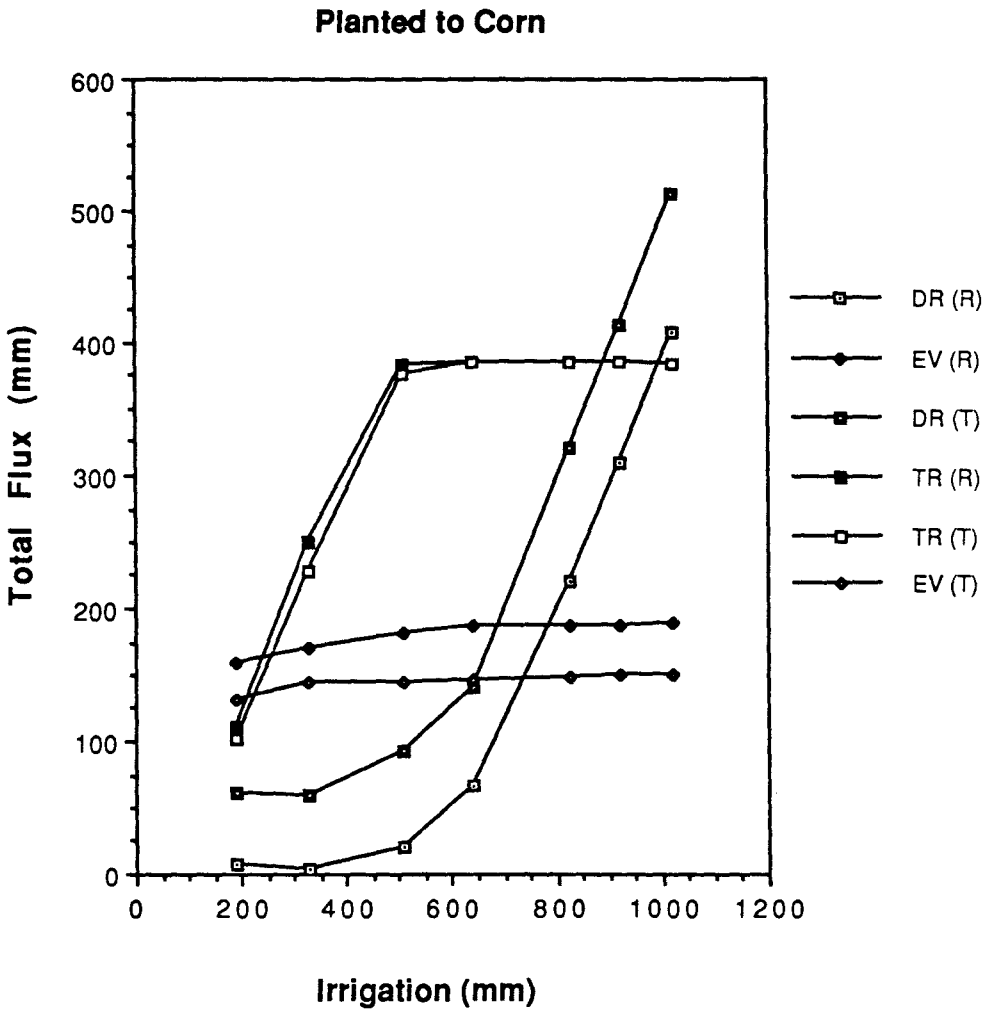

Figure 3.21 Predicted total amounts of drainage below 1.20 m (DR), predicted actual transpiration (TR) and predicted soil evaporation (EV) for cropped soil conditions over a range of irrigation water applications. a) predicted by the Richards equation (R) b) predicted by the Tipping Bucket routine (T).

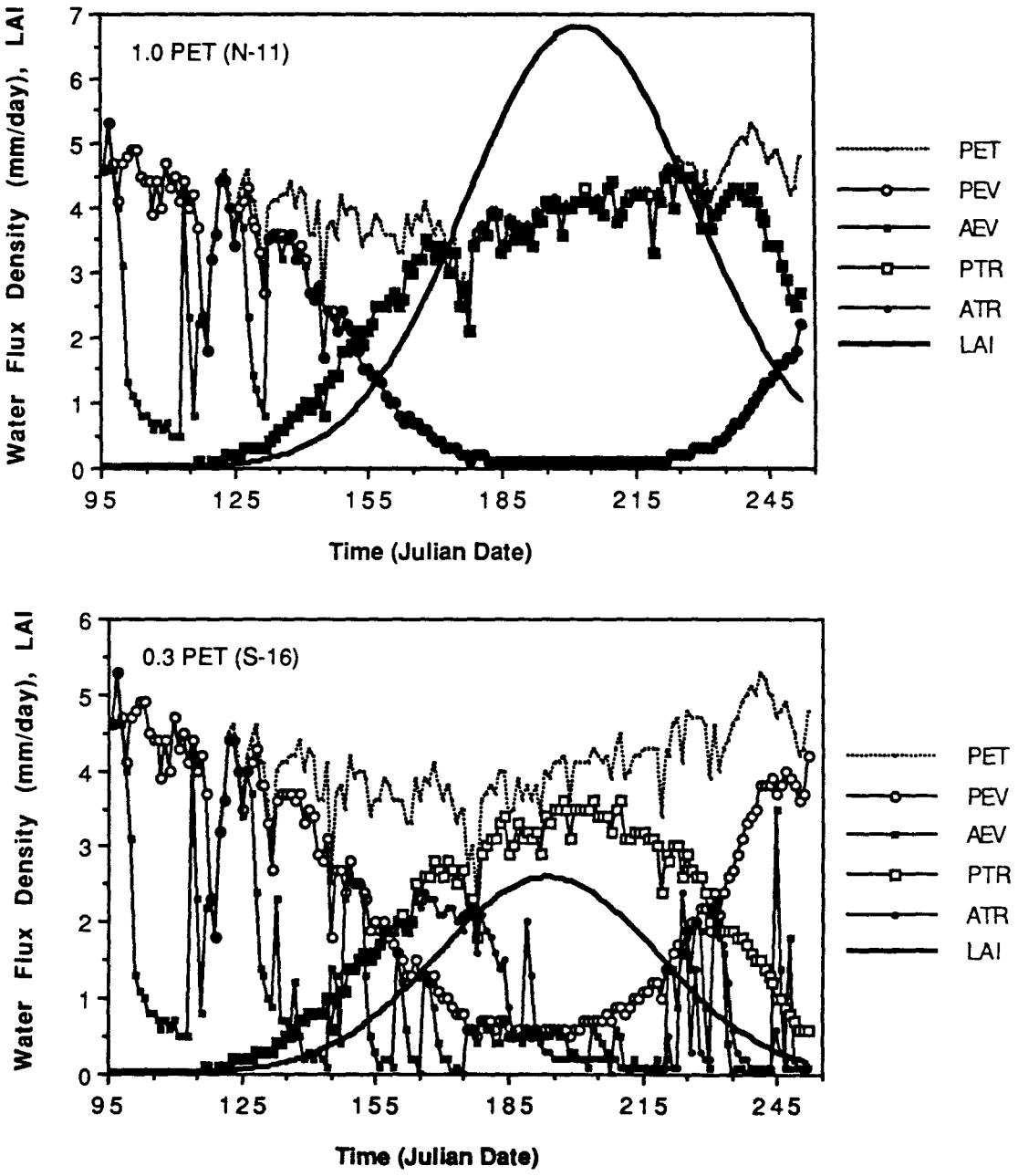

Figure 3.22 Partitioning of potential evapotranspiration as predicted by the Richards equation. a) under irrigation treatment 1.0 PET b) under irrigation treatment 0.3 PET.

Predictions of the total amount of water in the profile using either method are in good agreement with the measurements for the excess irrigation treatment (1.6 PET) (Fig. 3.23). For the well-watered treatment (1.0 PET) predictions by the Richards equation deviate after Day 180, after which water uptake is under-predicted. This is also obvious from Fig. 3.11 and 3.12, where predicted soil water contents are compared to the measured ones. In the deficit (0.3 PET) treatments, water uptake as predicted by both the Richards equation and the Tipping Bucket routine is similar and fits observations well. The under-prediction of water uptake by the Richards equation in the well-watered treatment could be the result of advection, which has been identified as an important factor in the energy budget under Cerrado conditions (Luchiari, 1988). This is supported by the comparison of Priestley-Taylor predicted ET rates with 'Class A' pan measurements. The drastic increase in evaporative demand after day 180 reflected in the pan data is not represented by Priestley-Taylor predictions. A higher value for the Priestley-Taylor coefficient would have to be used under these circumstances (Luchiari, 1988).

Interception of precipitation or irrigation water could have an effect on the water budget of the soil-plant system. A value of 2.5 mm was reported as the maximum interception capacity of a corn canopy (Sudar et al,. 1981) and used in the simulations. Including canopy

Figure 3.23 Total amounts of water contained in the 1.80 m soil profile planted to corn as measured and as predicted by the Richards equation and the Tipping Bucket procedure. For irrigation treatments a) 1.6 PET b) 1.0 PET c) 0.6 PET and d) 0.3 PET.

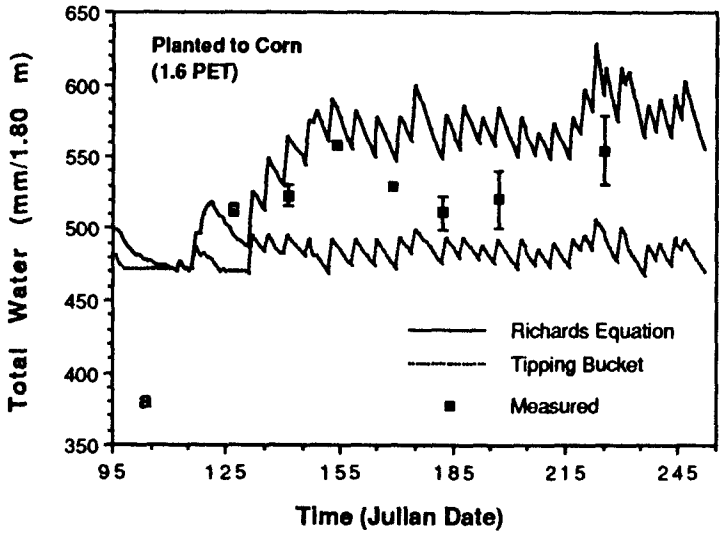
Planted to Corn
(1.6 PET)
Richards Equation
Tipping Bucket
Measured
a
Total Water (mm/1.80 m)
Time (Julian Date)
650
600
550
500
450
400
350
95
125
155
185
215
245

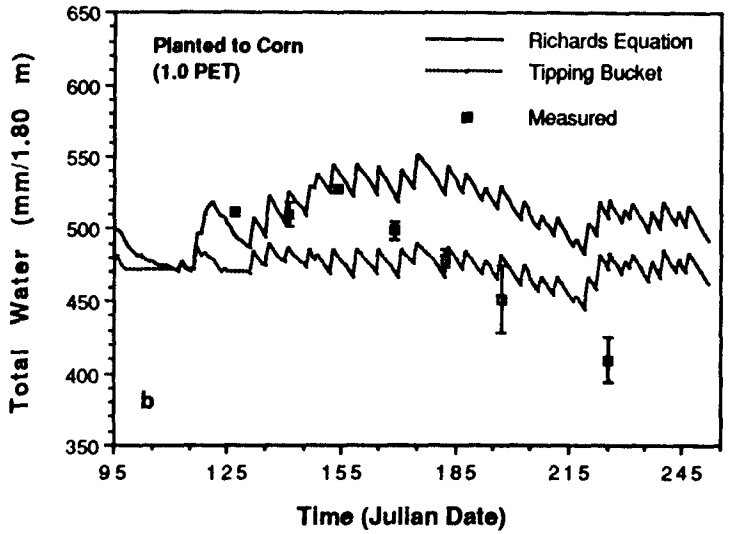
Planted to Corn
(1.0 PET)
Richards Equation
Tipping Bucket
Measured
b
Total Water (mm/1.80 m)
Time (Julian Date)
650
600
550
500
450
400
350
95
125
155
185
215
245

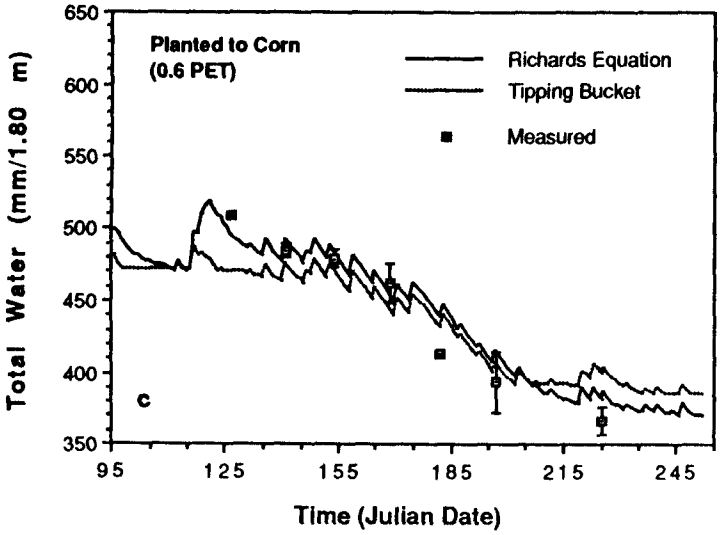
Planted to Corn
(0.6 PET)
Richards Equation
Tipping Bucket
Measured
c
Total Water (mm/1.80 m)
Time (Julian Date)
650
600
550
500
450
400
350
95
125
155
185
215
245

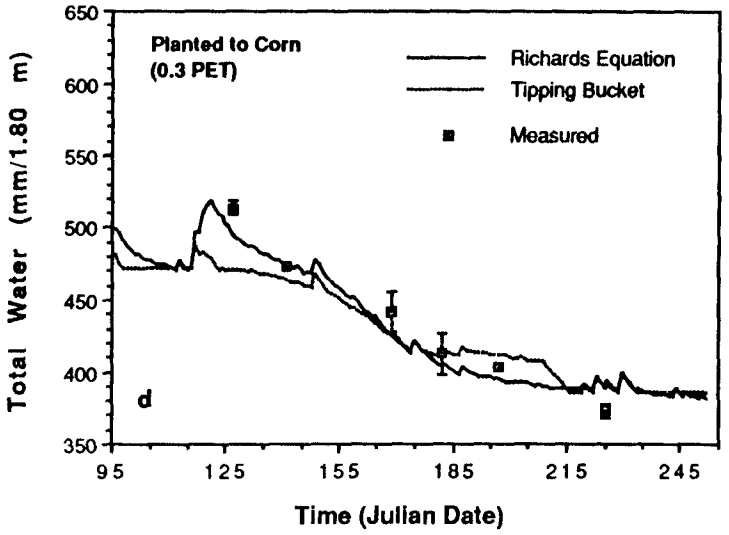
Planted to Corn
(0.3 PET)
Richards Equation
Tipping Bucket
Measured
d
Total Water (mm/1.80 m)
Time (Julian Date)
650
600
550
500
450
400
350
95
125
155
185
215
245

interception as a simulated process led to a reduction of transpiration by the amount intercepted (60 mm) and evaporated off the leaves, but did not affect predicted drainage or soil evaporation significantly. Also, soil water contents were barely affected by the inclusion of interception.

3.4 SUMMARY AND CONCLUSIONS

Comparisons between the Richards equation and capacity-type, water content based representations of soil water flow have been limited (Da Silva and de Jong, 1986). This is partly due to the difficulties encountered when comparing two different simulation models that contain other component processes besides the ones to be compared. GAPS provides an environment in which two alternative representations can be compared without changing the other component processes given that both modules provide the needed output for the other procedures in use. Choosing one of these two water flow models has clear effects on the freedom of choice regarding other component parts, e.g. a potential driven plant water uptake routine can not be linked to the Tipping Bucket routine since the latter does not provide needed estimates of soil water potentials over time and space.

Both the Richards equation and the Tipping Bucket water flow models were found to predict soil profile water contents well, when compared to field measured data. Both

methods have their respective strengths and weaknesses. The Richards equation performed better in predicting soil water contents over the whole range of irrigation water treatments and is better able to predict soil profile water content distributions. Drainage fluxes predicted by the Richards equation are continuous as opposed to the more discrete flux events predicted by the Tipping Bucket method. The soil evaporation component of the Tipping Bucket routine would have to be made more complex, possibly including upward flow, in order to simulate soil evaporation better.

Capacity-type flow representations such as the Tipping Bucket routine are used extensively in crop simulation models due to their perceived conceptual simplicity and computational efficiency. It is also often argued that input parameters for the latter model are more easily available than the parameters necessary to estimate water content-water potential relationship needed for the Richards equation. The Tipping Bucket water flow procedure is sensitive to the value chosen for field capacity water content. This was particularly obvious in the simulations of fallow soil conditions. Given this sensitivity, the choice of the appropriate soil water potential for field capacity becomes crucial.

Clearly, the predictions of water contents and potentials as well as predicted plant water uptake, using the Richards equation and potential driven water uptake,

are highly sensitive to the parameters calculated for the moisture release curve. This sensitivity does not always become apparent, especially if only tested under a narrow set of environmental conditions. The wide range of irrigation water treatments used in this study made the sensitivity of the predictions to moisture release parameters under certain condition apparent.

Several soil properties specific for highly weathered Oxisols have important implications for water flow modeling. The soil moisture release curve of the Oxisol studied in this research resembled a silt loam on the wet end and a clay on the dry end. The power function used to model the moisture release curve (Campbell, 1974, 1985) does not appear to provide a good enough fit to moisture release data for these Oxisols, when fitted over the whole range of water potentials to -1500 J kg^{-1}. If the emphasis of the modeling effort is the prediction of water flow and water contents under well irrigated conditions, it is advisable to use parameters fitted to the wet range (to -100 J kg^{-1}) only. Under irrigated conditions, the soil would not reach water potentials of less than -100 J kg^{-1}. Ideally, a different function better describing he unique behavior of this soil should be used.

Field saturated water contents never reach total porosity in the field, and the percentage of total porosity at field saturated water contents appears to be much lower than the percentages assumed for temperate

soils. A knowledge of the soil water content at saturation in the field is essential in order to predict soil water contents correctly, using the Richards equation. The effect of decreased total porosity due to compaction and reflected in increased bulk densities does not result in an equivalent decrease in saturated water contents under field conditions.

Limited measurements on rooting depths and distributions were available for this study. No differences in rooting depth or density were assumed between the different irrigation treatments. The deviation of predicted from measured soil water potentials in the dry treatments indicates that root water uptake was underpredicted in the soil surface and overpredicted at deeper soil depths. The occurrence of advective conditions in the Cerrado was reported by Luchiari (1988) and further evidence for the frequency of their occurrence was evidenced in this experiment.

REFERENCES

Bouldin, D. R., S. Mughogho, D. J. Lathwell, and T. W. Scott. 1979. Nitrogen fixation by legumes in the tropics. Cornell Int. Agric. Mimeo 75. Cornell University, Ithaca NY.

Buttler, I. W. and S. J. Riha. 1987. General purpose simulation model of water flow in the soil-plant-atmosphere continuum. Appl. Agr. Res. 2:230-234.

Buttler, I. W. and S. J. Riha. 1988. GAPS - A general purpose simulation model of the soil-plant-atmosphere. User's manual (Draft). Cornell University, Ithaca, NY.

Campbell, G. S. 1974. A simple method for determining unsaturated conductivity from moisture retention data. Soil Sci. 117:311-314.

Campbell, G. S. 1985. Soil physics with BASIC: Transport models for soil-plant systems. NY Elsevier.

Da Silva, C. C. and E. de Jong. 1986. Comparison of two computer models for predicting soil water in a tropical monsoon climate. Agr. and Forest Meteorology 36:249-262.

EMBRAPA/CPAC. 1981. (in portuguese) Relatorio Tecnico Anual do Centro de Pesquisa Agropecuaria dos Cerrados 1979-1980. Planaltina-DF, Brazil.

EMBRAPA/CPAC. 1978. (in portuguese) Relatorio Tecnico Anual do Centro de Pesquisa Agropecuaria dos Cerrados 1976-1977. Planaltina-DF, Brazil.

Fisher, M. J., Charles-Edwards, D. A., and M. M. Ludlow. 1981. An analysis of the effects of repeated short term soil water deficits on stomatal conductance to carbon dioxide and leaf photosynthesis by the legume Macroptilium atropurpureum cv. Siratro. Aust. J. Plant Physiol. 8:347-357.

Foth, H. D. 1962. Root and tap growth of corn. Agron J. 54:49-52.

Gardner, W. R. 1960. Dynamic aspects of water availability to plants. Soil Sci. 89:63-73.

Gardner, W. R. and C. F. Ehlig. 1962. Some observations on the movement of water to the plant. Agron.J. 54:453-456.

Garrido, W. C., Silva, E. M., and O. C. Souza. 1979. Water-use efficiency by wheat varieties in the cerrado soil of Brazil. In: Soil physical properties and crop production in the tropics (eds. R. Lal and D.G. Greenland), Wiley, New York.

Gee, G. W. and J. W. Bauder. 1985. Particle-size analysis. In: Methods of soil analysis. Part 1 - Physical and mineralogical methods. A. Klute (ed.). 2nd edition, ASA, MAdison, WI.

Gonzales-Erico, E., Kamprath, E. J., Naderman, G. C., and W. V. Soares. 1979. Effect of depth of lime incorporation on the growth of corn on an Oxisol of central Brazil. Soil Sci. Soc. Am. J. 43:1155-1158.

Goodwin, J. B., Garacorry, F. L., Espinoza, W., Sans, L. M., and L. J. Youngdahl. 1982. Modelling soil-water-plant-relationships in the Cerrado soils of Brazil: The case of maize. Agric. Systems 8:115-127.

Grove, T. L., K. D. Ritchey, and G. C. Naderman, Jr. 1979. Nitrogen fertilization of maize on an Oxisol of the Cerrado of Brazil. Agronomy J. 72:261-265.

Hanks, R. J., J. Keller, V. P. Rasmussen, and G. D. Wilson. 1976. Line source sprinkler for continuous variable irrigation-crop production studies. Soil Sci. Soc. Am. Proc. 40:426-429.

Jones, C. A. and J. R. Kiniry. (eds). 1986. CERES-Maize. A simulation model of maize growth and development. Texas A&M University Press, College Station. 194 pp.

Klute, A. and C. Dirksen. 1985. Hydraulic conductivity and diffusivity: Laboratory methods. In: Methods of soil analysis. Part 1 - Physical and mineralogical methods. A. Klute (ed.). 2nd edition, ASA, Madison, WI.

Lobato, E. and D. K. Ritchey. 1979. Improvement and fertilization of the savanna in Brazil. Tropical agriculture research series 15.

Luchiari, A. 1988. Measurements and predictions of evaporation rates from irrigated wheat in the Cerrados region of central Brazil. Ph.D. thesis, Cornell University, Ithaca, NY.

Macedo, J. and R. B. Bryant. 1987. Morphology, mineralogy, and genesis of a hydrosequence of Oxisols in Brazil. Soil Sci. Soc. Am. J. 51:690-698.

Norman, J. N., and G. S. Campbell. 1983. Application of a plant-environmental model to problems in irrigation. Adv. Irrig. 2:155-188.

Priestley, C. H. B. and B. J. Taylor. 1972. On the assessment of surface heat flux evaporation using large-scale parameters. Mon. Weather Rev. 100:81-92.

Pruntel, J. 1975. Water availability and soil suitability for irrigation water impoundments in the Federal District of Brazil. M.S. thesis. Cornell University. Ithaca, NY.

Riha, S. J. and G. S. Campbell. 1985. Estimating water fluxes in Douglas-fir plantations. Can. J. For. Res. 15:701-707.

Ritchey, K. D. 1979. Potassium fertility in oxisols and ultisols of the humid tropics. Cornell Intern. Agr. Bulletin 37. Cornell University, Ithaca, NY.

Ritchey, K. D. 1982. Calcium deficiency in clayey B-horizons of savanna Oxisols. Soil Sci. 133:378-382.

Ritchie, J. T. 1972. Model for predicting evaporation from a row crop with incomplete cover. Water Resources Res. 8:1204-1213.

Ritchie, J. T., J. R. Kining, C. A. Jones and P. T. Dyke. 1986. Model Inputs. In: CERES-Maize. A Simulation Model of Maize Growth and Development. C. A. Jones and J. R. Kiniry (Eds). Texas A&M University Press, College Station. 194 pp.

SAS Institute Inc., 1985. SAS user's guide: Basics. SAS Institute Inc., Cary, NC.

Stockle, C., and G. S. Campbell. 1985. A simulation model for predicting effect of water stress on yield: an example using corn. Adv. in Irrigation 3:283-323.

Sudar, R. A., K. E. Saxton, and R. G. Spomer. 1981. A predictive model of water stress in corn and soybeans. Transactions of the ASAE 24:97-102

Van Wambeke, A., Hastings, P., and M. Tolomeo. 1986. Newhall Simulation Model. Department of Agronomy, Cornell University, Ithaca, NY.

Wagenet, R. J. and J. L. Hutson. 1986. Predicting the fate of nonvolatile pesticides in the unsaturated zone. J. Environ. Qual. 15:315-322.

Wolf, J. M. 1975. Water constraints to corn production in Central Brazil. Unpublished Ph.D. Thesis, Cornell University.

Chapter IV

PREDICTING CORN GROWTH AND YIELDS UNDER VARIABLE WATER INPUTS

4.1 INTRODUCTION

The specific soil and climatic conditions of the Cerrado region in Brazil make an understanding of plant-water relations a prerequisite for a wide range of agricultural research objectives. Extremely low water holding capacities of the predominant soil orders (Oxisols and Ultisols) in combination with frequently occurring drought periods (veranicos) during the wet season (September to March) can cause water stress and yield reductions in crops (Wolf, 1975; Goodwin, et al. 1982). During the occurrence of a one to two week drought, the survival of the crop is largely determined by the amount of stored water that is accessible to the root system. The highly weathered acid soils restrict rooting depth to the zone where Al-toxicity and Ca-deficiency have been corrected by soil amendments (Ritchey, 1982). Deep incorporation of lime was shown to effectively reduce water stress and avoid concomitant reductions in yield in this region (Bandy, 1976). When water stress equivalent to a typical veranico was imposed on a corn crop, leaf water potentials were shown to drop less and recover earlier in the day in the deep lime treatment compared to treatment receiving no lime amendment. Grain yields in

these experiments were reduced 42% in the no-lime treatment compared to 8% in the limed treatment. Increased rooting depth was suggested as the most likely mechanism to account for the drought avoidance.

Components of a corn growth simulation model previously implemented by Stockle and Campbell (1985) was incorporated into the General Purpose Simulation Model GAPS (Buttler and Riha, 1987) and its applicability to Cerrado conditions tested. A crop growth component model that can respond to climate and soil water status is necessary for predicting crop response over a broad region, as well as a precursor to analysis of other production constraints, such as nitrogen. The objective of this research was to determine the effect of limiting water on corn growth and yield, in order to be able to predict the effects of varying inputs on corn yield and water fluxes under a range of soil fertility and climatic conditions found in the savanna regions of the tropics.

In chapter III, water flow components of the GAPS model were shown to satisfactorily simulate soil water fluxes and budgets under Cerrado conditions under bare soil as well as cropped conditions. For the simulations of cropped conditions, functions fitted to measured experimental data were used to provide leaf area index over time for different irrigation treatments. In this chapter, growth of the crop, including simulation of leaf area index, is predicted through simulation of

photosynthesis and dry matter accumulation. Photosynthesis and dry matter accumulation, in turn, are linked to routines describing water flow through the soil-plant-atmosphere system.

4.2 MATERIALS AND METHODS

The experimental site was located on the EMBRAPA-CPAC (Cerrado Agricultural Research Center) research station in the Federal District of Brazil. The soil is classified as an Oxisol (Typic Haplustox, isohyperthermic, fine, kaolinitic) or a Dark-red Latosol in the Brazilian classification system (Macedo and Bryant, 1987). Corn (Zea mays L., 'Cargill 111 S') was planted on 21 April in 80 cm wide rows at a final population density of 62,500 plants/ha. The crop was grown during the dry season to have optimal control of irrigation water treatments.

A line-source sprinkler irrigation system (Hanks et al., 1976) was used to establish a gradient of irrigation water application across a plot perpendicular to the irrigation line. For a detailed description of the irrigation water treatments see chapter 3.2. Results from four sampling locations (N-01, N-11, N-16, and S-16) are reported here, corresponding to approximately 1.6, 1.0, 0.6, and 0.3 potential evapotranspiration (PET), respectively, when averaged over the whole growing season. For the comparisons of predicted versus measured leaf area development and dry matter accumulation,

measured data from several rows was pooled according to amounts of irrigation water received, where appropriate. 'A4' refers to a pooling of irrigation treatments N-01, S-01, and N-06, and 'A3' to a pooling of N-11 and S-06 (see also Fig. 3.1 b).

Sequential harvests of the above-ground portion of the corn plants were conducted weekly for the first five weeks starting 31 days after emergence and then biweekly for a total of 10 sampling dates. Five plants (one consecutive meter) were sampled per row, corresponding to a specific irrigation treatment. Green and dry leaf area were determined with a leaf area meter. Dry weight of stalks, green leaves, flag leaf, dry leaves, tassel, and spikes was determined separately and are summed as total above-ground dry weight. For the final harvest on 22/23 September, all corn rows not previously used for sequential harvests were used. The six central meters of every row were harvested, and total dry matter and grain yield were determined.

4.3 SIMULATION OF CROP GROWTH

Components of a corn growth simulation model (Stockle and Campbell, 1985) were recoded and translated into PASCAL, in some instances revised, and incorporated into the General Purpose Simulation Model GAPS (Buttler and Riha, 1987). Photosynthesis is calculated on the basis of photosynthetically active radiation (PAR) intercepted

by the canopy using an equation proposed by Norman (1982) to estimate PAR, an equation to estimate the canopy extinction coefficient as given by Campbell (1977) and equations proposed by Hesketh and Baker (1967) for relating photosynthetic rate to intercepted PAR. The estimate of photosynthetic rate incorporates the effects of temperature assuming leaf temperature equal to air temperature.

Growth is directly related to photosynthesis by using an average conversion factor of 0.40 as suggested by Monteith (1981). This conversion factor was not varied as done by Stockle and Campbell (1985). The estimate of photosynthetic rate is used to calculate a no-stress canopy resistance for vapor transport. The concept of critical leaf water potential (Fisher et al, 1981; Turner, 1974) is used to calculate actual transpiration. It is assumed that canopy resistance responds little to a lowering in leaf water potential until a critical value is reached, at which resistance increases rapidly over a relatively narrow range. A critical leaf water potential of -1.4 MPa was used. Leaf water potential is calculated from hourly simulation of root water potential.

Knowing the canopy resistance as a function of leaf water potential, the reduction in potential transpiration can be calculated. The photosynthetic rate previously calculated for the non-stressed condition is reduced proportionally to the decrease in transpiration rate.

Photosynthetic rates are calculated on an hourly time step, summed for one day and converted into dry matter. The daily accumulated dry matter is partitioned into top and root dry matter using data presented by Foth (1962). Rooting depth is empirically related to root dry matter (Acevedo, 1975). No correction for water stress on partitioning as included in Stoeckle and Campbell (1985) was used for these simulations. Table 4.1 lists differences in processes and parameter values between Stockle and Campbell's model and this particular implementation.

A function for accumulated thermal time (FT) was used to separate corn phenological stages into vegetative (FT < 33), pollination (33<= FT <40), and grain filling (40 <= FT < 49) stages (Coelho et al. 1980).

To convert above-ground dry matter into leaf area during the vegetative phase the relationships originally included in Stockle and Campbell's model, and based on independent data sets of Acevedo (1975) were used. During pollination, leaf area is reduced as a function of attained leaf area index and thermal time (Dale et al., 1980) with a correction for water stress as proposed by Stockle and Campbell (1985). The more water stress has been accumulated during the vegetative phase, the more rapid will the decline of leaf area occur. After the end of the pollination phase, leaf area declines as a function of time (Dale et al., 1980).

TABLE 4.1

Differences in processes modeled and parameter values between this simulation and the implementation of Stockle and Campbell (1985).

Process / Parameter	Current Implementation	Stockle and Campbell (1985)
Water Stress Correction on partitioning of dry matter	(not included)	
Root resistances as a function of time	(not included)	
Root Density as function of root dry matter and thermal time	(not included)	
Critical leaf water potential	-1400 J kg^{-1} (1)	-1800 J kg^{-1}
Conversion factor photosynthesis to dry matter	0.40(2)	0.46-0.50 (3) 0.31-0.34 (4)
Exponent of F for reduction of photo-synthetic rate	1.0	0.8 - 1.2

(1) : after Stockle (1983)
(2) : Monteith (1981)
(3) : during early vegetative phase
(4) : during late vegetative phase

4.4 RESULTS AND DISCUSSION

4.4.1 Effect of Amount of Irrigation Water on Dry Matter Accumulation And Leaf Area Development

4.4.1.1 Sequential Harvests

Leaf area for the 1.0 PET (100 % of potential evapotranspiration) and the 0.6 PET (60 % of potential evapotranspiration) irrigation treatments developed similarly until day 180, when they reached a peak leaf area index (LAI) of about 5.0 (Fig. 4.1 a). After day 180, which coincides with time of tasseling, leaf area in treatment 0.6 PET decreased more rapidly than in the well watered (1.0 PET) treatment, indicating the effect of water stress. The 0.3 PET treatment exhibits a pronounced reduction in leaf area development from the beginning. Leaf area peaked around day 180 at a LAI of about 2.5, before starting to decline. Interestingly, a decrease in initial rate of leaf area development and dry matter accumulation was observed in treatment 1.6 PET (Fig.4.1 a). Later in the season, treatment 1.6 PET was able to maintain a higher leaf area for a longer time than treatment 1.0 PET. This resulted in continued dry matter accumulation after day 220, when dry matter accumulation rates in the other treatments had already slowed (Fig. 4.1 b). Treatment 1.6 PET eventually reached the highest dry matter and also the highest grain yield.

The leaf area ratio (LAR), the dry weight of leaves as a fraction of total above-ground dry matter decreased with

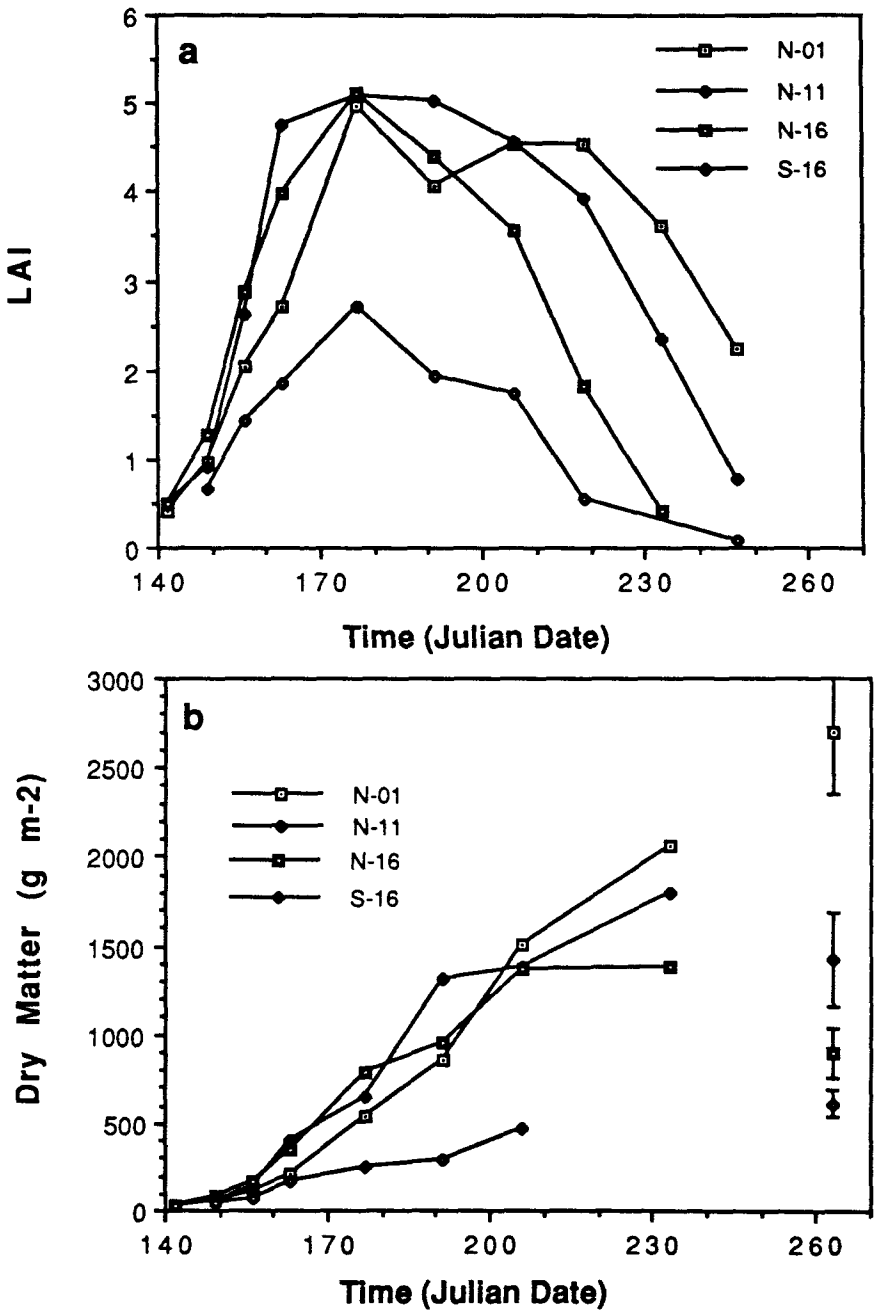

Figure 4.1 Crop growth under different irrigation treatments: N-01 (1.6 PET), N-11 (1.0 PET), N-216 (0.6 PET) and S-16 (0.3 PET). a) Leaf area index b) total above-ground dry matter. Error bars represent ±1 Ú.

time (Fig. 4.2), and was not statistically different between irrigation treatments.

4.4.1.2 Final Harvest

The increase in above-ground dry matter accumulation was nearly linear with the amount of irrigation water applied to an amount equivalent to potential evapotranspiration (641 mm) (Fig. 4.3 a). After that, final dry matter levelled off, although considerable variability in final dry matter is exhibited at high water levels. Final dry matter yields estimated using the regression equation fit to the data in Fig 4.3 a are 26 Mg/ha at 1020 mm of water applied (1.6 PET) compared to 21 Mg/ha at an irrigation corresponding to 1.0 PET.

Increase in grain yields with increased amounts of irrigation water applied were nearly linear over the whole range. Grain yields reached 9.2 Mg/ha at 1020 mm of irrigation water applied compared to 6.0 Mg/ha at an irrigation amount corresponding to PET (Fig. 4.3 b). Grain yield was clearly more severely effected by water deficit than total above-ground dry matter as shown by a rapid decrease in harvest index at irrigation amounts less than PET (Fig. 4.3 c). At irrigation levels above PET the harvest index leveled off around values of 0.33 to 0.34.

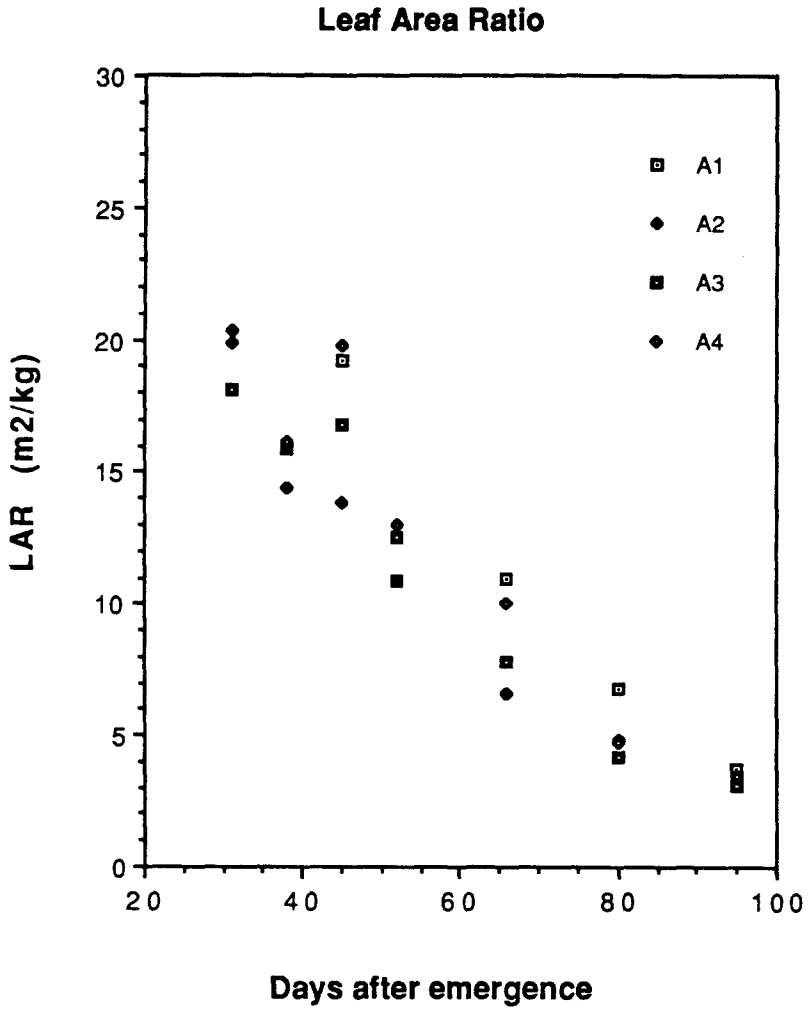

Figure 4.2 Leaf area ratios (leaf area/total above-ground dry weight) for different irrigation treatments: A4 (N-01, N-06, S-01), A3 (N-11, S-06), A2 (N-16, S-11), and A1 (S-16).

Figure 4.3 Yield as a function of applied irrigation water (PET = 641 mm): a) final above-ground dry matter, b) grain yield and c) harvest index.

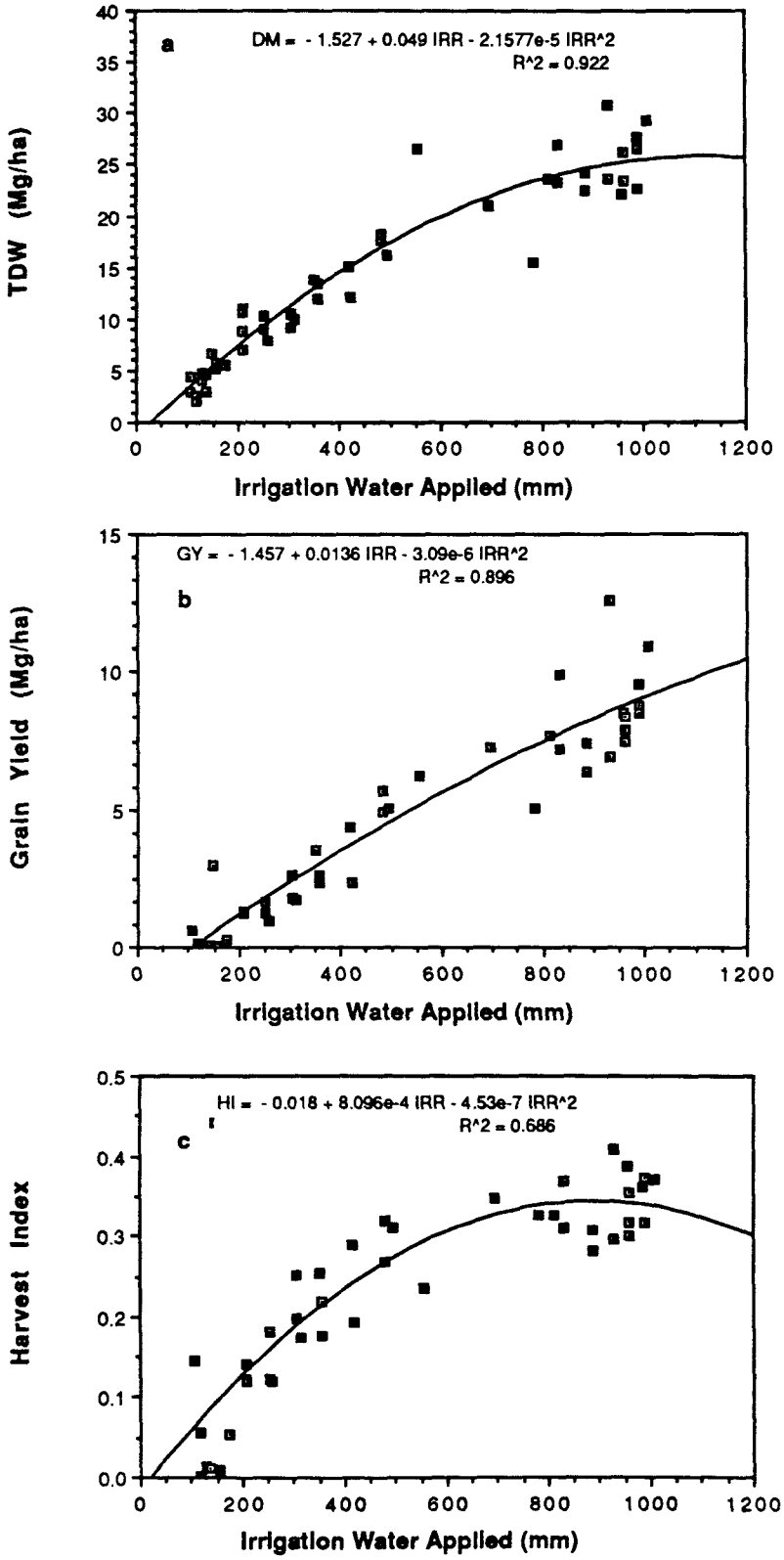
a
DM = - 1.527 + 0.049 IRR - 2.1577e-5 IRR^2
R^2 = 0.922
TDW (Mg/ha)
Irrigation Water Applied (mm)
b
GY = - 1.457 + 0.0136 IRR - 3.09e-6 IRR^2
R^2 = 0.896
Grain Yield (Mg/ha)
Irrigation Water Applied (mm)
c
HI = - 0.018 + 8.096e-4 IRR - 4.53e-7 IRR^2
R^2 = 0.686
Harvest Index
Irrigation Water Applied (mm)

4.4.2 Comparison of Measured and Predicted Crop Growth and Development

Model predictions of dry matter accumulation and leaf area for the 1.6 PET and 1.0 PET treatments are identical, since neither treatment experienced any water stress that would have resulted in a reduction of simulated growth rates. Predictions of accumulated top dry matter for treatment 1.0 PET correspond very well with measured data (Fig 4.4). The course of dry matter accumulation until day 205, which corresponds to about 15 days after tasseling, is very well simulated (Fig. 4.4 b). The end of further dry matter accumulation in the model is triggered when maturity (FT > 49) is reached. Leaf area after this date starts declining rapidly as a function of time (Dale, et al., 1980) and accumulated stress (Stockle and Campbell, 1985). Although the time course of leaf area decline is simulated well, final dry matter is being overpredicted.

The lower measured dry matter accumulation in treatment 1.6 PET (Fig. 4.5 b) as compared to the predictions as well as the measured dry matter accumulation in 1.0 PET could be the result of early leaching losses of applied fertilizer nitrogen below the root zone of the young corn plant, which might have delayed initial growth.

The time course of leaf area development corresponds to measured data (Fig. 4.5 a), although the initial rate

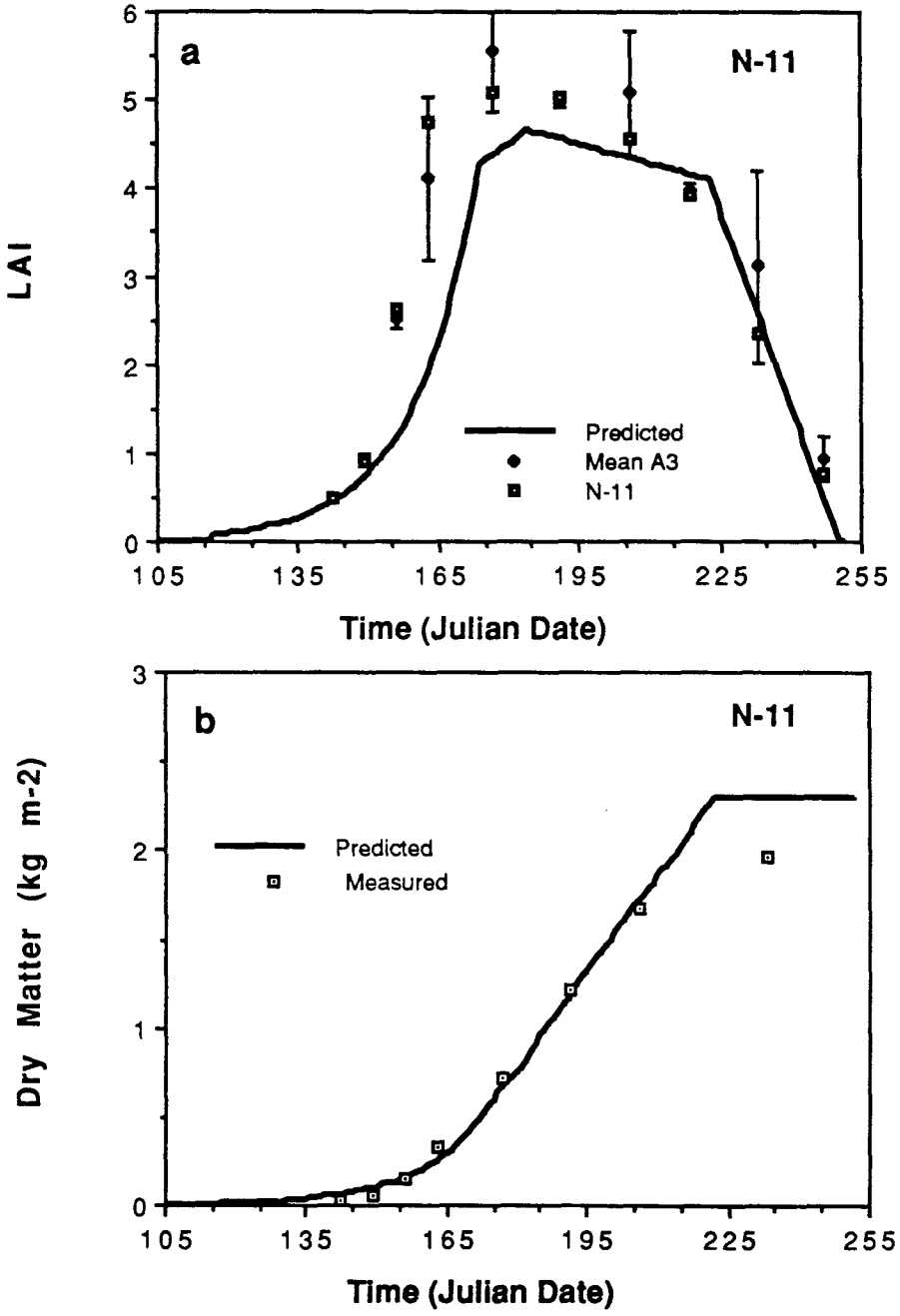

Figure 4.4 Comparison of measured and predicted crop growth for irrigation treatment N-11 (1.0 PET): a) leaf area and b) accumulated dry matter. Means of leaf area for plants in group A3 (N-11, S-06) ±1 Ú. Also, the measured value for N-11 is included.

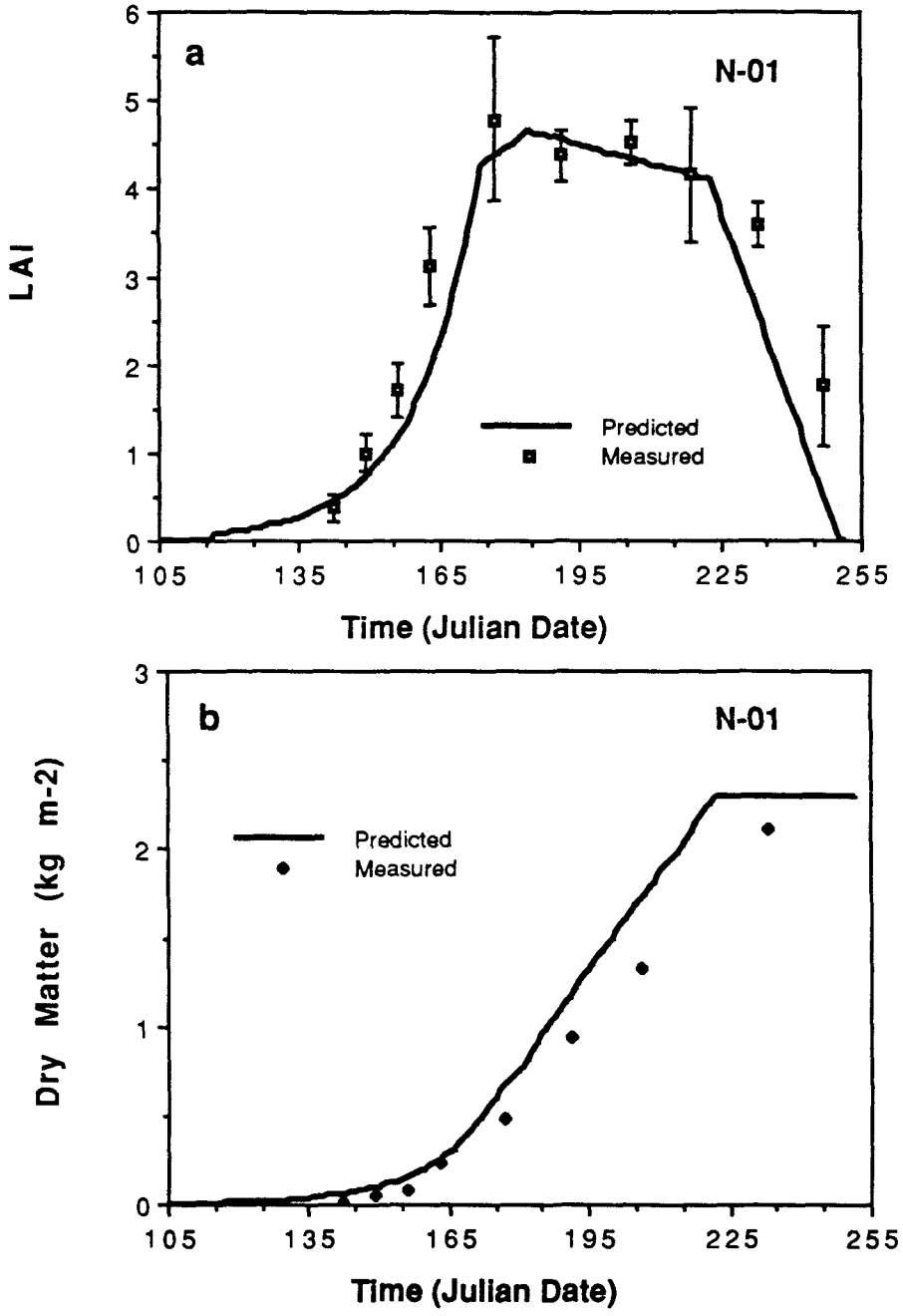

Figure 4.5 Comparison of measured and predicted crop growth for irrigation treatment N-01 (1.6 PET): a) leaf area and b) accumulated dry matter. Means of leaf area for plants in group A4 (N-01, N-06, S-06) ±1 Ú. Also, the measured value for N-01 is included.

of leaf area increase is underestimated. Several parameters influence the prediction of leaf area. The most important one is the leaf area ratio (LAR) assumed for the conversion of dry matter into leaf area. For the simulations presented here, relationships derived from a California data set were used (Acevedo, 1975). Leaf area ratios varied with time after emergence and was initially much higher than the constant value for LAR of 7.6 used in the model (see Fig. 4.2).

For the two water stressed treatments, 0.6 PET and 0.3 PET, comparisons of predicted and measured values are shown in Fig. 4.6 and Fig. 4.7, respectively. Dry matter accumulation in treatment 0.6 PET is being slightly underpredicted in the beginning, possibly for the reasons relating to leaf area ratio, and overpredicted after day 185, when simulated dry matter accumulations proceeds at an almost unchanged rate, whereas the measured data shows a clear depression in growth rate. The relative overprediction of dry matter accumulation is even more pronounced in the 0.3 PET treatment. Simulated leaf area reaches values greater than four before getting reduced rapidly as the result of accumulated stress. Measured leaf areas were maintained somewhat longer, which tends to balance out the overestimation in the early season and results in a satisfactory prediction of final dry matter.

Several reasons could cause an overprediction of dry matter accumulation in the extreme water stress treatment.

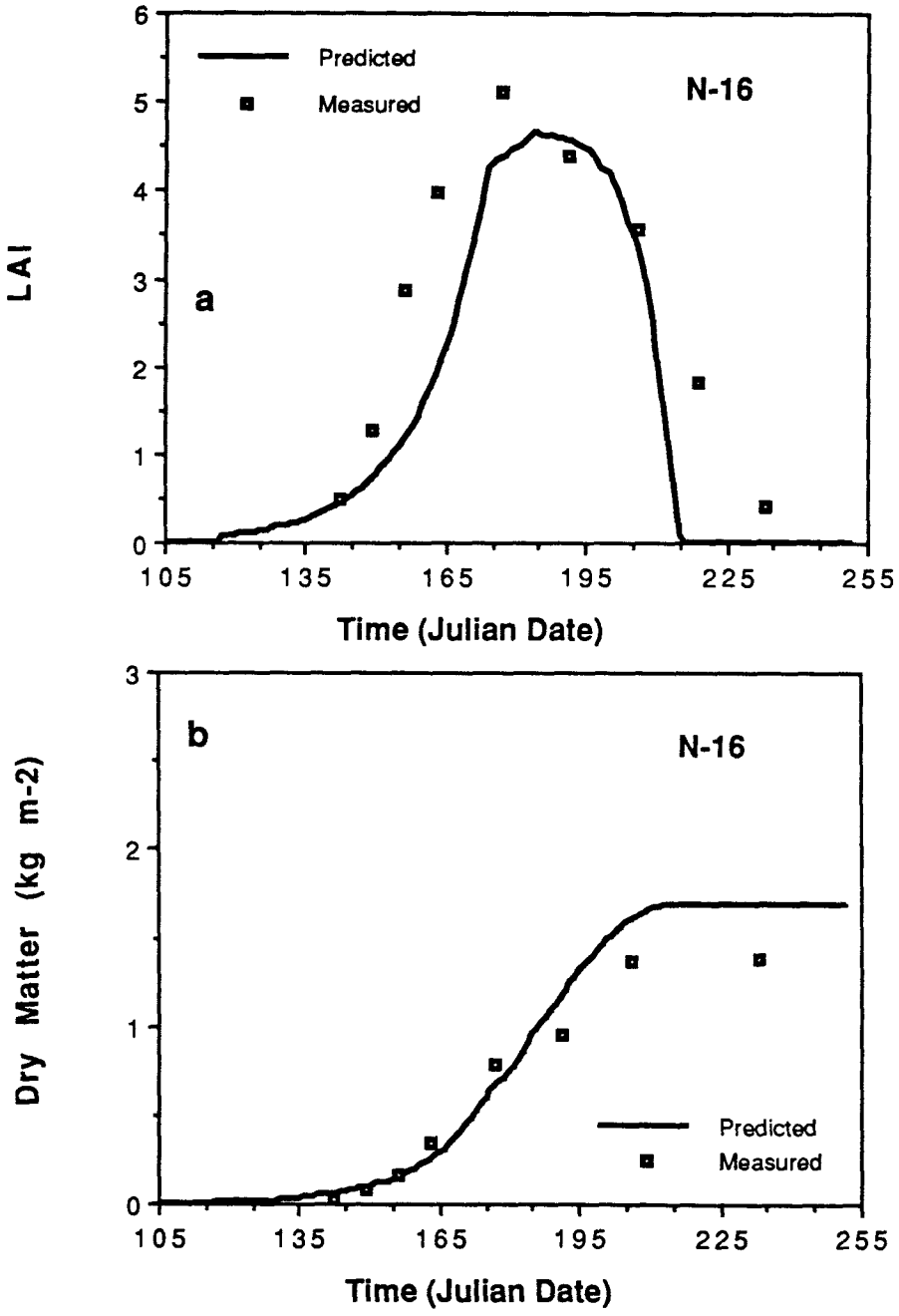

Figure 4.6 Comparison of measured and predicted crop growth for irrigation treatment N-16 (0.6 PET): a) leaf area and b) accumulated dry matter.

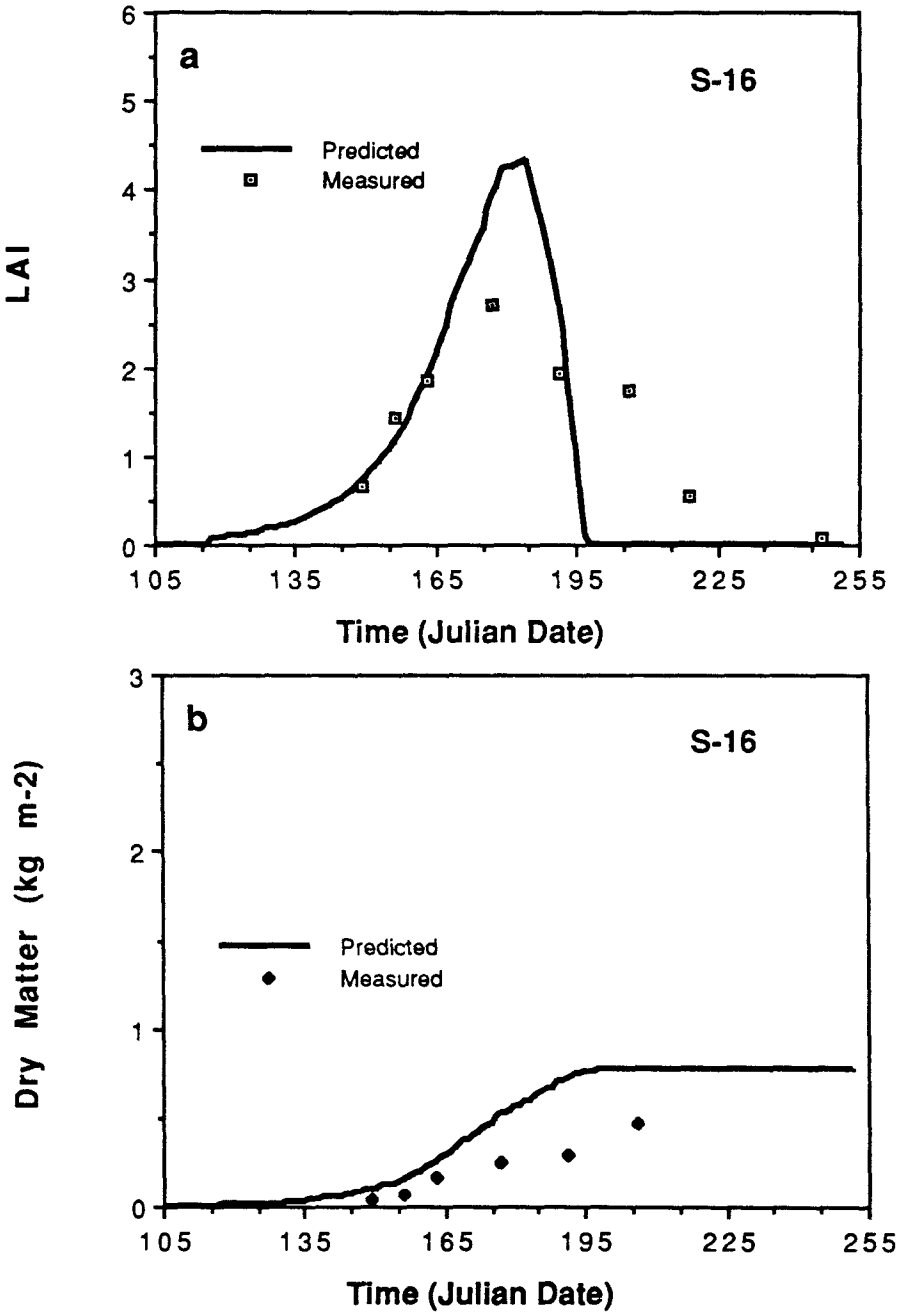

Figure 4.7 Comparison of measured and predicted crop growth for irrigation treatment S-16 (0.3 PET): a) leaf area and b) accumulated dry matter.

The equation modeling radiation partitioning between crop and soil surface will effect potential transpiration and therefore initial rate of use of soil water. More radiation partitioned to the crop results in stress occurring sooner. The choice of the value for critical leaf water potential will effect the response of the canopy resistance to leaf water potential. A less negative value would result in earlier closure of stomates and a concomitant reduction in photosynthetic rate, leading in turn to lower dry matter accumulation and reduced leaf area. Further, assumptions about root distribution and density might not be valid for the deficit irrigation treatments. Generally though, root growth is assumed to be enhanced under water stress conditions relative to shoot growth. If one assumes, that the model is an accurate representation of the effects of water stress on growth, the deviations observed in the water deficit treatments could be attributed to factors other than water, for example phosphate deficiency. While the plant might be able to fulfill transpirational demand by tapping water at lower depth, phosphate concentrated mostly in the upper 15 to 20 cm of the soil profile might be unavailable due to the extremely low water contents there. This could also partially explain the slight overprediction of dry matter accumulation in treatment 0.6 PET. In the field, the effect of water stress and nutrient stress cannot be easily separated. A better

knowledge and understanding of root growing patterns and distributions and at the same time an improved ability to model growing root systems will enhance our understanding of the interactions of water and nutrient stresses on plant growth.

A comparison of final measured and predicted above-ground dry matter for seven irrigation treatments is shown in Fig. 4.8. The slope of the linear regression of measured on predicted total above-ground dry matter indicates that, on the average, measured total dry matter is being overpredicted by eleven percent. Measured field top dry matter as a function of applied irrigation water for amounts less than potential evapotranspiration are shown in Fig. 4.9 b. When predicted values were plotted for this same range of irrigation water treatments (Fig 4.9 a) it was found that the best fit regression had a similar intercept and slope. However, the predicted increase in dry matter with irrigation is slightly higher than the measured one.

4.4.3 Simulation of the Dynamics of Water Stress

Leaf water potentials are one indication of plant water stress. Simulated mid-day leaf water potentials at 14:00 hours for the four irrigation treatments are shown in Fig. 4.10 a. As expected, the simulated leaf water potentials of the well watered (1.0 PET) and the excess watered (1.6 PET) treatments never attain water potentials

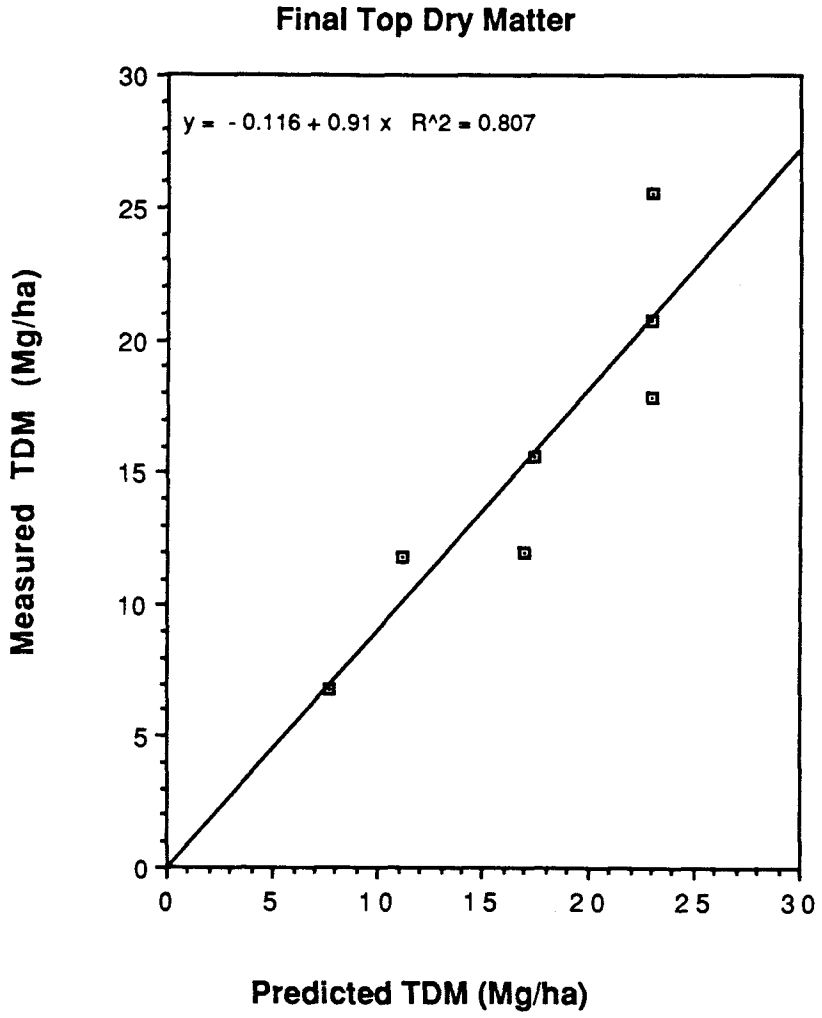

Figure 4.8 Comparison of measured and predicted final top dry matter for irrigation treatments less than PET.

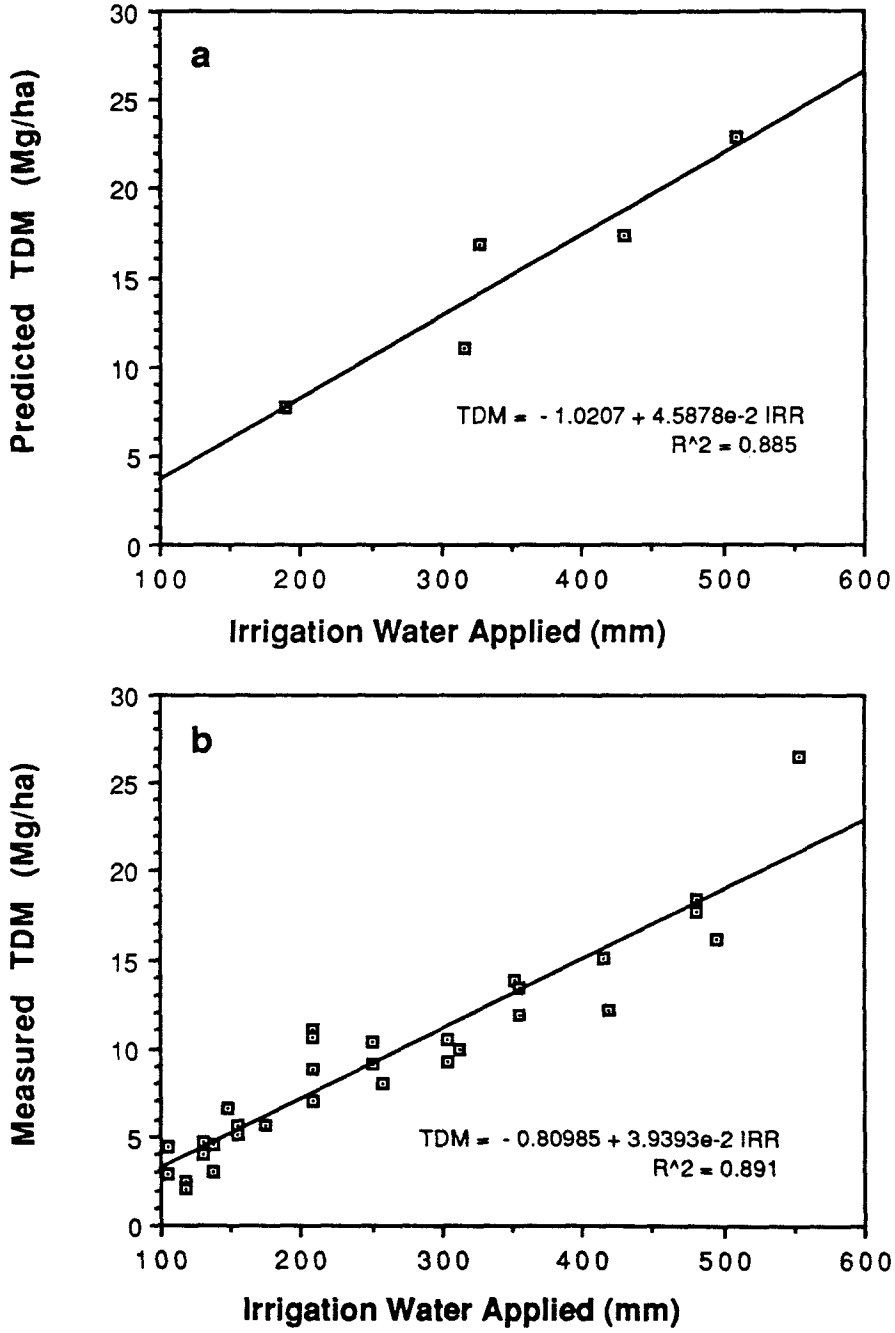

Figure 4.9 Final top dry matter as a function of the amount of irrigation water received. a) simulated and b) measured.

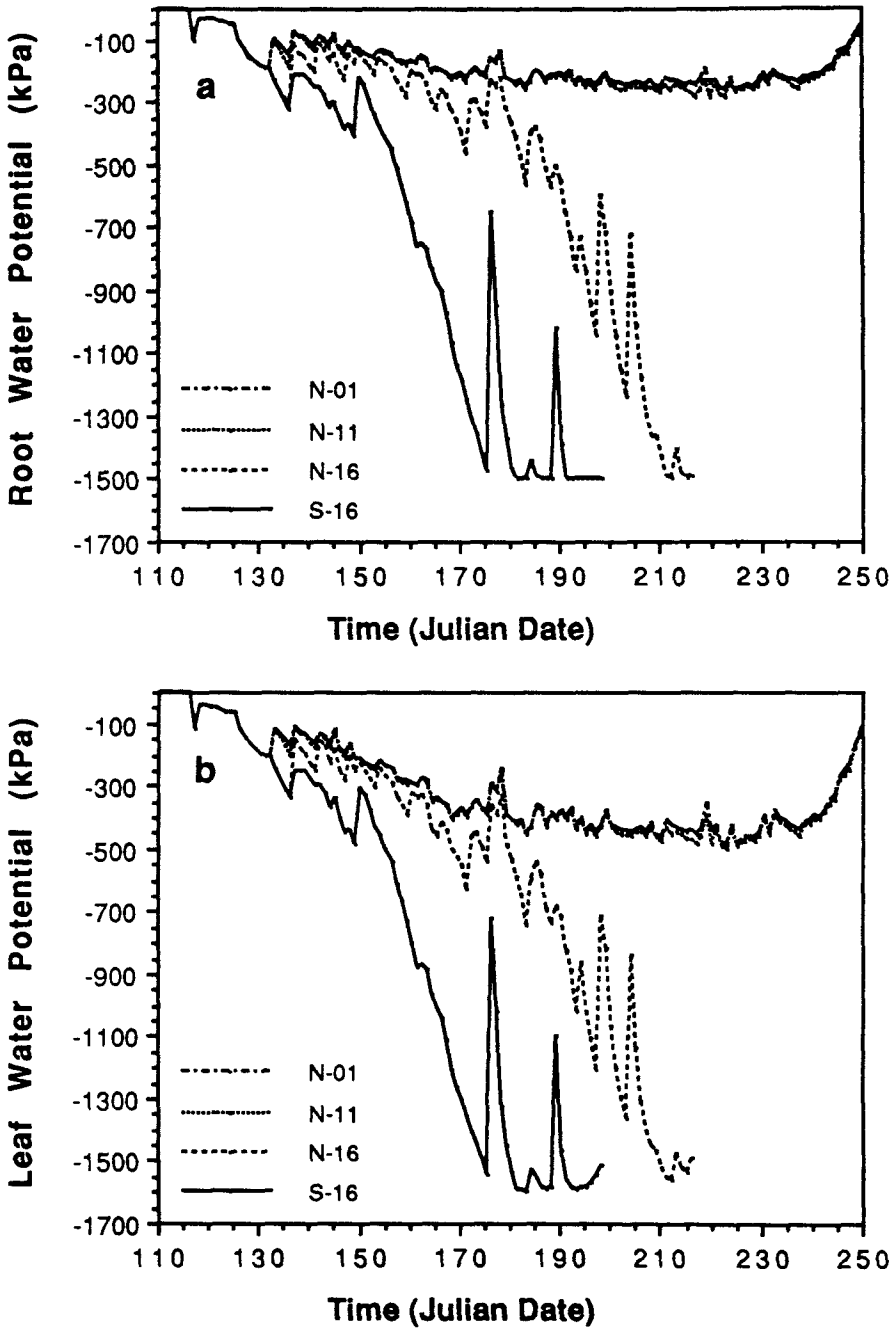

Figure 4.10 Simulated plant water potential at 14:00 hrs. a) root and b) leaf.

indicative of water stress. This is not the case for the two water stress treatments 0.6 PET and 0.3 PET. In treatment 0.3 PET, predicted leaf water potential drops soon after the initiation of irrigation water treatments, on day 132. After day 155 potentials become increasingly negative. Treatment 0.6 PET was able to maintain higher leaf water potentials for a longer time, but potentials start to drop after day 180. This corresponds to the time when observed leaf area indices start to deviate from the well watered treatments (see Fig. 4.1 a). While treatments 0.6 PET only deviates after day 180, the leaf area development in 0.3 PET was delayed from the onset. Corresponding root water potentials, which are always slightly more positive, are shown in Fig. 4.10 a for the same treatments. A lower limit of -1500 kPa was used and the root water potential was not allowed to drop below this value.

As leaf water potential become more negative, the canopy resistance to vapor transport is affected, and actual transpiration will be reduced from potential transpiration (Fig. 4.11 a). The same relative reduction as calculated for transpiration is applied to photosynthetic rate, assuming that carbon dioxide diffusion through the stomates is limiting photosynthetic rate. Fig 4.11 b depicts daily totals of simulated photosynthetic rates for the well-watered and the two deficit treatments. The reduction in photosynthetic rate

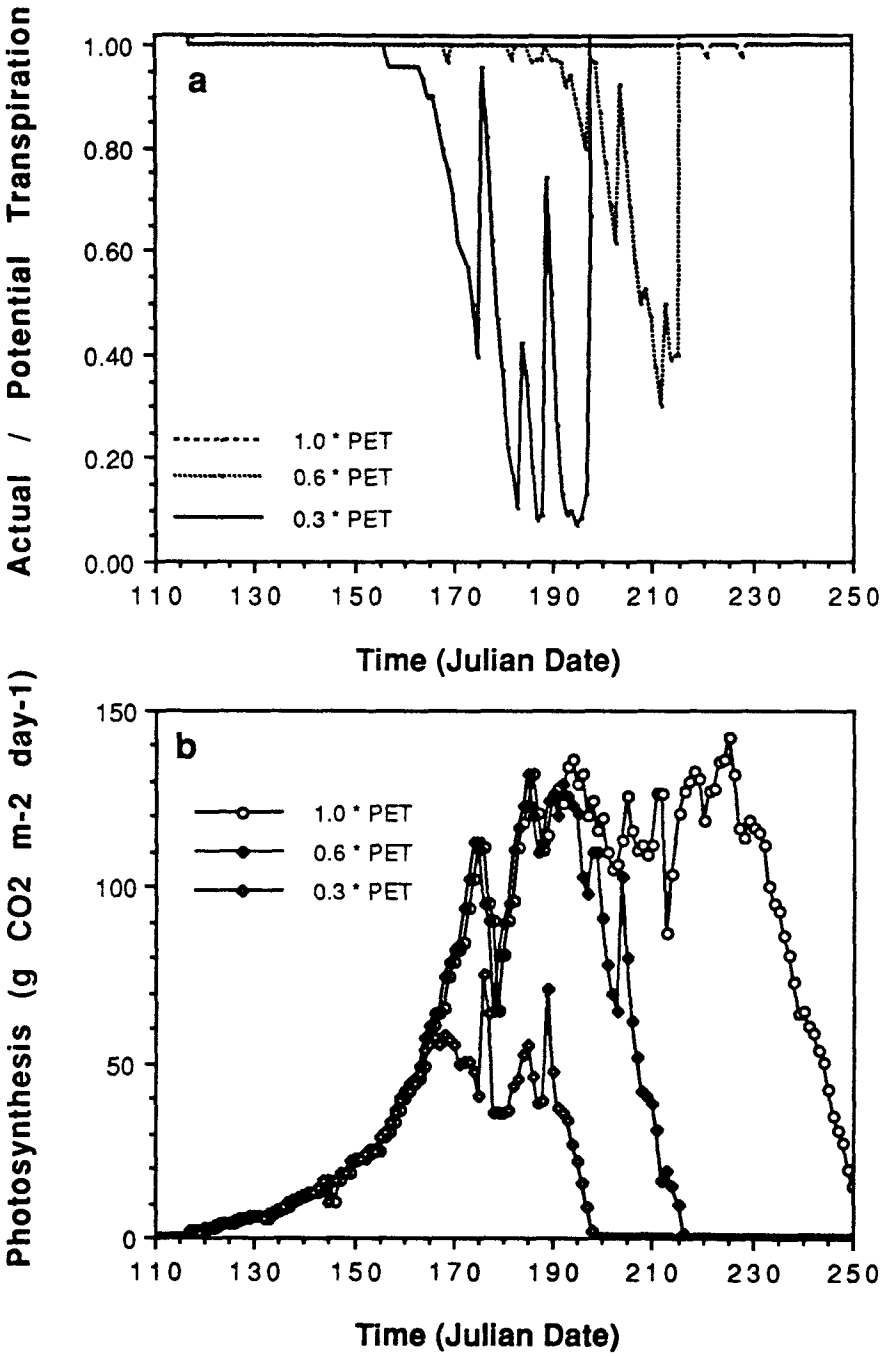

Figure 4.11 Simulated water stress on a daily basis over the growing season for three irrigation treatments N-11 (1.0 PET), N-16 (0.6 PET) and S-16 (0.3 PET). a) ratio of actual to potential transpiration and b) photosynthesis.

parallels the time course of transpirational deficit (Fig. 4.11 a), although it is effected as well by the predicted leaf area of the crop. The reduced rate of photosynthesis will in turn translate into reduced dry matter and a reduction in rate of leaf area expansion.

Simulated plant water potentials, actual and potential transpiration rates, and rates of photosynthesis are shown in Fig. 4.12 on an hourly scale for treatment 1.0 PET (1.0 PET). During the six days depicted, an irrigation event occurred on day 203 after dusk. Leaf water potentials in the well watered treatment drop to about - 700 kPa during mid-day, and recover to values above - 100 kPa at night. Actual transpiration proceeds at potential rates during all days between the two irrigations, indicating the lack of water stress. Simulated photosynthetic rates (Fig. 4.12 c) reach peak values of 16 g m^{-2} $hour^{-1}$ around mid-day, which compares favorably with reported peak rates of carbon dioxide fixation of 17.4 g m^{-2} $hour^{-1}$ (37 mg dm^{-2} leaf area $hour^{-1}$, at LAI of 4.7) reported for corn by Stoskopf (1985), and are about 80 percent of the maximum peak photosynthetic rate measured in corn in the Cerrado of 22.6 g m^{-2} $hour^{-1}$ (48 mg CO2 dm^{-2} leaf area $hour^{-1}$, at LAI of 4.7) (Luiz Carvalho, pers. communication).

In treatment 0.6 PET predicted leaf water potentials drop rapidly between irrigations and reach values less than -1200 kPa, below which canopy resistance increases rapidly and leads to a reduction in potential

Figure 4.12 Simulated water stress on an hourly basis between irrigation events for treatment N-11 (1.0 PET): a) plant water potential, b) actual and potential transpiration, and c) non-waterstressed and stressed photosynthesis.

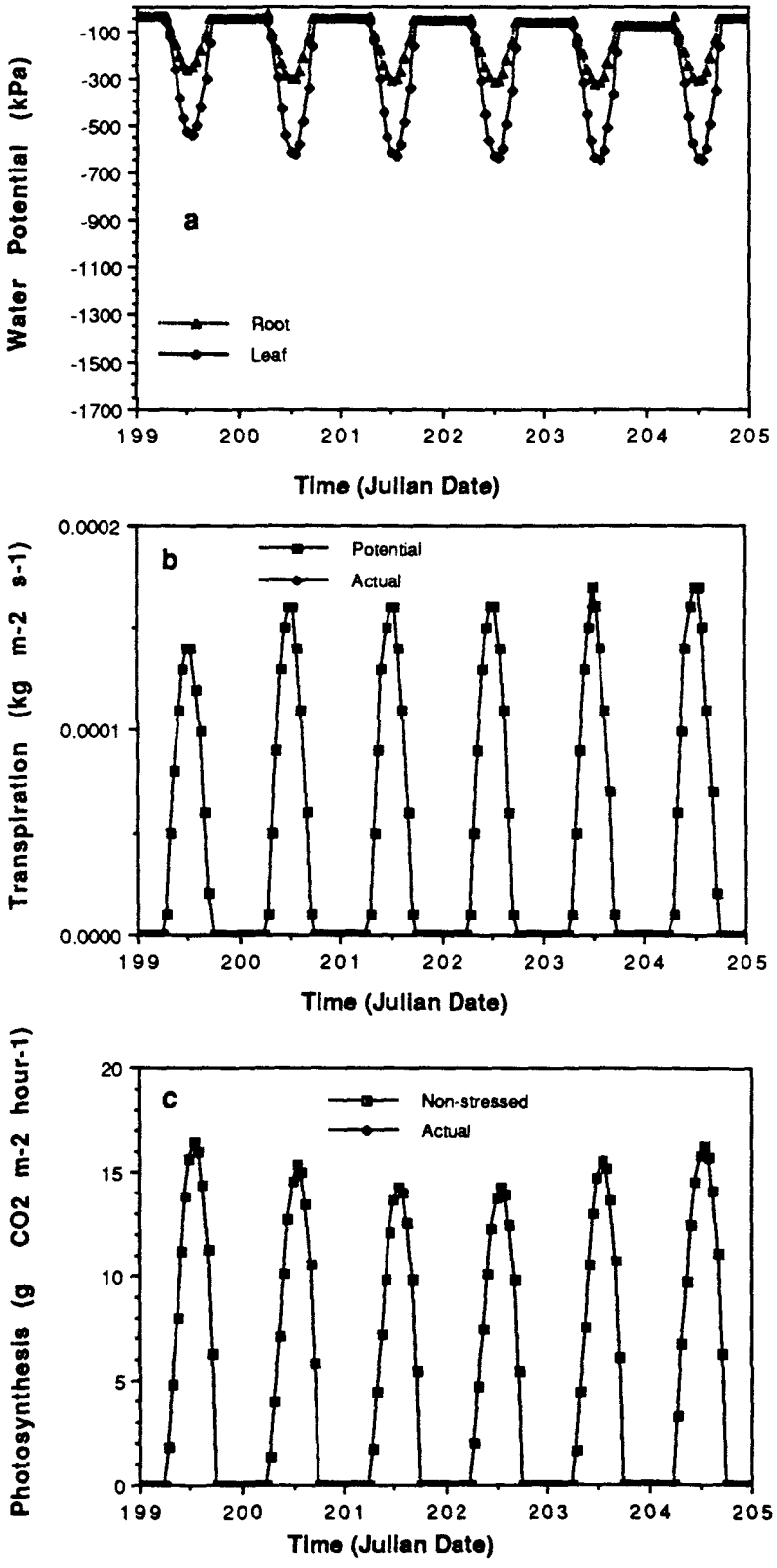
Water Potential (kPa)
-100
-300
-500
-700
-900
-1100
-1300
-1500
-1700
a
Root
Leaf
199
200
201
202
203
204
205
Time (Julian Date)
Transpiration (kg m-2 s-1)
0.0002
0.0001
0.0000
b
Potential
Actual
199
200
201
202
203
204
205
Time (Julian Date)
Photosynthesis (g CO2 m-2 hour-1)
20
15
10
5
0
c
Non-stressed
Actual
199
200
201
202
203
204
205
Time (Julian Date)

transpiration and concomitant reductions in photosynthetic rate (Fig. 4.13). Both recover rapidly the morning after the irrigation on day 203, although water potentials in 0.6 PET do not recover fully to non-stressed levels.

Predictions of root water uptake have been shown to be more sensitive to rooting depth than to root density (Da Silva and de Jong, 1986). Limiting the maximum rooting depth obtainable had no effect on predictions of actual transpiration in treatment 1.0 PET. In the water-stress treatments predicted actual transpiration and dry matter accumulation were reduced when rooting depth was not allowed to exceed a maximum value in the simulation (Table 4.2).

Stoeckle and Campbell (1985) presented a correlation between water stress accumulated during pollination (SIp) and the harvest index (HI), which did not apply well to the experimental results and simulations presented here. Predicted harvest index using their regression equation on accumulated stress index during pollination and measured harvest index are compared in Table 4.3. Measured harvest index in this experiment was poorly related to predicted accumulated stress during pollination (Fig. 4.14 a), but more closely related to total accumulated stress during the whole growing season (Fig. 4.14b).

Figure 4.13 Simulated water stress on an hourly basis between irrigation events for treatment N-16 (0.6 PET): a) plant water potential, b) actual and potential transpiration, and c) non-waterstressed and stressed photosynthesis.

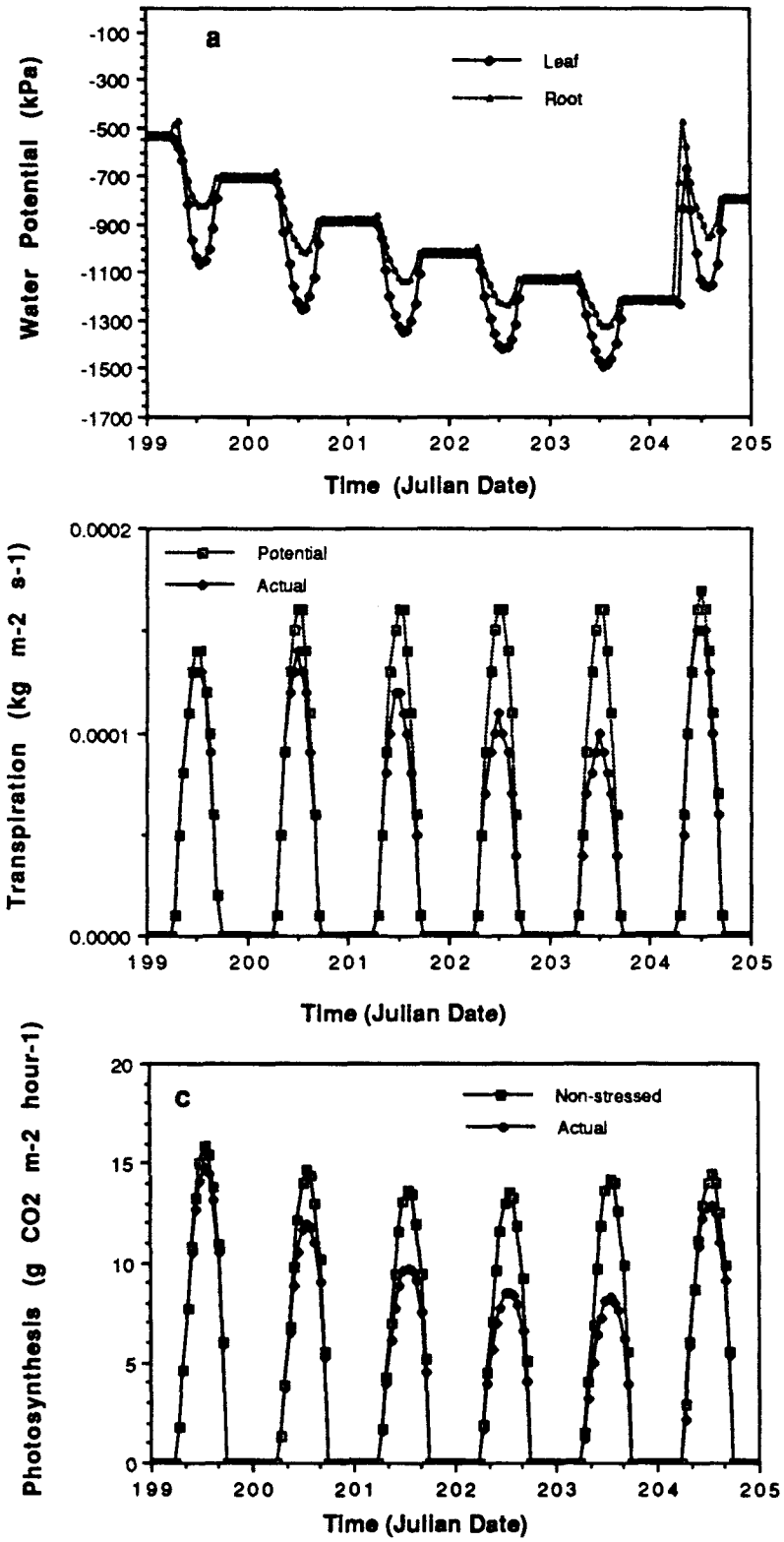
a
Leaf
Root
Water Potential (kPa)
-100
-300
-500
-700
-900
-1100
-1300
-1500
-1700
199
200
201
202
203
204
205
Time (Julian Date)
Potential
Actual
Transpiration (kg m-2 s-1)
0.0002
0.0001
0.0000
Time (Julian Date)
c
Non-stressed
Actual
Photosynthesis (g CO2 m-2 hour-1)
20
15
10
5
0
Time (Julian Date)

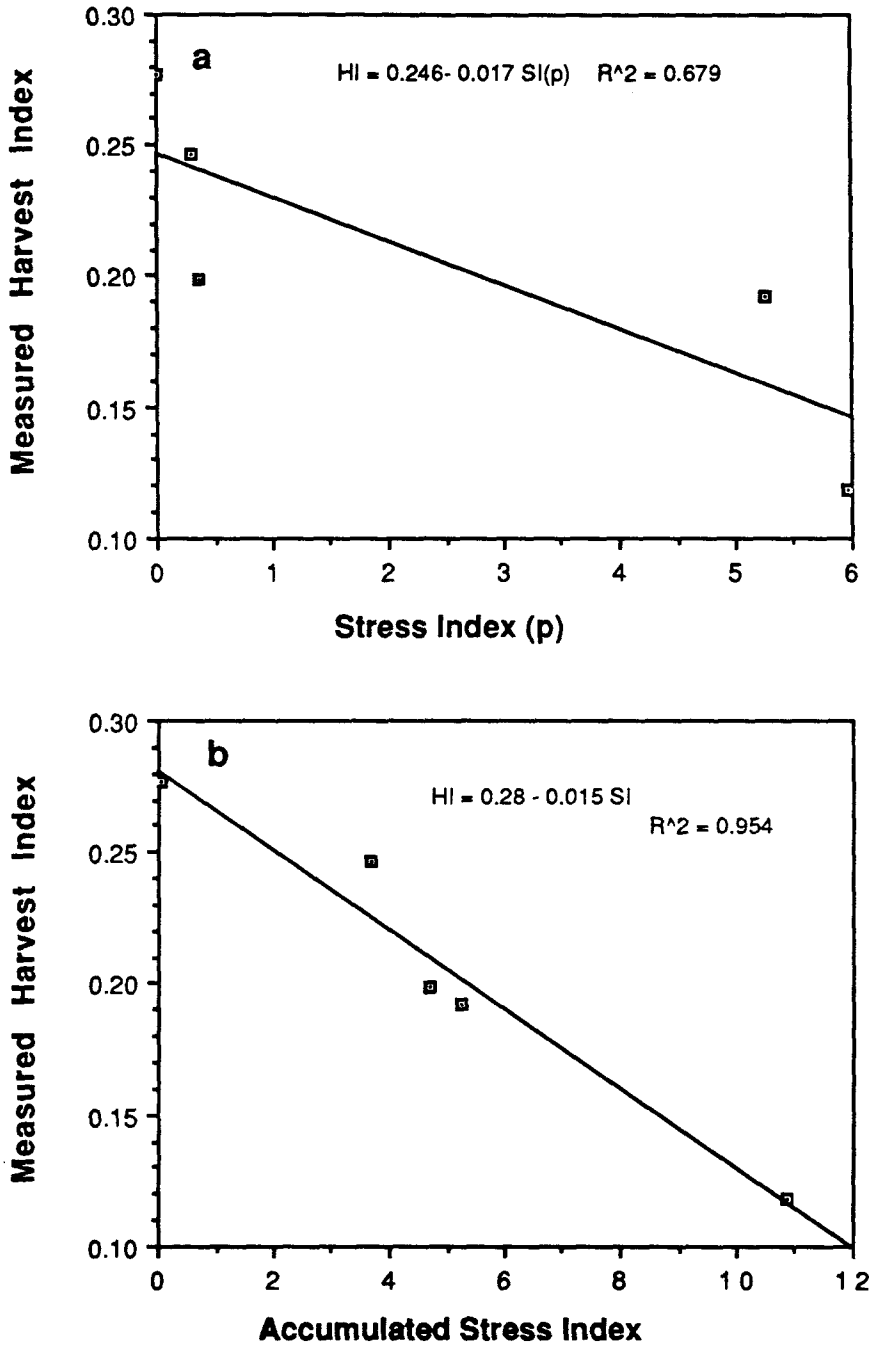

Figure 4.14 Measured harvest index as a function of accumulated water stress during a) pollination and b) the whole growing season.

TABLE 4.2

Simulated effects of limiting potential maximum rooting depth (0.38 m, 0.53 m, 0.75 m, and 1.05 m) on actual (mm/day) / potential transpiration (mm/day) (TR), deep drainage (mm) (DR) and final above-ground dry matter (kg/m2) (Y) under different irrigation water treatments.

Irrigation treatment								
1.0 PET			0.6 PET			0.3 PET		
TR	DR	Y	TR	DR	Y	TR	DR	Y
			0.38 m :					
363/364	70	2.30	164/201	13	1.32	75/145	11	0.56
			0.53 m :					
364/364	69	2.30	177/211	11	1.45	87/154	9	0.65
			0.75 m :					
364/364	68	2.30	193/223	9	1.59	102/161	7	0.77
			1.05 m :					
364/364	67	2.30	208/232	5	1.69	102/161	7	0.77

TABLE 4.3

Harvest index estimated from experimental data (HI_m), and predicted (HI_p) from accumulated stress during pollination (SI_p).

Irrigation (mm)	SI_p [1]	SI_t [2]	HI_p	HI_m
509	0.01	0.04	0.479	0.277
430	0.29	3.68	0.463	0.246
327	0.36	4.70	0.458	0.198
316	5.25	6.88	0.165	0.193
188	5.96	10.86	0.122	0.118

1 - SI_p predicted from regression from stockle and Campbell (1985)
2 - SI_t is the total accumulated stress index for the whole season

4.4 SUMMARY AND CONCLUSIONS

The assumptions relating to the effect of water stress on crop growth inherent in the crop simulation model (Stockle and Campbell, 1985) used here, appear to be valid when applied to Cerrado conditions. Temperature and light effects on photosynthesis are considered in the calculation of a non-stressed photosynthetic rate, which is dependent on the amount of photosynthetically active radiation intercepted by the canopy. Thus, model predictions are sensitive to the predicted partitioning of potential evapotranspiration. Photosynthetic rate in the model is reduced when leaf water potentials drop below a critical leaf water potential for stomatal closure. The

reduced photosynthetic rates translates directly into reduced dry matter accumulation and a reduced leaf area. Water stress is accumulated as a water stress index and effects the reduction of leaf area index after the end of the vegetative phase.

Predicted leaf area indices and dry matter accumulation over time compared well with measured data. Dry matter and leaf area were overpredicted in the most extreme water stress treatment, possibly due to soil fertility/water interactions not represented in the model. Important parameters effecting predictions are leaf area ratios, which vary with variety and were shown to decline over time for the variety used here, while an average leaf area ratio was used in the simulations. Model predictions are sensitive to the time, when phenological stages of pollination and maturity are reached. Simulated final dry matter is very sensitive to the thermal time chosen for maturity, since further dry matter accumulation is discontinued after the crop reaches maturity.

Harvest index was related more to water stress accumulated throughout the growing season, than to water stress accumulated during pollination, as was suggested by Stockle and Campbell (1985).

Hourly predicted leaf water potential changes and corresponding changes in transpiration and photosynthetic rate represented the dynamics of water stress realistically and were consistent with expectations.

REFERENCES

Acevedo, E. 1975. The growth of maize (Zea mays L.) under field conditions as affected by its water relations. Ph.D. thesis, Univ. of California, Davis. 253 p.

Bandy, D. 1976. Soil-plant=water relationships as influenced by various soil and plant management practices on Campo Cerrado soil in the Central Plateau of Brazil. Ph.D. thesis, Cornell University, Ithaca. 236 p.

Buttler, I. W. and S. J. Riha. 1987. General purpose simulation model of water flow in the soil-plant-atmosphere continuum. Appl. Agr. Res. 2:230-234.

Buttler, I. W. and S. J. Riha. 1988. GAPS - A general purpose simulation model of the soil-plant-atmosphere. User's manual. Version 1.1. Cornell University, Ithaca, NY.

Campbell, G. S. 1985. Soil physics with BASIC: Transport models for soil-plant systems. NY Elsevier.

Coelho, D. T. and R. F. Dale. 1980. An energy-crop growth variable and temperature function for predicting corn growth and development: planting to silking. Agron. J. 72:503-510.

Dale, R. F., Coelho, D. T., and K. P. Gallo. 1980. Prediction of daily green leaf area index for corn. Agron. J. 72:999-1005.

Fisher, M. J., Charles-Edwards, D. A., and M. M. Ludlow. 1981. An analysis of the effects of repeated short term soil water deficits on stomatal conductance to carbon dioxide and leaf photosynthesis by the legume Macroptilium atropurpureum cv. Siratro. Aust. J. Plant Physiol. 8:347-357.

Foth, H. D. 1962. Root and tap growth of corn. Agron J. 54:49-52.

Gonzales-Erico, E., Kamprath, E. J., Naderman, G. C., and W. V. Soares. 1979. Effect of depth of lime incorporation on the growth of corn on an Oxisol of central Brazil. Soil Sci. Soc. Am. J. 43:1155-1158.

Goodwin, J. B., Garacorry, F. L., Espinoza, W., Sans, L. M., and L. J. Youngdahl. 1982. Modelling soil-water-plant-relationships in the Cerrado soils of Brazil: The case of maize. Agric. Systems 8:115-127.

Hanks, R. J., Keller, J., Rasmussen, V. P., and G. D. Wilson. 1976. Line source sprinkler for continuous variable irrigation-crop production studies. Soil Sci. Soc. Am. J. 40:426-429.

Hesketh, J. and D. Baker. 1967. Light and carbon assimilation by plant communities. Crop Sci. 7:285-293.

Macedo, J. and R. B. Bryant. 1987. Morphology, mineralogy, and genesis of a hydrosequence of Oxisols in Brazil. Soil Sci. Soc. Am. J. 51:690-698.

Monteith, J. L. 1981. Climatic variation and the growth of crops. Q.J.R. Meteorol. Soc. 107:749-774.

Norman, J. M. 1982. Simulation of microclimates. "Biometeorology in integrated pest management". Academic Press, New York.

Norman, J. M., and G. S. Campbell. 1983. Application of a plant-environmental model to problems in irrigation. Adv. Irrig. 2:155-188.

Priestley, C. H. B. and B. J. Taylor. 1972. On the assessment of surface heat flux evaporation using large-scale parameters. Mon. Weather Rev. 100:81-92.

Riha, S. J. and G. S. Campbell. 1985. Estimating water fluxes in Douglas-fir plantations. Can. J. For. Res. 15:701-707.

Ritchey, K. D. 1982. Calcium deficiency in clayey B-horizons of savanna Oxisols. Soil Sci. 133:378-382.

Stockle, C., and G. S. Campbell. 1985. A simulation model for predicting effect of water stress on yield: an example using corn. Adv. in Irrigation 3:283-323.

Stoskopf, N. C. 1985. Cereal Grain Crops. Reston Publishing, Reston. Virginia. 516 p.

Turner, N. C. 1974. Stomatal behavior and water status of maize, sorghum and tobacco under field conditions at low water potential. Plant Physiol. 53:360-365.

Wolf, J. M. 1975. Water constraints to corn production in Central Brazil. Unpublished Ph.D. Thesis, Cornell University.

Chapter V

SUMMARY AND CONCLUSIONS

The objective of the research program of which this project is a part is to determine crop water requirements for the Cerrado region of Brazil. Knowledge of the influence of evapotranspiration, soil hydraulic properties and water management on crop growth is important for both the agronomic and economic evaluation of irrigation development and the extension of rainfed agriculture. In the case of irrigation a knowledge of crop water requirements in relation to yield will allow for better irrigation planning and design, as well as more realistic comparison of the relative benefit of using water for irrigation rather than for other purposes. In the case of rainfed agriculture, such knowledge will allow for more realistic evaluation of the feasibility of extending agriculture into areas where dry spells during the wet season are likely to reduce yield potential, as well as establish a basis for improving crop tolerance to short droughts.

The relationship between evapotranspiration, soil water properties and crop growth is complex. For this reason, dynamic plant-environmental simulation models were developed and used to predict water budgets and crop growth under a range of irrigation water treatments. Specifically, a microcomputer-based program (GAPS) was

designed to allow construction of several simulation models from various mathematical representations of processes in the soil-plant-atmosphere system. These representations, for the most part, had been previously published but not extensively tested, especially by researchers other than the group responsible for their development. The use, testing, and refinement of previously published models was considered important in this research program both to test their applicability to regions of the world for which they were not originally developed (and thus determine the generality of the underlying assumptions) and to build on existing paradigms that have shown to work reasonably well.

The structure of GAPS allows for direct comparison of various representations of evapotranspiration, soil water flow, crop water uptake and crop growth. Two different representations of soil water flow and plant water uptake were considered in this study: a) a capacity-type water flow model (Tipping Bucket) combined with a plant water uptake model based on the concept of plant-available water, and b) a numerical solution to the Richards equation combined with a potential driven water uptake model. Both used the Priestley-Taylor method to estimate potential evapotranspiration. To test the applicability of these models to Cerrado conditions in the Cerrado of Brazil, a line source sprinkler experiment which provided a range of irrigation water application to corn from 0.3

to 1.6 potential evapotranspiration was established during the dry season of 1987.

Both the Richards equation and the Tipping Bucket routine simulated soil water contents well under a wide range of irrigation water treatments. The advantages of the Richards equation are that it better predicts the water content distribution in the soil profile, gives more continuous predictions of water fluxes, and provides estimates of water potentials as a function of time and space that can be linked to potential-driven root water uptake and crop growth procedures. However, the water content-potential relationship for this Oxisol was not well described by the Campbell moisture release equation, which assumes that the log-transformed moisture release data is linear. Furthermore, field satiated water contents, which are around 70% of total porosity, had to be known in order to predict water contents correctly. Soil compaction, as indicated by increased bulk densities, did not change satiated water contents in proportion to the decrease in total pore volume, presumably because the portion of porosity lost due to compaction was not water-filled at satiated water contents under non-compacted conditions. The Tipping Bucket routine was very sensitive to the value chosen for field capacity. The capacity-type water uptake procedure linked to the Tipping Bucket routine compared well with the potential-driven root water uptake procedure used together with the Richards equation,

especially under water-limiting conditions. The limited available data on rooting depth and relative root distributions together with the assumptions used in the root growth simulations seemed to provide satisfactory results, judged by the comparison of observed and predicted soil water extraction patterns. Advection was identified as a plausible factor in underpredicting evapotranspiration during the later part of the dry season.

The corn growth simulation model was developed and tested previous to this study for another variety of corn grown in California. Although this model was considered crop-specific by its developers, only a few procedures are based on empirical relationships derived from corn. These include the photosynthetic rate as a function of PAR, leaf area development and leaf area ratio. The model predicted the effects of water stress on leaf area development very well and also predicted the relative effect of water stress on above-ground dry matter accumulation. Final predicted above-ground dry matter production was approximately 11% higher than measured. Measured values ranged from 6 Mg/ha for an irrigation treatment equivalent to 0.3 PET to 25 Mg/ha at 1.6 PET.

The assumptions relating the effect of water stress to corn dry matter accumulation and leaf area development used in the growth component models appear to apply to Cerrado conditions. Predicted time courses of dry matter

accumulation and leaf area development compared well with measured data under a range of irrigation water treatments. The model predictions were sensitive to the partitioning of potential evapotranspiration. Partitioning more PET to transpirational demand in the early season led to faster development of water stress effects under the deficit irrigation treatments. The leaf area ratio used to convert dry matter to leaf area strongly effects early leaf area development and predictions of dry matter production. The critical leaf water potential used to increase canopy resistance as a function of leaf water potential will determine how soon potential transpiration (and thus photosynthesis) respond to water stress. The date of maturity used to end further dry matter production is critical in its effect of final yields. Reduced growth under the extreme water stress treatment appeared to be due to additional factors, possibly nutrient deficiency caused by the extremely dry topsoil.

We conclude that the linked water and crop growth model can generally predict water movement in Cerrado soils and can predict the water stress on corn yield. The model could be applied for irrigation planning purposes and prediction of the effects of dry spells on crop growth in the rainy season.

This study has also demonstrated that developing software that allows for multiple representations of

plant-environmental processes is a promising approach that should result in more extensive and continued improvement of plant-environmental simulation models.

APPENDIX A

GAPS User's Manual

G A P S

A General Purpose Simulation Model

of the

Soil-Plant-Atmosphere System

Version 1.1

User's Manual

(DRAFT)

by

Imo W. Buttler and Susan J. Riha

Cornell University

Acknowledgements

We would like to acknowledge several people who contributed, either directly or indirectly, to this program.

Prof. Gaylon Campbell greatly influenced both authors' approach to simulation modeling when they worked with him at Washington State University and through his recently published "Soil Physics with BASIC" (Elsevier).

Oner Bicakci played an instrumental role in designing the user interface, particularily the screen menus. Jennifer Sanchez assisted in the production of the dependency diagrams and proofread portions of the documentation. James Altucher helped trouble-shooting later versions of the program and developed much of the current version of the Plotter.

This program was developed as part of the doctoral research conducted by the senior author and supported in part by subgrant SM-CRSP-012 of the TropSoils program funded by USAID.

Table of Contents

1. Introduction to GAPS

GAPS is a general purpose simulation model of the soil-plant-atmosphere system. GAPS is programmed in TurboPascal 4.0 and can be implemented on the IBM PC/AT or fully IBM PC compatible computers. The program consists of three main parts: the Editor, the Simulator, and the Plotter. The **Editor** allows the user to create or edit all files that are necessary input to the simulator. The **Simulator** links and implements the simulation procedures selected by the user. The **Plotter** outputs results of a simulation run or input data files to a printer.

This manual is organized in three major sections. Chapter 2 describes the structure and function of the Editor and the structure of input data files. Chapter 3 contains the documentation of the currently existing procedures in the Simulator. Each procedure is documented in detail in a separate chapter. Some information on how to make changes to an existing procedure and on how to add additional procedures to the Simulator is contained in Appendix B. Changing existing procedures or adding new ones requires some programming experience. Chapter 4 introduces the user to the functions of the Plotter. The Plotter is the part of the program responsible for accessing simulation model output or input. Note that instantaneous output can be obtained during the simulation run using the run time plotting option (see Chapter 3.4).

1.1 GAPS Menus

The intention of GAPS is to provide a user friendly environment in which to use simulation models. All the interaction with the user is through menus. The menus used in GAPS all follow the same general

layout. The screen is partitioned into several windows in which different information is displayed. The main window contains the different options available to the user at a particular level in the program. The function keys on the left side of the screen are used to facilitate user response. The function keys correspond to the options displayed in the main window and their definition changes between different windows. If no function keys are available the user can respond with the first letter of the respective choice. In the lower right hand window input data file currently residing in memory are displayed after they have been loaded in by the user before running a simulation.

1.2 Getting Started

To run GAPS insert the GAPS runtime diskette into one of your disk drives and type 'RUNGAPS'. This will execute a batch file that will automatically change the default directory to the already created subdirectory \GAPS\DATA, where test versions of input data files reside and where you will store your own data files. It will then invoke GAPS. Before running a simulation program the input data files have to be loaded into memory. Once all the necessary files are loaded and their names are being displayed in the lower right hand corner of the screen, you are ready to construct a simulation model from the component parts currently existing in the simulator. Choose the option 'Procedures' from the Simulator menu. A new menu will appear giving you the choice between different component parts of the system such as 'Water Flow', 'Water Uptake', 'Potential Evapotranspiration', and 'Soil Temperature'.

Upon selecting one or more of these options, you will have to select between different representations of the respective process. You can also specify the first and last day of the simulation run and choose the time step to be used (option 'Time'), and select up to four variables to be plotted instantaneously on the screen during the simulation run (option 'View'). If you want to save output to disk, option 'Out' needs to be selected and filenames identified. Hourly and/or daily data can be saved and the days and hours when to save data can be determined (see Chp. 3.5) When you made all your selections you may choose 'Run' to actually run the simulation. After the simulation stops you can hit any key to return to the simulator menu. You can change any of your options in terms of input data files or the constellation of the simulation model and execute another run. If you want to have a hard copy of the plots generated during the simulation run you can dump them to the printer (shift-PrTSc).

After a run you can enter the Plotter via the GAPS main menu and obtain further output from the simulation model. You can obtain tabular output of the main variables that have been saved to a file during the simulation run.

For detailed information about the procedures currently contained in the Simulator please refer to Chapter 3, where each procedure is documented in detail in a separate chapter.

2. The Editor

2.1 Editing Data Files

All the interaction between GAPS and the user is through menus. The Editor can be entered from the GAPS main menu by selecting the appropriate function key (F1) or, if function keys are not available, by hitting the corresponding first letter of the respective choice, in this case by hitting an 'E' for 'Editor'. Upon choosing the Editor option, the Editor menu will appear. The user is given the choice which category of input data files to edit (Climate, Soil, Plant, or Location Files). Upon choosing one of the categories the respective menu will appear. The option 'Outp' lets the user specify on which days and at which hours to save simulation output to disk. Since the internal data structure of the input files is different in each case, the options available for editing the data files are too.

The Editor searches the default directory for existing files of the desired type (reckognized by a particular file extension) and displays the file names in the window at the center of the screen. The user can use the arrow keys to scroll up and down the list and select any of the files for further editing (option 'Load'). To construct a new file, a file name (<u>without</u> specifying a file extension) has to be given, and the 'Make' option selected. A blank spreadsheet in the format of the data file will appear on the screen and the user can input data.

Selecting the 'Quit' option in any of the menus will bring the user back to the next higher level menu and, if hit consecutively back to the GAPS main menu and eventually back to DOS.

Existing input data files can be accessed from the GAPS Plotter and printed (see Chp.4.2). A user does not have to provide all parameters included in an input file. Only the parameters used in a specific application have to be present. For example, to use the Richards_Equation procedure to simulate water flow, values for wilting point or field capacity are not needed. The corresponding spaces in the input file could be left blank.

2.1.1 Editing a Climate Data File

A Climate Data File can contain a maximum of one years' of data (365 days). Row #1 in the file corresponds to January 1, row #365 to December 31. If a climate data set starts for example on June 01, the first row to input data would be #152. The user can jump to any row (date) in the file by using the 'Jump' option. 'Insert' can be used to input data for the first time or to insert additional days of data in an existing file. 'Modify' allows changing data entries. Simply hit return for the parameters you do not want to change. 'Save' will save the file to the disk. Note that you can change the file name and thus save an edited version of the file under a different name. 'Load' will load an existing file into the Editor.

At this time the Editor only accepts daily climate data. Parameters included in the current version of the climate input file are listed below. The variable name, units, and procedures in which they are used are also given. In the computer code, all climate data variable names are preceded by the prefix 'clim.', e.g. clim.MaxTemp.

1. Maximum air temperature, MaxTemp, degrees C (..._Temperature-..._ETP)
2. Minimum air temperature, MinTemp, degrees C (")
3. Solar radiation, SolRad, MJ m^{-2} d^{-1} (Atmos_Trans, ..._ETP)
4. Precipitation, Precip, mm d^{-1} (..._Flow)
5. Relative humidity, RelHumid (..._ETP, Richards_Flow)
6. Wind speed, WindSpeed, m s^{-1}
7. Pan evaporation, PanEV, mm d^{-1} (Pan_ETP)

2.1.2 Editing a Soil Data File

A soil data file contains information on soil parameters as a function of depth. Any number of soil layers up to 20 can be specified and different properties can be assigned to each soil layer. The depth of each layer can be chosen by the user when setting up the soil data file. When using the numerical solution to the water flow equations the user should be aware of the effect of node spacing and time step size on the results of the numerical solution. Close node spacings at the soil surface are recommended. Parameters included in the current version of the soil input file are listed below. In the code, all soil input parameters carry the prefix 'soil.', as for example in soil.NodeDepth.

1. Node depth, NodeDepth, m (..._Flow, ..._Temperature, ..._Uptake)
2. Bulk density, BulkDens, Mg m^{-3} (..._Flow, Soil_Temperature, ..._Uptake)
3. Particle density, PartDens, MG m^{-3} (..._Flow)
4. Saturated hydraulic conductivity, HydCond, kg s m^{-3} (Richards_Flow)

5. Air Entry potential, AirEntryPot, J kg^{-1} (Richards_Flow)
6. Soil B-value, BValue, (Richards_Flow)
7. Initial node water content, InitWater, m3 m^{-3} (..._Flow)
8. Field capacity water content, DUL, m3 m^{-3} (Tipping_Flow)
9. Wilting point water content, LL, m3 m^{-3} (Tipping_Flow, Water_Budget)
10. Initial soil temperature, InitSoilTemp, degree C (Soil_Temp)

Empirical equations to estimate some of these parameters can be found in Appendix C.

2.1.3 Editing a Plant Data File

At this point GAPS does not contain any crop growth components. A static crop can be defined in terms of leaf area index and several root parameters. The plant data file contains the following parameters. The prefix for plant input variables is 'plant.', as for example in plant.LAI.

1. Initial leaf area index, LAI, (Canopy)
2. Root radius, RootRad, m (Water_Uptake)
3. Root density, RootDens, m m^{-3} (Water_Uptake)
4. First layer containing roots, FRoot (Water_Uptake)
5. Last layer containing roots, NRoot (Water_Uptake)
6. Root resistance, RootRes, (Water_Uptake)
7. Emergence date, EmergenceDate
8. Initial canopy height, CanopyHeight, m
9. Initial dry matter, InitialDryMatter, kg m-2
10. Maximum water interception capacity, MaxCanopy, mm

11. Resistance of open stomates, RCopen, s m-1
12. Critical leaf water potential, Critical_LeafWP, J kg-1
13. S parameter, S, (Critical_LWP)
14. Aerodynamic resistance, RA, s m-1

The user can scroll through the list of variables and input values for these parameters or change existing ones much in the same way as has been explained above.

2.1.4 Editing a Location Data File

The Location information contains the following site specific parameters. All location parameters carry the prefix 'loca.' in the code, for example loca.LAT.

1. Latitude, LAT (Solar_Angles)
2. Time of solar noon, TSN (Solar_Angles)
3. Priestley-Taylor Alpha value, ALPHA (Priestley_Taylor_ETP)
4. Short-wave absorptivity of the surface, AS (..._ETP)
5. Long-wave emissivity of the soil or canopy surface, ES (..._ETP)
6. Resistance to heat transport, RT, s m-1 (Penman_ETP)
7. Resistance to vapor transport, RV, s m-1 (Penman_ETP)
8. Boundary layer conductance, Cond, W m^{-2} K^{-1} (Soil_Temperature)
9. Pan coefficient, Kp (Pan_ETP)
10. Crop coefficient, Kc (Pan_ETP)
11. Finite difference weighing factor, F (Soil_Temp)
12. First hour of rain / irrigation, RainFirst
13. Last hour of rain / irrigation, RainLast

14. Elevation, elevation, m

15. Height of wind measurement, WindHeight, m

The menu is structured in a similar fashion as the plant editor menu.

2.1.5 Output Format File

If simulation output is to be saved to disk, the 'Out' option in the simulator menu has to be activated and output file name have to be specified (see Chpt. 3.5). The output format file can be used to specify on which days and at which hours to save output data. If a number greater than zero is specified for either 'Number of days' or 'Number of hours', the program will prompt you for the day or hour numbers, respectively, when you modify the 'days' or 'hours' options. This format file needs to be saved to be later called up from the simulator in conjunction with output file names.

3. The Simulator

3.1 Introduction

The purpose of this part of the GAPS user's manual is to allow the users of GAPS to understand all the equations, the solutions to the equations, the variables and constants used in each procedure. The user should understand these procedures for two reasons. First, the users must select between certain procedures depending on their objective and input data restrictions. Secondly, the user may wish to change certain parts of the procedure or add a new procedure. Understanding the

material in this manual is the first step in enabling the user to accomplish this.

This section documents all the procedures currently contained in the Simulator. It will be appended as additional procedures become available. To support the modular structure of the Simulator each procedure is documented in a separate chapter. Each chapter contains an explanation of the concepts and equations used in the procedure, a dependency diagram for the procedure, where considered appropriate, the computer code of the procedure, and a list of all variables used in the procedure. Where appropriate, these concepts and equations are referenced. All constants and variables used in an equation are given the same symbol in the documentation as they have in the computer program. All symbols are defined immediately after they are presented in a chapter, at the end of the chapter, and again in alphabetical order in the Dictionary (Chpt. 3.4). When a symbol is defined its dimensions are also specified. If it is a constant, its value is also specified. The dimensions of all variables and constants in the Simulator are in SI (Systeme Internationale) units.

Dependency diagrams are used to illustrate the flow of information from outside the procedure into the procedure, the main relations of variables inside the procedure, and the output variables that leave the procedure. The procedure presented in each chapter is represented by a large white box in the dependency diagram. Other procedures which produce variables that are needed as input for the main procedure are represented as smaller shaded boxes to the left of the main procedure. The variables produced by these other, shaded procedures are listed in

the shaded portion of the box. These variables are global variables because they are used in more than one procedure. They are defined in the chapter where they appear in equations and again at the end of each chapter under the heading 'Global Variables'. Important local variables appear in the main white box. Variables generated by the main procedure which are subsequently used by other procedures are indicated by arrows pointing to shaded boxes at the bottom of the diagram. These variables are also global variables.

The dependency diagrams should not be confused with traditional flow charts of computer programs. They merely intend to introduce users graphically to the structure of the procedure and help them visualize the general flow of information to, within, and from a procedure. The dependency diagrams might be a helpful reference when making changes to a particular procedure.

The procedure program (computer source code) is presented along with the dependency diagram. The program begins with the procedure title followed by a comment statement summarizing the objective of the procedure. Then local variables and constants are defined. This is followed by the solutions of the equations used to generate the necessary output variables.

A list of variables and constants used in each procedure follows the procedure program. Global variables that are output of the procedure are starred. Finally each chapter contains a list of references for the concepts, equations, numerical solutions and constants used in the procedure. Specific instructions on how to add a

new procedure and how to change an existing one are contained in Appendix D.

3.2 Documentation of modules

The first section of the GAPS Simulator uses various daily climate data to calculate or estimate climate data needed for input to other routines. Procedure **Air_Temperature** simulates hourly air temperatures given daily maximum and minimum air temperatures Procedure **Solar_Angles** uses latitude, day of the year and hour of the day to calculate the maximum solar irradiance. The procedure **Atmos_Trans** uses daily measured solar radiation to estimate an atmospheric transmission coefficient, for use in **..._ETP** procedures that need net radiation as an input.

The second section of the GAPS Simulator currently contains four routines to estimate evapotranspiration: **Priestley_Taylor_ETP**, **Penman_ETP**, **Pan_ETP**, **and Linacre_ETP**. The user can choose one of these depending on the particular objective and input data available.

The procedure **Max_Photosynthesis** calculates photosynthetic rate on the basis of photosynthetically active radiation intercepted by the canopy. Photosynthesis is directly related to dry matter accumulation in **Dry_Matter_Accumulation**. Growth is linked to water stress in procedure **Critical_Leaf_Water_Potential**. **Growth_Stages** allows to define different phenological stages using growing degree days.

Two alternate routines are available for simulating water flow through soil. The **Richards_Equation** procedure uses a numerical solution to the Richards equation to predict water flux and water potentials with depth and time. Actual soil evaporation is also calculated. The

Tipping_Bucket_Flow procedure uses a procedure for water flow adapted from the CERES maize model.

There are two different routines available for predicting water uptake by plants. **Water_Uptake** is a potential driven resistance approach, where water uptake is limited by a minimum root water potential. **Simple_Water_Uptake** uses an adsorption approach, where water uptake is limited by the volumetric water content at wilting point. The former routine can only be used with the Richards_Flow procedure, since it uses soil water potentials.

The user has the option to use the procedure **Soil_Temperature** which numerically solves the heat transport equation predicting soil temperature as a function of depth and time or to specify a constant soil temperature profile.

List of currently available Procedures:

- Solar_Angles
- Atmos_Trans
- Air_Temperature

- Priestley_Taylor_ETP
- Penman_ETP
- Pan_ETP
- Linacre_ETP

- Max_Photosynthesis
- Critical Leaf_Water_Potential
- Growth_Stages
- Dry_Matter_Accumulation

- Richards_Flow
- Tipping_Bucket_Flow
- Water_Budget

- Water_Uptake
- Simple_Water_Uptake

- Soil_Temperature
- Const_Soil_Temp

3.2.1 Procedure Solar_Angles

This procedure calculates the solar elevation angle for any given latitude, day of the year and hour of the day. First, the solar declination angle (angle which the sun's rays make with the earth's equatorial plane) is calculated knowing the day of the year. Then, the solar elevation angle is calculated on an hourly basis from the solar declination angle, latitude and time of day in relation to solar noon (when the sun is directly north or south of the point of observation). Knowing the solar elevation angle and the solar constant, i.e. the mean annual radient flux density outside the earth's atmosphere and normal to the solar beam (1360 W m^{-2}), the theoretical irradiance above the atmosphere can be estimated.

The irradiance above the atmosphere (SpaRad, W m^{-2}) at any time during the day can be calculated according to Campbell (1977):

(1) SpaRad = SolElA * SolarConstant

where:
SolarConstant is the solar constant (1360 W m^{-2})
SolElA is the sine of the solar elevation angle (degrees) at the time of the day

The sine of the solar elevation angle (SolElA) for any time of the day can be calculated as (Campbell 1977, 1985):

(2) SolElA = SolDcA * sin(loca.Lat*0.01745) + cos(loca.Lat*0.01745)
* cos(0.2618*(Time-loca.Tsn)/3600)) * CSolDcA

where:
SolDcA is the sine of the solar declination angle
CSolDcA is the cosine of the solar declination angle loca.Lat is the latitude (degrees)
loca.Tsn is the time of solar noon (sec)
Time is the time of the day (sec).

To determine solar noon accurately for a particular geographic location see Gates (1980).

The sine of the solar declination angle (SolDcA) can be computed according to Swift (1976):

(3) $SolDcA = 0.39785 \sin [4.869 + 0.0172\ JulDay + 0.03345 \sin(6.224 + 0.0172\ JulDay)]$

where:
JulDay is the day-of-year number or Julian date, i.e. January 01 = 1, December 31 = 365.

Solar elevation angles are calculated for every time step of the day and, if the angles are positive, the theoretical solar radiation for the hour is calculated. Before starting a daily loop the procedure is executed once for the whole day to arrive at an estimate of total theoretical solar radiation (SpaceSum). This value is needed to get an estimate of fractional cloud cover, which is calculated in procedure AtmosTrans.

List of References

Campbell, G.S. 1985. Soil physics with BASIC. Elsevier, Amsterdam. 150 pp.

Campbell, G.S. 1977. An introduction to environmental biophysics. Springer Verlag, New York. 159 pp.

Gates, D.M. 1980. Biophysical Ecology. Springer, New York. Appendix 4, p. 572.

Swift, L.W. 1976. Algorithm for solar radiation on mountain slopes. Water Res. Res. 12:108-112.

Computer Source Code

```
Procedure Solar_Angles(Day : integer; Time : real);
     {calculates solar declination (Swift, 1976) and elevation angles
     and the theoretical solar radiation above the atmosphere (Campbell,
     1977, 1985)}

     const
          SolarConstant  =    1360;     {solar constant, W m-2}

     var
          SolDcA         :    real;     {sine of the solar declination
                                         angle}

     function declination_angle(day : integer) : real;
          begin
          declination_angle := 0.39785*SIN(4.869 + 0.0172 * day +
                                    0.03345 * SIN(6.224+0.0172* day));
          end;  {declination_angle}


     function elevation_angle(dec_angle, lat, time : real) : real;
          var
            CSolDcA: real; {cosine of solar declination angle}

          begin
          CSolDcA := POW((1 - dec_angle * dec_angle),0.5);
          elevation_angle := SolDcA * sin(Lat*0.01745) +
               cos(Lat*0.01745) *  cos(0.2618*(Time - loca.Tsn)/3600)) *
               CSolDcA;
          end;  {elevation_angle}


     begin
          SolDcA := declination_angle(Day);
          SolElA := elevation_angle(SolDcA, Lat, Time);
          if SolElA <= 0 then SpaRad := 0
               else SpaRad := SolElA * SolarConstant;
     end;  {Solar_Angle}
```

List of Variables

Global Variables:

SolEla	:	sine of solar elevation angle
JulDay	:	Julian date (01 Jan = 1)
Time	:	ellapsed time of the day (sec)

Lat : latitude (degree)

Local Variables:

SolDcA : sine of solar declination angle

SpaRad : hourly irradiance above the atmosphere (W m^{-2})

CSolDcA : cosine of solar declination angle

Local Constants:

SolarConstant : solar constant (1360 w m^{-2})

3.2.2 Procedure Atmos_Trans

The procedure Atmos_Trans, called at the beginning of each day, uses the daily theoretical solar radiation above the atmosphere (SpaceSum), calculated once every day before entering the hourly loop and the measured daily solar radiation (clim.SolRad) to arrive at an estimate of fractional cloud cover and atmospheric transmission coefficient. In other procedures (e.g. in Priestley_Taylor_ETP and Penman_ETP) these estimates are needed to calculate atmospheric emissivity which will in turn be used to estimate longwave radiation.

The transmission coefficient (TTrans) of the atmosphere is simply the ratio of measured to potential daily global solar radiation:

(1) TTrans = clim.SolRad / SolRad

where:
clim.SolRad is the measured solar radiation (MJ m^{-2} d^{-1})
SolRad is the theoretical solar radiation (MJ m^{-2} d^{-1})

Cloudiness or fractional cloud cover can be calculated as (Campbell, 1985):

(2) Clouds = 2.33 - 3.33 * TTrans

and is valid only when Clouds has values between 0 and 1.

List of References

Campbell, G.S. 1985. Soil physics with BASIC. Elsevier, New York. 150 pp.

Computer Source Code

```
Procedure Atmos_Trans(day : integer);

     var
          SolRad    :    real; {theoretical solar radiation,MJ/m2/day}

     begin
          SolRad := SpaceSum * 0.0864;
                    {converts W m-2 into MJ m-2 day-1}
          TTrans := climate.solar_rad[day].value / SolRad;
          Clouds:= 2.33-3.33*TTrans;

          if Clouds < 0 then Clouds := 0;
          if Clouds > 1 then Clouds := 1;

     end;  {Atmos_Trans}
```

List of Variables

Global Variables:

Day	:	day number
SpaceSum	:	theoretical solar radiation (W m^{-2})
clim.SolRad	:	measured solar radiation (MJ m^{-2} d^{-1})
Clouds	:	fractional cloud cover

TTrans : total transmission coefficient for the atmosphere

Local Variables:

SolRad : theoretical solar radiation (MJ m^{-2} d^{-1})

Comment: multiplying by 0.0864 converts (W m^{-2}) into (MJ m^{-2} d^{-1})

3.2.3 Procedure Air_Temperature

In the procedure Air_Temperature, daily values of minimum and maximum measured air temperature are used to fit a sine function to approximate values of air temperature at any hour during the day. Maximum temperatures are assumed to occur at 1500 hours and minimum temperatures at 300 hours. To assure smooth interpolation, the minimum air temperature of the following day is used after 1500 hours, and the maximum of the preceding day prior to 300 hours.

(1) AirTemp = 0.5 * (TempSum + TempDiff * COS(Angle))

where:
TempSum is the sum of maximum and minimum air temperature
TempDiff is the difference between maximum and minimum air temperature
Angle is a function of time of day:

(2) Angle = 0.2618 * (Hour-15)

where Hour is the ellapsed hour of the day.

Minimum and maximum air temperatures are provided as input data in the climate input file (Chp. 2.1.1). To obtain a constant air temperature, simply set minimum temperature equal to maximum temperature.

Computer Source Code

```
Procedure Air_Temperature(Day, Hour : integer);

     var
          MinTemp : real; {minimum temperature for calculation}
          MaxTemp : real; {maximum temperature for calculation}
          Angle: real; {angle as a function of time of day}
          TempDiff: real; {difference between maximum and minimum temp}
          TempSum : real; {sum of maximum and minimum temp}

     begin
          MinTemp := clim.MinTemp[day].value;
          MaxTemp := clim.MaxTemp[day].value;

          if ((EllapsedDay<>1) or (Hour>3)) then
               begin
                    if Hour >= 15 then
                         MinTemp := clim.MinTemp[day+1].value;
                    if Hour <=  3 then
                         MaxTemp := clim.MaxTemp[day-1].value;
               end;
          Angle     := 0.2618*(Hour-15);
          TempDiff  := MaxTemp - MinTemp;
          TempSum   := MaxTemp + MinTemp;
          AirTemp   := 0.5 * (TempSum + TempDiff * cos(Angle));

     end;  {Air_Temperature}
```

List of Variables

Global Variables:

AirTemp	:	simulated hourly air temperature (°C)
clim.MinTemp	:	measured minimum daily air temperature (°C)
clim.MaxTemp	:	measured maximum daily air temperature (°C)
Day	:	day number
Hour	:	time of the day in hours

Local Variables:

MinTemp	:	appropriate minimum air temperature (°C)

MaxTemp	:	appropriate maximum air temperature (°C)
Angle	:	angle as a function of time of day
TempDiff	:	difference between maximum and minimum air temperature (°C)
TempSum	:	sum of maximum and minimum air temperature (°C)

3.2.4 Procedure Priestley_Taylor_ETP

Priestley and Taylor (1972) developed an equation for calculating potential evapotranspiration (ETP) for short vegetation, well-supplied with water under nonadvective conditions. This equation incorporates a proportionality factor known as the Priestley-Taylor factor (ALPHA) with an expression for equilibrium evapotranspiration based on radiation. The proportionality factor is supposed to compensate for the elimination of the aerodynamic component from the Penman equation (see Penman_ETP, 3.2.5). Priestley and Taylor experimentally determined an average value for ALPHA of 1.26, which is supported by the observation that the radiation component is generally four to five times as large as the aerodynamic component. An ALPHA very close to this value has since been confirmed by several investigators (Stewart and Rouse, 1977; Davies and Allen, 1973), when water supply to the evaporating surface is not a limiting factor. To improve estimates under advective conditions several attempts were made to estimate ALPHA from available climatic data such as air temperature (Jury and Tanner, 1975) or air temperature and net radiation (Nakayama and Nakamura, 1982). Others attempted to correlate ALPHA with soil surface moisture (Davies and Allen, 1973).The

Priestley-Taylor equation has also been used to predict evapotranspiration from forests (Shuttleworth and Calde, 1979).

Despite the empirical nature of the proportionality factor ALPHA, the Priestley Taylor equation is based on reasonable physical grounds. It reduces input data requirements and can be used in situations where wind speed data and aerodynamic resistances are not available.

The Priestley-Taylor equation for potential evapotranspiration (ETP) can be written as:

(1) sim.ETP = loca.ALPHA * (NetRad-G) * (SSVD/ (SSVD+PSYCON)) / LAMB

where:
sim.ETP is the pot. evapotranspiration (kg m^{-2} s^{-1})
loca.ALPHA is the Priestley-Taylor factor (1.08 - 1.34)
NetRad is the net radiation (W m^{-2})
G is the soil heat flux (W m^{-2})
SSVD is the slope of the saturation vapor density function (kg m^{-3} k-1)
PSYCON is the psychrometric constant (0.494 g m^{-3} K^{-1})
LAMB is the latent heat of vaporization of water (2450 J g-1, at 20 °C)

Net radiation (NetRad) is calculated as:

(2) NetRad = LWR + loca.AS * clim.SolRad * 11.574 * (SpaRad / SpaceSum)

where:
LWR is net longwave radiation (W m^{-2})
loca.AS is the short wave absorptivity of the plant canopy or soil surface (0.78)
clim.SolRad is measured solar radiation (MJ m^{-2} d^{-1}) being converted to (W m^{-2}) by multiplication with 11.574
SpaRad is the theoretical solar radiation above the atmosphere for a given time step (W m^{-2})
SpaceSum is the theoretical solar radiation for a day (W/m2)

Net Longwave radiation (LWR) is calculated assuming the soil or plant surface is equal to air temperature:

(3) LWR = (EA - loca.ES) * ST * (AirTemp+273)^4

where:
LWR is net longwave radiation (W m^{-2})
EA is the atmospheric emissivity
loca.ES is the emissivity of the soil or canopy surface (0.97)
ST is the Stephen-Boltzmann constant (5.67E-08 W m^{-2} K-4)
AirTemp is the air temperature (°C),being converted to (K) by adding 273

Atmospheric emissivity can be calculated according to Campbell (1985) as:

(4) EA = (1-0.84*Clouds) * (0.72+0.005 * AirTemp) + 0.84 * Clouds

where Clouds is the fractional cloud cover taking values between 0 and 1 and is calculated in procedure Atmos_Trans. The slope of the saturation vapor density function (SSVD, kg m^{-3} K^{-1}), i.e. the change in saturation vapor density with a change in temperature, is given by Fuchs et al. (1978):

(5) SSVD = SVD * (((LAMB*MW)/R) / (AirTemp+273)-1)/(AirTemp+273)

where:
LAMB is the latent heat of vaporization of water (2450 J g-1)
MW is the molecular weight of water (0.018 kg mol-1)
R is the gas constant (8.3143 J mol-1 K^{-1})
SVD is the saturation vapor density (g m^{-3}), given by Campbell (1981) as:

(6) SVD = (EXP(31.3716-6014.79/(AirTemp+273)-0.00792495
*(AirTemp+273))) / (AirTemp+273)

where:
AirTemp is the air temperature (°C)

List of References

Fuchs, M., Campbell, G.S. and R.I. Papendick. 1978. An analysis of sensible and latent heat flow in a partially frozen unsaturated soil. Soil Sci. Soc. Am. J. 42:379-385.

Campbell, G.S. 1985. Soil Physics with BASIC. Transport models for soil-plant systems. Elsevier, New York. 149 pp.

Davies, J.A. and C.D. Allen. 1973. Equilibrium, potential and actual evaporation from cropped surfaces in Southern Ontario. J. Appl. Meteorol. 12:649-657.

Jury, W.A. and C.B. Tanner. 1975. Advection modification of the Priestley-Taylor ET formula. Agron. J. 67:840-842.

Nakayama, K. and A. Nakamura. 1982. Estimating potential evapotranspiration by the Priestley-Taylor model. J. Agr. Met. 37:297-302.

Priestley, C.H.B. and B.J. Taylor. 1972. On the assessment of surface heat flux evaporation using large-scale parameters. Mon. Weather Rev. 100:81-92.

Sharma, M.L. 1985. Estimating Evapotranspiration. Advances in Irrigation 3:213-281.

Shuttleworth, W.J. and I.R. Calder. 1979. "Has the Priestley-Taylor equation any relevance to forest evaporation?" J. Appl. Meteorol. 18:639-646.

Stewart, R.B. and W.R. Rouse. 1977. Substantiation of the Priestley-Taylor parameter for potential evaporation in high latitude. J. Appl. Meteorol. 16:649-650.

Tanner, C.B. and W.A. Jury. 1976. Estimating evaporation and transpiration from a row crop during incomplete cover. Agron. J. 68:239-243.

Computer Source Code

```
Procedure Priestley_Taylor_ETP;

     const
          PSYCON    = 0.494;  {psychrometric constant, g m-3 K-1}
          G         = 0.0;    {soil heat flux, W m-2}
          LAMB      = 2450.0; {latent heat of vaporization of water, J
                               g-1}
          ST        = 5.67E-8;{Stephan-Boltzman constant, W m-2 K-4}
          MW        = 0.018;  {molecular weight of water, kg mol-1}
          R         = 8.3143; {gas constant, J mol-1 K-1}

     var
          EA        : real;   {atmospheric emissivity}
          LWR       : real;   {net longwave radiation, W m-2}
          NetRad    : real;   {net radiation,W m-2}
          SSVD      : real;   {slope of sat vapor density fct., kg m-3
                               K-1}
          SVD       : real;   {saturation vapor density, g m-3}

     begin
          SVD  := (EXP(31.3716-6014.79/(AirTemp+273) -
                    0.00792495*(AirTemp+273))) /(AirTemp+273);
          SSVD := SVD * (((LAMB*MW)/R)/(AirTemp+273)-1) / (AirTemp+273);
          EA   := (1-0.84*Clouds) * (0.72 + 0.005*AirTemp) +
                    0.84*Clouds;
          LWR  := (EA-loca.ES) * ST * POW((AirTemp+273.0),4.0);
          NetRad:= LWR + loca.AS * clim.SolRad[real_day].value * 11.574
                    * (SpaRad/SpaceSum);

          sim.ETP:= loca.ALPHA * (NetRad-G) * (SSVD/(SSVD+PSYCON))
                    /(LAMB*1000);

          if (clim.SolRad[real_day].value*(SpaRad/SpaceSum) = 0)
               then sim.ETP := 0;
          if sim.ETP < 0 then sim.ETP := 0;

     end;  {Priestley_Taylor_ETP}
```

List of Variables

Global Variables:

sim.ETP	:	potential evapotranspiration (kg m^{-2} s^{-1})
loca.Alpha	:	Priestley-Taylor factor, 1.08 to 1.34
clim.SolRad	:	measured daily solar radiation (MJ m^{-2} d^{-1})
AirTemp	:	hourly air temperature (°C)
loca.ES	:	long-wave emissivity of soil or canopy surface
loca.AS	:	short-wave absorptivity of surface
Clouds	:	fractional cloud cover
SpaRad	:	theoretical solar radiation above the atmosphere during a time step (W m^{-2})
SpaceSum	:	theoretical solar radiation for a given day (W m^{-2})

Local Variables:

EA	:	atmospheric emissivity
LWR	:	net longwave radiation (W m^{-2})
SVD	:	saturation vapor density (g m^{-3})
SSVD	:	slope of the saturation vapor density function (kg m^{-3} K^{-1})
NetRad	:	net radiation (W m^{-2})

Local Constants:

PSYCON	:	psychrometric constant (0.494 g m^{-3} K^{-1})
G	:	soil heat flux (0 W m^{-2})

LAMB : latent heat of vaporization of water (2450 J g-1, at 20 °C)

ST : Stephan-Boltzman const. (5.67E-08 W m^{-2} K-4)

3.2.5 Procedure Penman_ETP

The Penman-Monteith equation combines a vapor diffusion and energy budget approach to predict evapotranspiration from plant canopies. Monteith (1964) applied the Penman equation (1948) to crop canopies, arguing that the resistances to vapor diffusion from inside the leaves through the stomates, leaf boundary layer and canopy, could be incorporated into a single canopy resistance. Net radiation must be known, change in soil heat storage either known or assumed to be negligable, air temperature, relative humidity, and windspeed must be known.

The procedure Penman_ETP is divided into several smaller procedures in order to apply the equation to both soil and cropped surfaces. In the procedure Common, variables that are needed to predict evapotranspiration from either soil surfaces or crop canopies are calculated. First, the transmission coefficient of the canopy is calculated as a function of the leaf area index of the crop from an equation given by Stockle and Campbell (1985) and is subtracted from 1 in order to obtain the fraction of ETP allocated to transpiration.

TransFrac = 1 - (exp(-0.823 * LAI + 0.0286 * LAI^2))

where:
LAI is the leaf area index (m2 m-2).

The saturation vapor density (SVD) is calculated as a function of air temperature (Campbell 1985):

(1) SVD = (EXP(31.3716-6014.79 / (AirTemp+273)-0.00792495 * (AirTemp + 273))) / (AirTemp + 273)

where:
SVD is the saturation vapor density (g m-3)
AirTemp is air temperature (°C)

The slope of the saturation vapor density (SSVD) as a function of temperature at a given temperature is calculated (Campbell 1985):

(2) SSVD = SVD * (((LAMB*MW)/R) /(AirTemp + 273) - 1/(AirTemp + 273)

where:
SSVD is the slope of the saturation vapor density curve (g m-3 K-1)
LAMB is latent heat of vaporization (2430 J g-1)
MW is molecular weight of water (18 g mole-1)
R is the gasconstant (8.3143 J mole-1 K-1)

The actual vapor density (VD) is then calculated by multiplying the relative humidity by the saturated vapor density.

(3) VD = clim.RelHumid[day] * SVD

where:
VD is the vapor density of air (g m-3)
SVD is the saturated vapor density of air (g m-3)
clim.RelHumid is the relative humidity of the air

In the procedure Soil, variables in the Penman-Monteith equation are determined assuming the surface of interest is a soil. First, the aerodynamic resistance to vapor transfer (RA) for a soil surface is calculated based on the theory of turbulent transport if a windspeed at a specified height is known. For a soil surface, the zero plane displacement (D) is assumend equal to 0 m. The momentum roughness parameter (ZM) is assumed equal to 0.01 m. The vapor roughness

parameter (ZV) is assumed to be 20% of the height of the momentum roughness parameter.

```
RA = (ln((loca.WindHeight - D + ZV) / ZV) * ln((loca.Windheight - D
     + ZM) / ZM )) / (K^2 * clim.Windspeed)
```

where:
RA is the aerodynamic resistance to vapor transfer (s m-1)
loca.Windheight is the height above soil surface at which windspeed was measured (m)
D is the zero plane displacement (m)
ZM is the momentum roughness parameter (0.01 m)
ZV is the vapor roughness parameter (0.2 * ZM),
K is the von Karman constant (0.4),
clim.Windspeed is the measured windspeed (m s-1).

If windspeed is not known, the aerodynamic resistance to vapor transport is assigned a constant value of 90 s m-1. Also in this procedure, shortwave absorptivity (ABS) is assigned a value from the soil input file.

In the next procedure, Crop, an areodynamic resistance for the boundary layer abover the crop is calculated based on the same equation used for calculating the aerodynamic resistance of the boundary layer above a soil. However, in this case the height of zero plane displacement is no longer zero but assumed to be 64% of the canopy height (m). The momentum roughness parameter (ZM) is assumed to be 13% of the canopy height and again the vapor roughness parameter (ZV) is assumed to be 20% of ZM (Campbell 1977). If windspeed is not known, then some assumed value for the aerodynamic resistance is called from the plant input file. Within this procedure, the bulk canopy resistance can either be assigned and held constant or can be made a function of plant (leaf water potential), environmental (vapor density deficit) or soil (soil water potential) factors, depending on the crop being

modelled. Shortwave absorptivity is assigned a value from the plant input file.

The Penman-Monteith equation is applied in the procedure Penman. First, net radiation (sim.NetRad) is calculated as the sum of absorbed shortwave radiation and net longwave radiation.

```
sim.NetRad := LWR + ABS * clim.solrad[real_day].value *
                    11.574 * SpaRad/SpaceSum
```

where:
LWR is net longwave radiation (W m-2)
ABS is the shortwave absorptivity of the soil or crop
clim.SolRad is solar radiation (MJ m-2 d-1)
SpaRad is irradiance above the atmosphere (W m-2)
SpaceSum is theoretical solar radiation for a day (W m-2)
11.574 converts MJ m-2 d-1 into W m-2

Next, latent heat of evapotranspiration (LE) is calculated:

```
LE=(SSVD*(sim.NetRadG)+(RO*(SVD-VD)/RA))/((PSYCON*(1+RC/RA))+SSVD)
```

where:
LE is latent heat of evapotranspiration (J m-2 s-1)
RO is the specific heat capacity of air (J m-3 K-1)
RA is the canopy resistance to heat transport (s m-1)
PSYCON is the psychrometric constant (g m-3 K-1)
RC is the canopy resistance to vapor transport (s m-1)
SSVD is the slope of the saturation vapor density curve (g m-3 K-1)

Latent heat of evapotranspiration is then converted into evapotranspiration (sim.ETP) by dividing by the latent heat of vaporization.

(5) `sim.ETP = LE / (LAMB * 1000)`

where:
LAMB is the latent heat of vaporization (2430 J kg-1)
multiplication by 1000 converts g into kg

References

Campbell, G. S. 1985. Soil Physics with BASIC. New York: Elsevier.

Monteith, J. L. 1964. Evaportion and environment. In the State and Movement of Water in Living Organisms. 19th Symp. Soc. Exp. Biol.

Penman, H. L. 1948. Natural evaportion from open water bare soil and grass. Roy. Soc. London, Proc. Ser. A 193:120-146.

Computer Source Code

```
Procedure PenmanETP;

   const
      PSYCON= 0.494;       {psychometric constant, g m-3 K-1}
      RO    = 1200.0;      {specific heat capacity of air,, J m-3 K-1}
      LAMB  = 2430.0;      {latent heat of vaporization, J kg-1}
      R     = 8.3243;      {gas constant, J mole-1 K-1}
      MW    = 18.0;        {molecular weight of water, g mole-1}
      ST    = 5.67E-8;     {Stephan-Boltzman constant, W m-2 K-4}
      K     = 0.4;         {vonKarman constant}


   var
      TransFrac:  real;    {fraction of ETP allocated to transpiration}
      SVD  :  real;        {saturation vapor density, g m-3}
      SSVD :  real;        {slope of sat. vap. dens. curve, g m-3 K-1}
      VD   :  real;        {actual vapor density of air, g m-3}
      EA   :  real;        {atmospheric emissivity}
      LWR  :  real;        {net longwave radiation, W m-2}
      LE   :  real;        {latent heat of evapotranspiration, J m-2 s-1}

      RC   :  real;        {canopy resistance, s m-1}
      RA   :  real;        {aerodynamic resistance, s m-1}
      D    :  real;        {zero plane displacement, m}
      ZM   :  real;        {momentum roughness parameter, m}
      ZV   :  real;        {vapor roughness parameter, m}
      ABS  :  real;        {shortwave absorptivity}
      G    :  real;        {soil heat flux, W m-2}


  Procedure Common;      {Calculates variables for P.M. equation common
                to soil and plant canopies}

    begin
      TransFrac := 1 - exp(-0.823 * LAI + 0.286 * LAI^2);

      SVD    :=  (EXP(31.3716-6014.79/(AirTemp+273)
                    -0.00792495*(AirTemp+273))) / (AirTemp+273);
```

```
    SSVD   := SVD * (((LAMB*MW)/R)/(AirTemp+273)-1)/(AirTemp+273);
    VD     :=clim.relhumid[real_day].value * SVD;
    EA     := (1-0.84*Clouds) * (0.72 + 0.005*AirTemp) + 0.84*Clouds;
    LWR    := (EA-0.98) * ST * POW((AirTemp+273.0),4.0);
  end;

    {-------------------------------------------------}

Procedure Soil;        {Sets soil variables for P-M equation}
   begin
    if (clim.Windspeed[real_day].filled = 1)  then
       begin
        D  :=0;
        ZM :=0.01;
        ZV :=0.2 * ZM;
        RA := (ln((loca.WindHeight - D + ZV)/ZV)
              * ln((loca.WindHeight - D + ZM)/ZM))
              / (POW(K,2.0) * clim.Windspeed[real_day].value);
       end
    else
      begin
        RA := 90;
      end;

    ABS    := loca.AS;
    RC     := 0;
   end;

   {-------------------------------------------------}

Procedure Crop;       {Sets plant variables for P-M equation}

  Procedure AerodynamicR;
   begin
    if (clim.Windspeed[real_day].filled = 1)  then
       begin
        D  :=0.64 * CanopyHeight;
        ZM :=0.13 * CanopyHeight;
        ZV :=0.2 *ZM;
        RA := (ln((loca.WindHeight - D + ZV)/ZV)
              * ln((loca.WindHeight - D + ZM)/ZM))
              / (POW(K,2.0) * clim.Windspeed[real_day].value);
       end
    else
      begin
        RA := plant.RA;
      end;
   end;


  Procedure CanopyR;
```

```
   begin
        RC := plant.RCopen;
        if RC < plant.RCopen then RC:=plant.RCopen;
    end;

  begin

    ABS :=plant.AS;
    AerodynamicR;
    CanopyR;

  end;

   {-----------------------------------------------------}

Procedure Penman;   {Calculates Penman.ETP}

  begin

    if (clim.solrad[real_day].value*(SpaRad/SpaceSum)=0) then
         sim.ETP:=0
        else
         begin
             sim.NetRad := (LWR + ABS * clim.solrad[real_day].value *
                            11.574 *  SpaRad/SpaceSum) - G;
             G := 0.10 * sim.NetRad;
             LE     := (SSVD*(sim.NetRad-G)+(RO*(SVD-VD)/RA)) /
                        ((PSYCON*(1.0+RC/RA))+SSVD);
             sim.ETP:= LE/(LAMB*1000);
             if sim.ETP<0 then sim.ETP:=0;
         end;
  end;

   {-----------------------------------------------------}

begin
       CanopyHeight:=plant.CanopyHeight;
       RA := plant.RA;
       Common;
       Soil;
       Penman;
       sim.POTEVA := sim.ETP*(1.0-TransFrac);
       if there_is_a_plant then Crop;
       if there_is_a_plant then Penman;
       sim.POTTRANS := sim.ETP*Transfrac;
       sim.ETP:=sim.POTTRANS + sim.POTEVA;
end;
```

List of Variables

Global Variables:

sim.ETP	:	potential evapotranspiration (kg m-2 s-1)
AirTemp	:	air temperature (°C)
clim.RelHumid	:	relative humidity
clim.SolRad	:	Measured daily solar radiation (MJ m-2 d-1)
SpaRad	:	irradiance above the atmosphere (W m-2)
SpaceSum	:	theoretical solar radiation for a given day (W m-2)
loca.AS	:	short-wave absorptivity of the surface
loca.RT	:	resistance to heat transport (s m-1)
loca.RV	:	resistance to vapor transport (s m-1)

Local Variables:

SVD	:	saturation vapor density (g m-3)
SSVD	:	slope of sat. vap. dens. curve (g m-3 K-1)
VD	:	actual vapor density of air (g m-3)
LE	:	latent heat of evapotranspiration (J m-2 s-1)
G	:	soil heat flux (W m-2)

Local Constants:

PSYCON	:	psychometric constant, 0.494 g m-3 K-1
RO	:	specific heat capacity of air, 1200 J m-3 K-1
LAMB	:	latent heat of vaporization, 2430 J kg-1

MW : molecular weight of water, 18 g mole-1

R : gas constant, 8.3143 J mole-1 K-1

3.2.6 Procedure Pan_ETP

The procedure **Pan_ETP** uses daily measured values for pan evaporation provided in the climate input file (clim.PanEV) and distributes the evaporative demand during the day using a sine wave function. A pan coefficient (loca.Kp) and a crop coefficient (loca.Kc) can be specified in the location input file.

Computer Source Code

```
Procedure Pan_ETP;

  begin
     sim.ETP:= 2.3 * clim.PanEV[real_day].value
               * (0.05 + POW(SIN(0.0175*7.5 * ellapsed_hour),4)) /
               86400.0 * loca.Kc * loca.Kp;

     if SpaRad <= 0 then sim.ETP := 0;
  end;
```

List of Variables

Global Variables:

sim.ETP : potential evapotranspiration (kg m^{-2} s^{-1})

clim.PanEV : measured pan evaporation (mm d^{-1})

real_day : day number

ellapsed_hour : ellapsed hour

loca.Kc : crop coefficient

loca.Kp : pan coefficient

SpaRad : theoretical solar radiation above the atmosphere during a time step (W m^{-2})

3.2.7 Linacre_ETP

The procedure Linacre_ETP uses a simple empirical formula (Linacre, 1977) to estimate potential evapotranspiration from mean daily air temperature, mean daily dew-point temperature, elevation and latitude. If dew-point temperature is unavailable, minimum daily temperature can be used as an approximation.

The daily mean air temperature (TMean) is calculated as:

```
TMean := (clim.MinTemp[real_day].value +
          clim.MaxTemp[real_day].value) / 2;
```

where:
clim.MinTemp is the measured daily minimum air temperature
clim.MaxTemp is the measured daily maximum temperature

Daily potential evaporation (ETPdaily) is calculated as:

```
ETPdaily:= (700 * Tm/(100 - loca.latitude) + 15*(TMean-Td)) /
           (80-TMean);
```

where: Tm equals TMean + 0.006 * loca.elevation
Td is the dew-point temperature
loca.latitude is latitude
TMean is mean temperature (°C)

The daily evaporative demand is then distributed over the day using a sine function. The instantaneous rate of potential evapotranspiration (sim.ETP) is:

```
sim.ETP :=  2.3 * ETPdaily * (0.05 + POW(SIN(0.0175*7.5 *
            ellapsed_hour),4)) / 86400.0;
```

where:
ellapsed_hour is the ellapsed time in a day (hours)

If the sine of the solar elevation angle is less than 0, sim.ETP is set equal to 0. The potential evapotranspiration (sim.ETP) is partitioned into potential evaporation (sim.PotEva) and potential transpiration (sim.PotTrans) according according to Stockle and Campbell (1985):

```
TransFrac := 1 - exp(-0.823 * LAI + 0.286 * LAI * LAI);

sim.PotTrans := sim.ETP*Transfrac;

sim.PotEva   := sim.ETP*(1.0-TransFrac);
```

where:
LAI is the leaf area index

References

Linacre, E. T. 1977. A simple formula for estimating evaporation rates in various climates, using temperature data alone. Agric. Meteorol. 18:409-424.

Computer Source Code

```
Procedure Linacre_ETP;

  var
    Tm          : real;      {empirical parameter}
    TMean       : real;      {mean daily air temperature}
    Td          : real;      {mean dewpoint temperature}
    ETPdaily    : real;      {potential evapotranspiration, mm day-1)
    TransFrac   : real;      {fraction of ETP allocated to transpiration}


  begin
   TMean := (clim.MinTemp[real_day].value +
                clim.MaxTemp[real_day].value) / 2;
   Tm := TMean + 0.006 * loca.elevation;
   Td := clim.MinTemp[real_day].value;
   ETPdaily:= (700 * Tm/(100 - loca.latitude) + 15*(TMean-Td)) /
              (80-TMean);
```

```
   sim.ETP :=  2.3 * ETPdaily * (0.05 + POW(SIN(0.0175*7.5 *
               ellapsed_hour),4)) / 86400.0;

   if SolElA <= 0 then sim.ETP := 0;

   TransFrac := 1 - exp(-0.823 * LAI + 0.286 * LAI * LAI);

   sim.POTTRANS := sim.ETP*Transfrac;
   sim.POTEVA   := sim.ETP*(1.0-TransFrac);

  end;
```

List of Variables

Global Variables:

sim.ETP	:	potential evapotranspiration (kg m-2 s-1)
sim.PotTrans	:	potential transpiration (kg m-2 s-1)
sim.PotEva	:	potential soil evaporation (kg m-2 s-1)
clim.MinTemp	:	measured minimum air temperature (°C)
clim.MaxTemp	:	measured maximum air temperature (°C)
loca.elevation	:	elevation (m)
loca.latitude	:	latitude (degrees)

Local Variables:

Tm	:	empirical parameter
TMean	:	mean daily air temperature (°C)
Td	:	mean dewpoint temperature (°C)
ETPdaily	:	potential evapotranspiration (mm day-1)
TransFrac	:	fraction of ETP allocated to transpiration)

3.2.8 Procedure Max_Photosynthesis

The procedure Max_PhotoSynthesis is from a simulation model developed by Stockle and Campbell (1985) to predict the effects of water stress on corn yield. It is called on an hourly basis and implemented whenever there is daylight (sine of the Solar Elevation Angle is greater than 0). At night, photosynthesis is assumed to equal 0 and the stomatal resistance is set at a high value representative of closed stomates (3200 s m-1). During the day, photosynthesis is calculated as a function of photosynthetically active radiation and leaf temperature. This procedure also calculates a non-stressed canopy resistance to water vapor loss based on the maximum stomatal resistance required to achieve the predicted photosynthesis rate, assuming that internal leaf CO2 concentration, ambient CO2 concentration and the boundary layer resistance to CO2 are known or can be estimated. As written, this procedure can only be applied to homogeneous plant canopies and not to mixed plantings or isolated plants.

This procedure begins by determining the amount of leaf area that is sunlit. An extinction coefficient (K) for a spherical (random) leaf angle distribtion is calculated as a function of the sine of the solar elevation angle.

(1) K = 0.5 / SolElA

where:

SolElA is the sine of the solar elevation angle

This equation, as well as others for calculating extinction coefficients for different types of leaf inclination angles, is presented and discussed in Campbell (1977). The sunlit leaf area index (LAISun) is

then calculated as a function of the total leaf area and extinction coefficient.

(2) LAISun = (1 - EXP(-K * LAI)) / K

where:

LAI is the leaf area index (m2 leaves m-2 ground),
K is the canopy extinction coefficient.

The shaded leaf area index (LAIShade) is the difference between the total leaf and the sunlit leaf area (LAIShade = LAI - LAISun).

In the next section of the procedure direct and diffuse photosynthetically active radiation (PAR) is calculated. First, PAR is calculated from solar radiation assuming half of the short wave spectrum is PAR.

(3) PAR = 0.5 * (clim.SolRad[real_day].value * 11.574 SpaRad / SpaceSum)

where:
clim.SolRad is measured daily solar radiation (MJ m-2 d-1)
SpaRad is the theoretical solar radiation above the atmosphere during a time step (W m-2)
SpaceSum is the theoretical solar radiation for a given day (W m-2)

PAR for sunlit leaves (PARSun) is assumed to be a function of the proportion of the total transmission coefficient of the atmosphere (TTrans) that is direct radiation (1-DTrans/TTrans) multiplied by the canopy extinction coefficient (K) plus the proportion of the total transmission coefficient of the atmosphere that is diffuse radiation (DTrans/TTRans) (Norman 1982).

(4) PARSun = PAR (K * (1 - DTrans / TTrans) + DTrans / Trans)

where:
PAR is photosynthetically active radiation (W m-2),
K is the canopy extinction coefficient,

DTrans is the diffuse transmission coefficient of the atmosphere,
TTrans is the total transmission coefficient of the atmosphere.

PAR for shadelit leaves (PARShade) is calculated as a function of the proportion of the total transmission coefficient of the atmosphere that is the diffuse radiation coefficient multiplied by diffuse transmission coefficient of the canopy (Kd) plus the scattered irradiance within the canopy (ScIrr) (Norman 1982).

(5) PARShade = PAR * Kd * DTrans / TTrans + ScIrr

where:
PAR is the photosynthetically active radiation (W m-2)
Kd is the diffuse transmission coefficient for the canopy
DTrans is the diffuse transmission coefficient for the atmosphere
TTrans is the total transmission coefficient for the atmosphere
ScIrr is scattered radiation

Scattered irradiance is estimated as:

(6) ScIrr = (1-DTrans/TTrans) * PAR * 0.07 * (1.1-0.1*LAI) * EXP(-SolElA)

where:
DTrans is diffuse transmission coefficient of the atmosphere
TTrans is total transmission coefficient of the atmosphere
PAR is photosynthetically active radiation (W m-2)
LAI is leaf area index
SolElA is sine of solar elevation angle

Both sunlit (PSSun) and a shadelit (PSShade) rates of photosynthesis are then calculated assuming that photosynthesis is related to PAR according to an equation given for corn by Hesketh and Baker (1969). This rate is then modified for canopy temperature (assuming the leaf temperature equals air temperature) based on an equation from Stockle and Campbell (1985) derived from data of Hofstra and Hesketh (1969). To model photosynthesis for another crop, these

equations would have to be replaced by the appropriate functions for the crop of interest.

```
(7)  TempFac =   -1.37893 + 0.184573*LeafTemp - 7.6341E-03 *
                    POW(LeafTemp,2) + 1.98485E-04 * Pow(LeafTemp,3)  -
                    2.15152E-06 * POW(LeafTemp,4);
```

where:
LeafTemp is the leaf temperature (°C)

```
(8)  PSSun = 6.2527E-05 * POW(PARSun,0.507578) * TempFac / 0.7;
```

where:
PARSun is photosynthetically active radiation for sunlit LAI (W m-2)
TempFac is temperature function for photosynthesis

```
(9)  PSShade = 6.2527E-05 * POW(PARShade,0.507578) * TempFac / 0.7;
```

where:
PARShade is photosynthetically active radiation for shaded LAI (W m-2)
TempFac is temperature function for photosynthesis

Crop photosynthesis for the hour (PS) is then obtained by multiplying the photosynthetic rate for sunlit leaves (PSSun) by the sunlit leaf area index (LAISun) and adding to this the photosynthetic rate for shaded leaves (PSShade) multiplied by the shaded leaf area index (LAIShade).

```
(10) PS = (PSSun*LAISun + PSShade*LAIShade) * time_step;
```

where:
PSSun is photosynthetic rate of sunlit LAI (g m-2 s-1)
LAISun is sunlit leaf area index
PSShade is photosynthetic rate of shaded LAI (g m-2 s-1)
LAIShade is shaded leaf area index
time_step is the time step (s)

In the final section of the code, a "non-stressed" stomatal resistance to vapor loss is calculated for both shaded and sunlit leaves. This is accomplished by using Ohm's equation to model CO2

diffusion from the atmosphere into the leaves (PS = (COext-COint)/(RACO + RESCO)). This equation is rearranged to solve for RES and also divided by 1.65 to convert from CO2 to water vapor resistance (Campbell 1977).

ResSun = ((COext - COint) / PSSun - RaCO) / 1.65

ResShade = ((COext - COint / PSShade - RaCO) / 1.65

where:
ResSun is the sunlit stomatal resistance to water vapor transfer (s m-1),
ResShade is the shadelit stomatal resistance to water vapor transfer (s m-1),
COext is the atmospheric CO2 concentration (0.54 g m-3),
COint is the CO2 concentration internal to the leaf (assumed here to be 0.20 g m-3),
RaCO is the leaf boundary layer resistance to CO2 transfer,
PSSun is the photosynthesis rate of sunlit leaves (g m-2 s-1),
PSShade is the photosynthesis rate of shadelit leaves (g m-2 s-1).

To then obtain the whole canopy non-stress resistance to water vapor transfer the sun and shade lit resistances are weighted according to the proportion of sun and shade lit leaf area and added in parallel (Stockle and Campbell 1985).

NonStressRes = LAI / (LAISun / ResSun + LAIShade / ResShade)

This an optimization approach to predicting water vapor loss from a plant canopy since there is an implicit assumption that the plant only opens its stomates the amount necessary to achieve maximum photosynthesis and is never losing more water than required to achieve this rate.

List of References

Campbell, G.S. 1977. An introduction to environmental biophysics. Springer Verlag, New York. 159 pp.

Hesketh, J. and D. Baker. 1967. Light and carbon assimilation by plant communities. Crop Sci. 7:285-293.

Hofstra, G. and J. D. Hesketh. 1969. Effect of temperature on the gas exchange of leaves in the light and dark. Planta 85:228-237.

Norman, J. M. 1982. Simulation of microclimates. "Biometeorology in integrated pest management". Academic Press, New York.

Stockle, C., and G. S. Campbell. 1985. A simulation model for predicting effect of water stress on yield: an example using corn. Adv. in Irrigation 3:283-323.

Computer Source Code

```
Procedure Max_PhotoSynthesis;  {Light and temperature limited}

   const
    COext     =       0.54;  {external CO2 concentration, g m-3}
    COint     =       0.20;  {internal CO2 concentration, g m-3}
    RACO      =       100.0; {boundary layer resistance
                              for CO2 tranfer, s m-1}
  var
    LAISun    :       real;  {sunlit leaf area index}
    LAIShade  :       real;  {shaded leaf area index}
    PSSun     :       real;  {photosynthetic rate of sumlit LAI, g m-2
                              s-1}
    PSShade   :       real;  {photosynthetic rate of shaded LAI, g m-2
                              s-1}
    K         :       real;  {canopy extinction coefficient}
    Kd        :       real;  {diffuse transmission coefficient for the
                              canopy}
    LeafTemp  :       real;  {leaf temperature, °C}
    TempFac   :       real;  {temperature fct for photosynthesis}
    PAR       :       real;  {photosynthetically active radiation, W
                              m-2}
    ScIrr     :       real;  {scattered irradiance, W m-2}
    PARSun    :       real;  {photosynthetically active radiation
                              for sumlit LAI, W m-2}
    PARShade  :       real;  {photosynthetically active radiation
                              for shaded LAI, W m-2}
    ResSun    :       real;  {non-stress stomatal resistance
                              for sunlit leaves, s m-1}
    ResShade  :       real;  {non-stress stomatal resistance
                              for shaded leaves, s m-1}


   begin
    if SolElA <= 0 then
     begin
```

```
      PS:=0;
      NonStressRes:=3200; {stomates shut}
    end

  else
   begin
    K       := 0.5 / SolElA;
    Kd      := 1 - exp(-0.823 * LAI + 0.0286 * LAI * LAI);

  {calculate shaded and sunlit LAIs}
    LAISun    := (1-EXP(-K * LAI)) / K;
    LAIShade  := LAI - LAISun;
    PAR       := 0.5 * (clim.SolRad[real_day].value * 11.574 *
                   SpaRad/SpaceSum);
    PARSun    := PAR * (K*(1- DTrans/TTrans)+DTrans/TTRans);
    PARShade  := PAR * Kd * DTrans/TTrans + ScIrr;


  {calculate shade and sunlit PAR}
    ScIrr     := (1-DTrans/TTRans) * PAR * 0.07
                  * (1.1-0.1*LAI) * EXP(-SolElA);
    LeafTemp:= AirTemp;
    TempFac := -1.37893 + 0.184573*LeafTemp - 7.6341E-03 *
               POW(LeafTemp,2) + 1.98485E-04 * Pow(LeafTemp,3) -
               2.15152E-06 * POW(LeafTemp,4);

  {calculate shade and sunlit photosynthetic rates and stomatal
        resistances}
    PSSun     := 6.2527E-05 * POW(PARSun,0.507578) * TempFac / 0.7;
    PSShade   := 6.2527E-05 * POW(PARShade,0.507578) * TempFac / 0.7;
    PS :=  (PSSun*LAISun + PSShade*LAIShade) * time_step;


    ResSun    := ((COext - Coint) / PSSun - RACo)/1.65;
    ResShade  := ((COext - Coint) / PSShade - RACo)/1.65;

    NonStressRes:= LAI / (LAISun / ResSun + LAIShade / ResShade);
  end;


end; {Max_Photosynthesis}
```

List of Variables

Global Variables:

SolElA	:	sine of solar elevation angle
PS	:	photosynthesis (g m-2 hour-1)

NonStressRes: non-water-stressed stomatal resistance (s m-1)

AirTemp : air temperature (°C)

clim.SolRad: measured solar radiation (MJ m-2 day-1)

SpaRad : theoretical solar radiation above the atmosphere during a time step (W m-2)

SpaceSum : theoretical solar radiation for a given day (W m-2)

LAI : Leaf area index

DTrans : diffuse transmission coefficient of the atmosphere

TTrans : total transmission coefficient of the atmosphere

Local Variables:

LAISun : sunlit leaf area index

LAIShade : shaded leaf area index

PSSun : photosynthetic rate of sumlit LAI (g m-2 s-1)

PSShade : photosynthetic rate of shaded LAI (g m-2 s-1)

K : canopy extinction coefficient

LeafTemp : leaf temperature (°C)

TempFac : temperature fct for photosynthesis

PAR : photosynthetically active radiation (W m-2)

ScIrr : scattered irradiance (W m-2)

PARSun : photosynthetically active radiation for sumlit LAI (W m-2)

PARShade : photosynthetically active radiation for shaded LAI (W m-2)

ResSun : non-stress stomatal resistance for sunlit leaves (s m-1)

ResShade : non-stress stomatal resistance for shaded leaves (s m-1)

Local Constants:

COext : external CO2 concentration (0.54 g m-3)

COint : internal CO2 concentration (0.20 g m-3)

RACO : boundary layer resistance for CO2 tranfer (100 s m-1)

3.2.9 Procedure Critical_Leaf_Water_Potential

The procedure Critical_Leaf_Water_Potential is from a simulation model developed by Stockle and Campbell (1985) to predict the effects of water stress on corn yield. It can be called on an hourly basis whenever the simulated potential transpiration (sim.PotTrans) is greater than 0. This procedure uses an empirically derived equation that relates decreases in leaf water potentials to increases in stomatal resistance. The increase in stomatal resistance contributes to a simulated decrease in actual transpiration (ActTrans) below potential transpiration. Using Ohm's Law to model water flow through plants [ActTrans = (RootWP - LeafWP) / LeafRes] a new leaf water potential (LeafWP) based on the simulated actual transpiration is calculated. This leaf water potential, in turn, is used to calculate a new stomatal resistance, which then results in a new simulated ActTrans and LeafWP. This process is repeated until LeafWP changes less than 10 J kg-1 with successive iterations.

Initially, the saturation vapor density (SVD, g m-3) is calculated according to Campbell (1981) and the slope of the saturation vapor density function (SSVD, g m-3 K-1) is calculated according to Fuchs et al. (1978).

```
SVD = (EXP(31.3716-6014.79/(AirTemp+273)-
     0.00792495*(AirTemp+273)))/(AirTemp+273)
```

where:
AirTemp is the air temperature (°C)
SSVD = SVD * (((LAMB*MW/R) / (AirTemp+273)-1)/(AirTemp+273)
where:
LAMB is the latent heat of water vaporization (2450 J g-1),
MW is the molecular weight of water (2450 J g-1),
R is the gas constant (8.3143 J mol-1 K-1)

The stressed stomatal resistance (StressRes) is calculated next based on the work of Fisher et al. (1981) using values for corn given by Stockle and Campbell (1985).

```
StressRes = NonStressRes * (1 + (LeafWP /
                plant.CriticalLeafWP)^plant.S)
```

where:
NonStressRes is the non-stressed stomatal resistance
     calculated in the procedure Max_Photosynthesis (s m-1),
LeafWP is the simulated LeafWP calculated in the procedure
     Water_Uptake (J kg-1),
plant.CriticalLeafWP is a species dependent, empirically
     derived value (J kg-1),
plant.S is a species dependent, empirically derived constant.

The reduction in transpiration that occurs due to an increase in stomatal resistance is related to the contribution of stomatal resistance to the total resistance to vapor transport given by Campbell (1977). The ratio of non-stressed to stressed resistances (F) is calculated and this term is then multipled by potential transpiration (sim.PotTrans) to give actual transpiration (ActTrans).

```
F = (SSVD + PSCON * (NonStressRes + plant.RA)/Re) / (SSVD +
     PSYCON * (StressRes + plant.RA)/Re)
```

where:
SSVD is the slope of the saturation vapor density function (g m-3 K-1),
PSYCON is the psychrometric constant (0.494 g m-3 K-1),
Plant.RA is the crop boundary layer resistance (s m-1),
Re is the combined resistance for convection and longwave radiation heat transfer (s m-1).

After calculating simulated actual transpiration (ActTrans = F * sim.PotTrans) a new simulated leaf water potential (LeafWP) is calculated.

```
LeafWP = RootWP - ActTrans * LeafRes
```

where:
RootWP is the root water potential calculated in the procedure Water_Uptake (J kg-1),
LeafRes is the leaf resistance to liquid water transport (m4 s-1 kg-1) assumed equal to 2 x 10^6 (Campbell 1985).

The hourly photosynthetic rate (PS) is also reduced as a function of the stressed stomatal resistance (PS = F*PS).

In this last section of this procedure, a stress factor which affects leaf area index development is calculated if actual transpiration is less than 90% of potential transpiration.

```
LAIStressFact = LAIStressFact + sim.PotTrans/ActTrans*0.8
```

The transpiration deficit is accumulated on an hourly basis and used outside this procedure to calculate a stress index.

```
Stress = 1 - ActTrans/sim.PotTrans
```

References

Campbell, G.S. 1977. An introduction to environmental biophysics. Springer Verlag, New York. 159 pp.

Campbell, G.S. 1981. Fundamentals of radiation and temperature relations. Physiological Plant Ecology I. Encyclop. Plant Physiol., New Ser. 12A.

Fisher, M. J., Charles-Edwards, D. A., and M. M. Ludlow. 1981. An analysis of the effects of repeated short term soil water deficits on stomatal conductance to carbon dioxide and leaf photosynthesis by the legume Macroptilium atropurpureum cv. Siratro. Aust. J. Plant Physiol. 8:347-357.

Fuchs, M., Campbell, G.S. and R.I. Papendick. 1978. An analysis of sensible and latent heat flow in a partially frozen unsaturated soil. Soil Sci. Soc. Am. J. 42:379-385.

Stockle, C., and G. S. Campbell. 1985. A simulation model for predicting effect of water stress on yield: an example using corn. Adv. in Irrigation 3:283-323.

Computer Source Code

```
Procedure Critical_Leaf_Water_Potential;

  const
    LAMB     = 2430.0;     {latent heat of vaporization, J kg-1}
    R        = 8.3243;     {gas constant, J mole-1 K-1}
    MW       =   18.0;     {molecular weight of water, g mole-1}
    Re       =     40;     {combined resistance for convective and LWR
                                        heat transfer, s m-1}
    PSYCON   =  0.494;
    LeafRes  =  2E+06;

   var
    SVD      :   real;   {saturation vapor density, g m-3}
    SSVD     :   real;   {slope of sat. vap. dens. curve, g m-3 K-1}
    StressRes:   real;   {stomatal response as a fct of leaf  water
                             potential}
    I        :integer;   {counter variable}
    LastLWP  :   real;
    DeltaLWP :   real;

  begin
   SVD   :=  (EXP(31.3716-6014.79/(AirTemp+273) - 0.00792495 *
              (AirTemp+273))) / (AirTemp+273);
   SSVD  := SVD * (((LAMB*MW)/R) /(AirTemp+273)-1)/(AirTemp+273);

   Repeat
      StressRes:= NonStressRes * (1+ POW((LeafWP /
                   plant.CriticalLeafWP),plant.S));
      LastLWP:=LeafWP;
      F:= (SSVD + PSYCON * (NonStressRes + plant.RA)/Re) /
          (SSVD + PSYCON * (StressRes + plant.RA)/Re);
      ActTrans := F * sim.PotTrans;
      LeafWP := RootWP - ActTrans * LeafRes;
      DeltaLWP:= ABS(LeafWP-LastLWP);
   until DeltaLWP < 10;

   PS := PS * F;

 if sim.PotTrans > 0 then
   begin
     Stress:= (1 - ActTrans / sim.PotTrans);
     if (ActTrans/sim.PotTrans) < 0.9 then
       LAIStressFact:= LAIStressFact + sim.PotTrans / ActTrans * 0.8;
   end;

  end; {Critical_Leaf_Water_Potential}
```

List of Variables

Global Variables:

PS	:	photosynthesis (g CO2 m-2 hour-1)
F	:	ratio of nonstressed to stressed resistances
AirTemp	:	air temperature (°C)
NonStressRes	:	non-stressed stomatal resistance (s m-1)
LeafWP	:	leaf water potential (J kg-1)
plant.CriticalLeafWP	:	crop dependent parameter (J kg-1)
plant.S	:	crop dependent parameter
plant.RA	:	boundary layer resistance (s m-1)
ActTrans	:	actual transpiration (kg m-2 s-1)
sim.PotTrans	:	potential transpiration (kg m-2 s-1)
RootWP	:	root water potential (J kg-1)
Stress	:	hourly relative transpiration deficit
LAIStressFact	:	stress index for leaf area development

Local Variables:

SVD	:	saturation vapor density (g m-3)
SSVD	:	slope of sat. vap. dens. curve (g m-3 K-1)
StressRes	:	stomatal response as a fct of leaf water potential
LastLWP	:	leaf water potential of last time step (J kg-1)

DeltaLWP : change in leaf water potential over one time step (J kg-1)

I : counter variable

Local Constants:

LAMB : latent heat of vaporization (2430.0 J kg-1)

R : gas constant (8.3243 J mole-1 K-1)

MW : molecular weight of water (18.0 g mole-1)

Re : combined resistance for convective and LWR heat transfer (40 s m-1)

PSYCON : psychrometric constant (0.494 g m-3 K-1)

LeafRes : leaf mesophyll resistance to liquid flow (2E+06 m4 s-1 kg-1)

plant.S : crop specific constant

3.2.10 Growth Stages

Computer Source Code

```
Procedure Growth_Stages;

  var
    TMean    :     real;   {mean daily air temperature}
    DD       :     real;   {degree days}
    T1,T2    :     real;   {upper and lower limits of air temperature
                           for growing degree day calculations}

  begin
    TMean := (clim.MinTemp[real_day].value +
                clim.MaxTemp[real_day].value) / 2.0;

    If (TMean >= 6.0) and (TMean < 21.0)
      then DD := 0.027 * TMean - 0.162;
    If (TMean >= 21.0) and (TMean < 28.0)
      then DD := 0.086 * TMean - 1.41;
    If (TMean >= 28.0) and (TMean < 32.0)
      then DD := 1.0;
    If (TMean >= 32.0) and (TMean < 44.0)
      then DD := -0.083 * TMean +3.67;
    If (TMean >= 44.0) or (TMean < 6.0)
      then DD := 0;
    AccDD := AccDD + DD;

    T2 := clim.MaxTemp[real_day].value;
    T1 := clim.MinTemp[real_day].value;
    if T2 > 30 then T2 := 30;
    if T1 < 10 then T1 := 10;
    GDD := GDD + ((T1+T2)/2) - 10;

  end;
```

3.2.11 Dry_Matter_Accumulation

Computer Source Code

```
Procedure Dry_Matter_Accumulation;

  var
   DAE        : integer;     {days after emergence}
   PartFactor:     real;     {factor for partitioning}
   PartRatio :     real;     {shoot/root partitioning}
   DryMatter :     real;     {dry matter accumulation rate, kg m-2
                              day-1}
   LAR        :    real;     {leaf area ratio, m2 leaf area kg-1 dry
                              matter}
   MaxRootingDepth: real;

 procedure Root_Growth;
    var I : integer;
    begin
      for I:= plant.FRoot to soil.LastLayer do
        begin
         if (RootingDepth / 100) >= LowBound[I]
           then plant.NRoot := I+1;
        end;
     if plant.NRoot <= plant.FRoot then plant.NRoot:=Plant.FRoot;
     if plant.NRoot >= 8 then plant.NRoot:= 8;
    end;

  begin
   {calculate partitioning}
    MaxRootingDepth := plant.MaxRootDepth;
    DAE := Real_day - Plant.EmergenceDate;
    If DAE < 50 then PartFactor := 0.125 * DAE;
    If DAE < 16 then PartFactor := 2;
    If DAE >=50 then PartFactor := 0.135 * DAE;
    PartRatio := PartFactor / (PartFactor+1);

   {dry matter production}
    DryMatter:= 0.40 * (SumPS / 1000.0);
    if AccDD >= 33 then DryMatter:= 0.33 * (SumPS / 1000.0);   {after
                                                               pollination
    if AccDD >=  49
                then DryMatter:=0  ;        {after maturation}


   {dry matter accumulation}
    AccTotalDryMatter := AccTotalDryMatter + DryMatter;
    AccTopDryMatter   := AccTopDryMatter + DryMatter * PartRatio;
    AccRootDryMatter  := AccRootDryMatter + DryMatter * (1-PartRatio);
```

```
   {calculate LAI and Root Density}
    if (accdd < 33) {vegetative phase} then
     begin
     LAI := 7.6 * AccTopDryMatter;
      if LAI >= 4.1 then
       LAI := 3.61173 + 1.15435 * AccTopDryMatter;
     end;

      if (accdd >= 33) and (AccDD < 49) {pollination phase} then
       begin
        if CropPollinated = false then
          begin
           LastLAI := LAI;
           CropPollinated := true;
          end;
       LAI := LastLAI - 0.035 * (AccDD-33) * AccLAIStressfact;
       if LAI <= 0 then cropmatured := true;
       end;

      if (AccDD >= 49) or (AccTopDryMatter >= plant.MaxTopDM) then
{matured}
       begin
        if CropMatured = false then
          begin
           MatDay := real_day;
           LastLAI := LAI;
           CropMatured := true;
          end;
        LAI := LastLAI - 0.15 * (real_day - MatDay);
       end;

    If LAI < 0.001 then LAI := 0;

     RootingDepth:= 1174.8 * AccRootDryMatter;

     if RootingDepth >= 82  then
       RootingDepth:=72.8 + 121.3 * AccRootDryMatter;
     if RootingDepth > 165 then
       RootingDepth:= 112.6 + 70.4 * AccRootDryMatter;
     if RootingDepth > MaxRootingDepth then
       RootingDepth:= MaxRootingDepth;


   Root_Growth;

  end;
```

3.2.12 Procedure Richards_Equation

The soil-water balance is obtained by a numerical solution of the Richards equation, which describes water flow and storage in soil. This equation is obtained by applying the continuity equation to Darcy's law (Hillel, 1980):

$$w*CP*\ dWP/dt = d/dt\ (K(WP)\ *\ dWP/dz + K(WP)*GR + U$$

where:
w is the density of water (kg m^{-3})
CP is the specific water capacity (CP = d Õ/d WP)
Õ is the volumetric soil water content ($m^3\ m^{-3}$)
WP is the soil water potential (J kg^{-1})
t is time (s)
z is depth (m)
k(WP) is the soil hydraulic conductivity (kg s m^{-3}), which is a function of the water potential
GR is the acceleration of gravity (9.8 m s^{-2})
U is a source/sink term (kg $m^{-2}\ s^{-1}$)

This equations has to be solved numerically for realistic boundary conditions.

The model makes use of a network analysis approach to describe water transfer. The soil profile is divided into a number of layers whose properties are assumed to be concentrated at the nodes. The nodes are connected through conductors and associated with capacitors analogous to the electrical circuit problem (Campbell, 1985). The network problem can be solved numerically to determine the change in water potential and water content with time at each node. Steady flow occurs within each element. Storage is assumed to occur only at the nodes. Mass balance equations are written for each node of the profile and solved for the unknowns using an iterative process, the Newton Raphson procedure (Campbell, 1985). Similar schemes have been used by

Stoeckle (1985), Weaver (1984) and Bristow (1983) to describe different aspects of the soil-plant-atmosphere continuum.

The procedure **Richards_Flow** simulates infiltration, redistribution, and soil evaporation. Input requirements for the procedure Richards_Flow include soil physical parameters such as bulk density, partical density, saturated hydraulic conductivity, air entry potential, and soil b-value. If these parameters have not been measured, they can be estimated from soil textural data (Campbell, 1985). The procedure Richards_Flow is divided into separate procedures. These procedures will be discussed in the sequence of their being called in the procedure Richards_Flow.

The procedure **Hydraulic_Conductivities** calculates unsaturated hydraulic conductivities for each layer using the soil water potentials of the most recent time step (or the initial soil water potentials at the beginning of a simulation). The unsaturated hydraulic conductivity (K) for each soil profile layer is calculated according to Campbell (1974):

(1) K(I) = soil.HydCond(I) * (soil.AirEntryPot(I) / sim.WP(I))^N(I)

where:
soil.HydCond is the saturated hydraulic conductivity (kg s m^{-3})
soil.AirEntryPot is the air entry potential (J kg^{-1})
sim.WP is the soil water potential (J kg^{-1})
N = 2+3/soil.BValue, where
soil.BValue is the slope of the water release curve, when plotted on log / log scale.

The procedure **Soil_Evaporation** determines actual soil evaporation. First, the relative humidity (HA) of the soil surface layer is calculated from the soil water potential:

(2) HA = exp(MW*sim.WP[2]/(R*(sim.SoilTemp[2]+273)))

where:
MW is the molecular weight of water (0.018 kg $mole^{-1}$)
sim.WP[2] is the soil surface node water potential (J kg^{-1})
R is the gas constant (8.3143 J $mole^{-1}$ K^{-1})
sim.Soiltemp is the soil temperature (°C)
(Addition of 273 converts °C into Kelvin).

The actual evaporative flux (EV) of water from the surface layer is then calculated as:

(3) sim.EV[1] = sim.PotEva * (HA-clim.RelHumid[day])/(1-clim.RelHumid[-day]))

where:
sim.PotEva is the potential soil evaporation rate (kg m^{-2} s^{-1})
clim.RelHumid is the relative humidity of the air
HA is the relative humidity of the soil surface node

Evaporation during second and third stage drying is controlled by the humidity of the evaporative surface and the liquid flux to the soil surface from deeper soil layers. The derivative of the evaporative flux is calculated for use later:

(4) DEV[I]=sim.PotEva*MW*HA/(R*(sim.SoilTemp[2]+273)*(1 - clim.RelHumid[DAY]))

In the procedure **Jacobian** the components of the Jacobian matrix and mass balance terms are calculated. The water flux (WFlux) (positive downward) in element I is:

(5) sim.WFlux(I) = -(K[I+1]*sim.WP[I+1] - K[I]*sim.WP[I])
/((soil.NodeDepth[I+1]-soil.NodeDepth[I])*(1-N))

where:
soil.NodeDepth is the depth of the soil node (m)

Combining this equation with the mass balance equation for a layer:

(6) FGauss[I]=WFlux[I-1]-WFlux[I]+U(I-1)-U(I)+ Volume[I]*(WN[I]-W[I]) * time_step

and letting U[I] = GR*K[I] yields the mass balance error (FGauss) for each node:

$$(7)\quad FGauss[I] = \frac{K[I]*sim.WP[I] - K[I-1]*sim.WP[I-1]}{(1-N)*(NodeDepth[I]-NodeDepth[I-1]} -$$

$$\frac{K[I+1]*sim.WP[I+1] - K[I]*sim.WP[I]}{(1-N)*(NodeDepth[I+1]-NodeDepth[I]} - GR*(K[I-1]-K[I]) +$$

$$\frac{(sim.WN[I]-W[I])*Volume[I]}{time\_step}$$

where:
K is the element hydraulic conductivity (kg s m^{-3})
sim.WP is the node water potential (J kg^{-1})
NodeDepth is the node depth (m)
time_step is the time step (s)
W is the old water content (m3 m^{-3})
sim.WN is the new water content (m3 m^{-3})
N is the power for hydraulic conductivity function
Volume is the element volume per unit surface area multiplied by the density of water

An appropriate mean water potential is calculated for each node using a weighted mean of the water potential at the i-th time step and the water potential at the (i+1)th time step:

(9) WP[I] = n * WP[I][J+1] + (1-n) * WP[I][J]

where J denotes time, and I denotes the node number and n is a weighing factor between 0 (forward difference or 'explicit' method) and 1 (backward difference or 'implicit' method). When using the forward difference method, fluxes, conductivities, and capacities are calculated using the water potential gradient at the beginning of the time step. If n=1, fluxes are evaluated using the new water potentials only. If n=0.5 the method is called 'time-centered' or the Crank-Nicholson method

and the arithmetic average of the water potential at the beginning and end of the time step is used to calculate fluxes of water. The choice of n depends on the time constant of the system and strongly affects the numerical stability and accuracy of the solution. When n=0 the solution can be unstable if the time steps chosen are too large or the fluxes of water entering the profile are great. For water flow problems, n=1 almost always gives the best results and will be used hereafter.

Other sources/sinks not represented in Eq. 6, such as root extraction, gravitational flux, precipitation, or irrigation, are added explicetly to the mass balance term in equation 7 and such become part of the solution.

Eq. 7 can be written for each node in the simulated soil profile resulting in LastLayer equations in LastLayer+2 unknowns. Boundary conditions are used to reduce the number of unknowns by two so that the system of equations can be solved simultaneously. The three basic choices for boundary conditions are measured values, assumed constant flux and assumed constant potential. For the profile's upper boundary, the soil water potential can be set to the air entry potential during infiltration in order to simulate saturation, or to a specified flux density in the case where the water input is less than the infiltration rate. At the bottom of the profile, the potential is usually set to a known value, for example zero for a water table. The potential could be set at some value that can be considered constant for the duration of the run. Or there could be some depth at which no water flux is assumed to occur.

Writing Eq. 7 for each node and expressing the set of simultaneous equations as a tridiagonal matrix results in the Jacobian matric:

BGauss(1)	CGauss(1)	0	0	DP(1)	FGauss(1)
AGauss(2)	BGauss(2)	CGauss(2)	0	DP(2)	FGauss(2)
0	AGauss(3)	BGauss(3)	CGauss(3)	DP(3)	FGauss(3)
0	0	AGauss(4)	BGauss(4)	DP(4)	FGauss(4)

where:
FGauss[I] is the mass balance error for node I,

(10) CGauss[I] = d FGauss[I]/d sim.WP[I+1] =
-K[I+1]/(NodeDepth[I+1)-NodeDepth[I])

(11) BGauss[I] = d FGauss[I]/d sim.WP[I] = K[I]/(NodeDepth[I]-
NodeDepth[I-1])+K[I]/(NodeDepth[I+1] -
NodeDepth[I])+CP[I]) - GR*N[I]*K[I]/sim.WP[I] +
sim.DEV[I-1]-sim.DEV[I]

(12) AGauss[I] = d FGauss[I]/d WP[I-1] = -K[I-1]/(NodeDepth[I]-
NodeDepth[I-1]) + GR*N[I]*K[I-1]/sim.WP[I-1]

DP[I] is the change in water potential over one iteration.

The node soil water capacity term (CP) is calculated as:

(8) CP[I] = -Volume[I] * sim.WN[I]/(soil.BValue[I]*
sim.WP[I]*time_step)

where:
Volume is the volume per unit area of the soil
time_step is the time step (sec)
sim.WN is the water content (m^3 m^{-3})
soil.BValue is the soil b-value (slope of the water release curve)

The coefficient matrix consists of the partial derivatives (AGauss,BGauss, and CGauss) of each FGauss[I] with respect to each node water potential influencing it.

After each iteration, the total mass balance error (SE) for the whole soil profile is evaluated by summing the mass balance errors from all the nodes:

(13) SE=SE+ABS(FGauss[I])

Convergence is determined by checking whether the FGauss[I]'s are sufficiently close to zero. When the total mass balance error is less than the allowable mass balance error the procedure is completed.

In the procedure **Thomas_Algorithm** the set of equations is solved by Gauss elimination and a new set of soil water potential changes (DP[I]) is found and once again substituted into the Jacobian matrix. The soil water potential changes for each layer (DP[I]) are calculated and the old water potential is updated for each node:

(14) DP[I] = FGauss[I] - CGauss * DP[I+1]

(15) sim.WP[I] = sim.WP[I] - DP[I]

When the DP[I]'s for all the nodes in the profile become zero, the correct values for the soil water potentials have been found. Convergence is determined by checking whether the FGauss[I]'s are sufficiently close to zero. When the total mass balance error (IM) is less than the allowable mass balance error the procedure is completed. These are also the values at which mass balance is assured. The water potential is not allowed to exceed the air entry value and is set to the air entry value if the calculated new water potential exceeds the air entry potential.

In the procedure **New_Water_Contents** the new water contents (WN) for each layer are calculated from the updated water potentials:

(16) sim.WN[I] = WS[I] * (soil.AirEntryPot[I] / sim.WP[I])^B1[I]

where:
WS is the saturated water content (m3 m^{-3})
soil.AirEntryPot is the air entry potential (J kg^{-1})
sim.WP is the water potential (J kg^{-1})
B1 is the inverse of the soil B-value.

Once the solution satisfies mass balance criteria, the procedure **Calculate_Fluxes** calculates the changes in amount of water for each layer and the whole profile. Fluxes between layers are also calculated and the new water contents for the next time step are updated.

At each time step the water content change for each node in the profile is calculated:

(20) Node_WC_Chg[I] = Volume[I]*(sim.WN[I]-W[I])

where:
Volume is the volume of soil per unit area soil surface (m)
sim.WN is the water content of the next time step (m3 m-3)
W is the old water content (m3 m-3)

The changes for each node are summed up to get the change in amount of water for the whole profile, and the rate of change is calculated:

(21) Profile_WC_Chg:= Profile_WC_Chg + Node_WC_Chg[I]

(22) Profile_WC_Chg_Rate:= Profile_WC_Chg / time_step

where:
Profile_WC_Chg is the change in amount of water in the profile over one time step
Profile_WC_Chg_Rate is the rate of change of water content for the profile
Time_step is the time step (sec)

The new water contents for the next time step are updated:

(23) sim.WN[I] = W[I]

and the drainage from the lower boundary of the soil profile is calculated. Assuming no matric potential induced flux at the bottom of the soil profile the drainage rate is:

(24) Drain_Rate = GR * K[NLayer]

where:
GR is the acceleration of gravity (9.8 m s-2)
K[NLayer] is the hydraulic conductivity of the bottom layer (kg s m-3)

List of References

Bristow, K.L. 1983. Simulation of heat and moisture transfer through a surface residue-soil system. Ph.D. thesis. Washington State University, Pullman.

Campbell, G.S. 1985. Soil Physics with Basic. Transport Models for Soil-Plant Systems. Elsevier, New York. 149 pp.

Campbell, G.S. 1974. A simple method for determining unsaturated hydraulic conductivity from moisture retention data. Soil Sci. 117:311-314.

Hillel, D. 1980. Fundamentals of Soil Physics. Academic Press, New York.

Stoeckle, C.O. 1985. Simulation of the effect of water and nitrogen stress on growth and yield of spring wheat. Ph.D. thesis. Washington State University, Pullman.

Weaver, H.L. 1984. A mechanistic model of evapotranspiration from Saltcedar. Ph.D. thesis. Washington State University, Pullman.

Computer Source Code

```
Procedure Richards_Equation;
  const
    GR        = 9.8;          {accelleration of gravity, m s-2}
    IM        = 1E-6;         {allowable mass balance error, kg m-2
                                s-1}
  var
    SE        :  real;        {mass balance error, kg m-2 s-1}
    K         :  depth;       {unsaturated hydr. conductivity, kg s
                                m-3 }
    AGauss,
    CGauss,
    BGauss    :  depth;       {partials in Jacobian matrix}
    FGauss    :  depth;       {mass balance term, kg m-2 s-1}
    I         :  integer;     {counter variable}
       {-------------------------------------------------------}

  Procedure Campbell_Hydraulic_Conductivities;
  var      I : integer;
    begin
      For I := 2 to soil.LastLayer+1 do
       K[I] := soil.HydCond[I].value *
                 POW((soil.AirEntryPot[I].value/sim.WP[I]),N[I]);
    end;   {Hydraulic_Conductivities}

       {-------------------------------------------------------}
```

```
Procedure Soil_Evaporation;
  const
    MW = 0.018;                 {molecular weight of water}
    R  = 8.31;                  {gasconstant}
  var
    HA : real;                  {soil surface relative humidity}
  begin
    HA := EXP( MW * sim.WP[2] / (R*(sim.SoilTemp[2]+273)));
    sim.EV[1]  := sim.PotEva*(HA-clim.RelHumid[real_day].value)/
                              (1-clim.RelHumid[real_day].value);
    DEV[1] := sim.PotEva*MW*HA/ (R*(sim.SoilTemp[2]+273) *
                              (1-clim.RelHumid[real_day].value));
  end;  {Soil_Evaporation}

     {-------------------------------------------------------}

Procedure Jacobian;
  var
    CP : depth;                  {soil node water capacity}
    I  : integer;
  begin
    K[1]:=0;
    SE := 0;
    For I:=2 to soil.LastLayer do
      begin
        CP[I] := -Volume[I]*sim.WN[I]/(soil.BValue[I].value
                  *sim.WP[I]*time_step);
        AGauss[I]:=-K[I-1]/(soil.NodeDepth[i].value -
                  soil.NodeDepth[i-1].value)+GR
                   *N[I]*K[I-1]/sim.WP[I-1];
        CGauss[I]:=-K[I+1]/(soil.NodeDepth[i+1].value -
                        soil.NodeDepth[i].value);
        BGauss[I]:=K[I]/(soil.NodeDepth[i].value -
                  soil.NodeDepth[i-1].value)+K[I]/
                  (soil.NodeDepth[i+1].value -
                  soil.NodeDepth[i].value) + CP[I]
                  -GR*N[I]*K[I]/sim.WP[I]+DEV[I-1]+DEV[I];
        FGauss[I]:=((sim.WP[I]*K[I]-sim.WP[I-1]*K[I-1])/
                  (soil.NodeDepth[i].value -
                  soil.NodeDepth[i-1].value)-
                  (sim.WP[I+1] * K[I+1] - sim.WP[I] * K[I])/
                  (soil.NodeDepth[i+1].value -
                  soil.NodeDepth[i].value))/N1[I]+Volume[I]
                  *(sim.WN[I]-W[I])/time_step
                  - GR*(K[I-1]-K[I])+sim.EV[I-1]
                  -sim.EV[I]+sim.WUptake[I]-WInput[I];
        SE := SE+ABS(FGauss[I]);

      end;
  end; {Jacobian}

     {-------------------------------------------------------}
```

```
      Procedure Thomas_Algorithm;
        var DP  :  depth;     {change in water potential}
            I : integer;
        begin
        {Gauss elimination}
          for I:=2 to soil.LastLayer-1 do
            begin
              CGauss[I]   := CGauss[I]/BGauss[I];
              FGauss[I]   := FGauss[I]/BGauss[I];
              BGauss[I+1] := BGauss[I+1]-AGauss[I+1]*CGauss[I];
              FGauss[I+1] := FGauss[I+1]-AGauss[I+1]*FGauss[I];
            end;

DP[soil.LastLayer]:=FGauss[soil.LastLayer]/BGauss[soil.LastLayer];

sim.WP[soil.LastLayer]:=sim.WP[soil.LastLayer]-DP[soil.LastLayer];
if sim.WP[soil.LastLayer]>soil.AirEntryPot[soil.LastLayer].value
            then sim.WP[soil.LastLayer]
                  := soil.AirEntryPot[soil.LastLayer].value;

        {back substitution}
          for I:=soil.LastLayer-1 downto 2 do
            begin
              DP[I]:=FGauss[I]-CGauss[I]*DP[I+1];
              sim.WP[I]:=sim.WP[I]-DP[I];
              if sim.WP[I] > soil.AirEntryPot[I].value
                then sim.WP[I] := soil.AirEntryPot[I].value;
            end;
        end; {Thomas_Algorithm}

           {-------------------------------------------------------}

      Procedure New_Water_Contents;
      var      I : integer;
        begin
          for I:=2 to soil.LastLayer do
             sim.WN[I]:=WS[I]*POW(soil.AirEntryPot[I].value/sim.WP[I],
                                  1/soil.BValue[I].value);
            sim.WP[soil.LastLayer+1] := sim.WP[soil.LastLayer];
            sim.WN[soil.LastLayer+1] := sim.WN[soil.LastLayer];
        end; {New_Water_Contents}

           {-------------------------------------------------------}

  Procedure Calculate_Fluxes;
    var
      Profile_WC_Chg  :  real;
      Node_WC_Chg     :  depth;
      I : integer;
    begin
      {calculate changes in water contents}
```

```
    Profile_WC_Chg:=0;
    For I:=2 to soil.LastLayer do
      begin
        Node_WC_Chg[I]:= Volume[I] * (sim.WN[I]-W[I]) ;
        Profile_WC_Chg:= Profile_WC_Chg + Node_WC_Chg[I];
        WC_Change:= Profile_WC_Chg / time_step;
        sim.WFlux[I]:=((K[I]*sim.WP[I] - K[I+1]*sim.WP[I+1])/
                       ( N1[I] * (soil.NodeDepth[I+1].value -
                       soil.NodeDepth[I].value)) + GR *
                       K[I]);
      end;

    {reset water contents for next time step}
    For I:= 2 to soil.LastLayer do
      W[I]:=sim.WN[I];

    Drain_Rate:=  GR * K[soil.LastLayer];

  end; {Calculate_Fluxes}


    begin       {Richards_Equation}
      Repeat
        Campbell_Hydraulic_Conductivities;
        Soil_Evaporation;
        Jacobian;
        Thomas_Algorithm;
        New_Water_Contents;
      Until (SE < IM);
      Calculate_Fluxes;
    end;        {Richards_Equation}
```

List of Variables

Global Variables:

sim.WP	:	soil water potential (J kg^{-1})
W	:	soil water content (m3 m^{-3})
sim.WN	:	new soil water content (m3 m^{-3})
soil.HydCond	:	Saturated soil hydraulic conductivity (kg s m^{-3})
sim.EV	:	soil evaporative flux (kg m^{-2} s^{-1})
sim.WUptake	:	root water uptake (kg m^{-2} s^{-1})
WInput	:	Irrigation and/or precipitation (kg m^{-2} s^{-1})

sim.SoilTemp	:	Soil temperature (°C)
sim.PotEva	:	potential soil evaporation (kg m^{-2} s^{-1})
Volume	:	Volume of soil layer per unit area multiplied by the density of water
DEV	:	derivative of evaporative flux

Local Variables:

K	:	soil hydraulic conductivity (kg s m^{-3})
SE	:	mass balance error (kg m^{-2} s^{-1})
I	:	counter variable
HA	:	relative humidity of the surface node
DP	:	change in water potential over a time step
CP	:	node water capacity (d Õ/d WP)
AGauss	:	partial derivative of FGauss with respect to WP[I-1] (sub diagonal element in tridiagonal matrix)
BGauss	:	partial derivative of FGauss with respect to WP[I] (diagonal element in tridiagonal matrix)
CGauss	:	partial derivative of FGauss with respect to WP[I+1] (super diagonal element in tridiagonal matrix)
FGauss	:	node mass balance error (kg m-2 s^{-1})

Local Constants:

MW	:	Molecular weight of water (0.018 kg $mole^{-1}$)
R	:	gas constant (8.3143 J $mole^{-1}$ K^{-1})
GR	:	acceleration of gravity (9.8 m s-2)
IM	:	maximum allowable mass balance error (1E-06 kg m^{-2} s^{-1})

3.2.13 Procedure Tipping_Bucket_Flow

This procedure uses the soil water flow approach as contained in the CERES Maize model (Jones and Kiniry, 1986). The code as contained in CERES Maize was translated into Pascal with concommitant changes in the programming but without altering the general computational method.

As the name of this procedure suggests the soil is conceptualized as consisting of a series of tipping buckets each having a specified capacity to hold water. Each 'bucket' corresponds to a soil layer the dimensions and properties of which have to be specified in the soil input data file. Basically, water is transferred from one layer to the next downward in the soil profile if the amount entering the layer exceeds the layer's water holding capacity. The capacity of each soil layer to hold water is calculated as the difference between the saturation water content (WS) and the current volumetric water content. Input requirements for this procedure include values for bulk density and particle density to calculate saturation water content, field capacity or 'Drained Upper Limit' (DUL) and wilting point or 'Lower Limit' volumetric water contents (LL). The values of DUL and LL can be estimated from soil textural data and organic carbon content using empirical equations contained in CERES Maize (Ritchie et al., 1986). Ideally, values for DUL and LL should be obtained from field measurements as described by ..... ( ). Empirical equations to estimate these parameters can be found in Appendix A.

The Profile Drainage Coefficient (Profile_SWCON) used in calculating the amounts of water drained from a layer is estimated in the procedure **Estimate_Parameters** by calculating a Drainage coefficient for each layer (SWCON) and using the smallest one as the value for the whole profile.

(1) SWCON[I]:=(PO[I]-soil.DUL[I])/PO[I]

where:
PO is the soil total porosity
soil.DUL is the field capacity water content

The procedure **Clear** sets the variables Drain_Rate and Flux[I] to zero before each time step calculation.

In the procedure **Water_Application** the flux into the first soil layer (Flux[2]) is set equal to precipitation. The daily amount of water is distributed evenly over the whole day by dividing the amount of water added by the number of time steps in a day:

(2) Flux[2]:=(clim.Precip[real_day].value)/ num_of_time_steps;

where:
clim.Precip is measured daily precipitation (mm/day)
num_of_time_steps is the number of time steps per day

If the resulting flux is greater than zero the procedure **Infiltration** is called. In this procedure the amount of water the layer can hold is calculated as the amount of water between saturation water content and the current water content:

(3) Hold:=(WS[I]-sim.WN[I]) * Volume[I]

where:
Volume is the volume of the soil layer per unit surface area (m)
WS is the saturation water content (m3 m^{-3})
sim.WN is the soil layer water content (m3 m^{-3})

If the flux into the layer is greater than Hold the procedure **Saturated_Flow** calculates the water draining to the next layer (Drain),

the new water content of the node (sim.WN) and updates the flux to be passed on to the next downstream layer.

(4) Drain:=Profile_SWCON*(WS[I]-DUL[I])*Volume[I]

(5) sim.WN[I]:=WS[I]-Drain/Volume[I];

(6) Flux[I]:=Flux[I]-Hold+Drain;

If the flux does not exceed Hold the old water content of the layer is updated:

(7) sim.WN[I]:=sim.WN[I]+Flux[I]/Volume[I];

If this new water content exceeds the Drained upper limit water content (field capacity) the procedure **Unsaturated_Flow** is called to calculate fluxes, new water contents and update the flux passed to the downstream layer similiar to procedure Saturated_Flow.

(8) Drain:=Profile_SWCON*(sim.WN[I]-DUL[I])* Volume[I]

(9) sim.WN[I]:=sim.WN[I]-Drain/Volume[I]

(10) Flux[I]:=Drain

The amount of water returned in Flux[I] from the procedure Infiltration is passed on to the next soil layer repeating the process until the bottom layer of the soil profile has been reached. If there is a residual flux left after satisfying the water holding capacity of all layers in the soil profile the remaining flux is declared drainage from the bottom of the profile (Drain_Rate).

Soil evaporation is included in the Tipping Bucket water flow procedure as simple first-stage evaporation, which is allowed to proceed until the soil water content reaches 50 % of its value at permanent wilting point. Soil evaporation occurs only from the surface soil node. No upward water flow is simulated. First, the amount of water available

for soil evaporation is calculated as half the amount of water between the permanent wilting point (LL) and the current soil water content (WN):

```
AvailableWater := (Volume[I] * (sim.WN[I]-soil.DLL[I].value/2))
```

Actual soil evaporation is allowed to proceed at potential rates and is limited only by the amount of water present in the uppermost soil layer. Under non-limiting conditions:

```
sim.Ev[1] = sim.PotEva
```

When the amount of water present becomes limiting, soil evaporation is limited to that amount:

```
sim.Ev[1]:=  AvailableWater / time_step
```

Then the water contents are updated:

```
sim.WN[I]:=sim.WN[I] - ((sim.EV[1]*time_step)/volume[I])
```

At the end of the time step the procedure **Calculate_Fluxes** calculates the changes in water contents for each node and the overall profile, as well as fluxes of water between the layers. The old water contents are updated:

```
(11) W[I]:=sim.WN[I];
```

At each time step the water content change for each node in the profile is calculated:

```
(12) Node_WC_Chg[I] =  Volume[I]*(sim.WN[I]-W[I])
```

where:
Volume is the volume of soil per unit area soil surface (m)
sim.WN is the water content of the next time step (m3 m-3)
W is the old water content (m3 m-3)

The changes for each node are summed up to get the change in amount of water for the whole profile, and the rate of change is calculated:

```
(13) Profile_WC_Chg:= Profile_WC_Chg + Node_WC_Chg[I]
```

(14) Profile_WC_Chg_Rate:= Profile_WC_Chg / time_step

where:
Profile_WC_Chg is the change in amount of water in the profile over one time step
Profile_WC_Chg_Rate is the rate of change of water content for the profile
Time_step is the time step (sec)

List of References

Jones, C.A. and J.R. Kiniry. (eds). 1986. CERES-Maize. A simulation model of maize growth and developement. Texas A&M University Press, College Station. 194 pp.

Jones, C.A., J.T Ritchie, J.R. Kining and D.C. Godwin. 1986. Subroutine Structure. In: CERES-Maize. A Simulation Model of Maize Growth and Development. C.A. Jones and J.R. Kiniry (Eds). Texas A&M University Press, College Station. 194 pp.

Ritchie, J.T., J.R. Kining, C.A. Jones and P.T. Dyke. 1986. Model Inputs. In: CERES-Maize. A Simulation Model of Maize Growth and Development. C.A. Jones and J.R. Kiniry (Eds). Texas A&M University Press, College Station. 194 pp.

Computer Source Code

```
Procedure Tipping_Bucket_Flow;

{"tipping bucket" water balance approach as used in CERES MAIZE,
Ritchie et al., 1986.}

var
   J             :  integer;   {counter variable}
   I             :  integer;   {counter variable}
   Hold          :  real;      {amount of water soil can hold above
                                   present level,cm}
   Flux          :  depth;     {flux of water into next layer, cm}
   SWCON         :  depth;     {layer drainage coefficient}
   Profile_SWCON :  real;      {profile drainage coefficient}
   Drain         :  real;      {drainage = flux, cm}
   PO            :  depth;     {soil porosity, cm3/cm3}


Procedure Estimate_Parameters;
 var I : integer;
```

```
 begin
   Profile_SWCON:=1.00;
   For I:= 2 to soil.LastLayer do
    begin
     PO[I]:= WS[I];
     SWCON[I]:=(PO[I]-soil.DUL[I].value)/PO[I];
     If SWCON[I] < Profile_SWCON
          then Profile_SWCON:=SWCON[I];
    end; {for layers do..}
 end;  {Estimate_Parameters}

{-----------------------------------------------}
Procedure Null_Setting;
  var I : integer;
  begin
   for I:=2 to soil.LastLayer do
      Flux[I]  :=  0.0;
   Drain_Rate  :=  0.0;
  end; {Null_Setting}

{-----------------------------------------------}
Procedure Soil_Evaporation;
 var
  I                : integer;
  AdditionalDemand : real;
  AvailableWater   : real;

  begin
   AvailableWater:=0;
   AdditionalDemand:=0;

         For I:= 2 to 2 do
          begin
            AvailableWater := (Volume[I] * (sim.WN[I] -
                              soil.DLL[I].value/2));
            if AvailableWAter <= 0 then AvailableWater := 0;
             sim.Ev[1]:= sim.PotEva;
             if (sim.PotEva*time_step) > AvailableWater then
               begin
                AdditionalDemand:= sim.PotEva*time_step -
                                   AvailableWater;
                sim.Ev[1]:=  AvailableWater / time_step;
               end;

             sim.WN[I]:=sim.WN[I] - ((sim.EV[1]*time_step)/volume[I]);
            end;

  end; {Soil_Evaporation}

{-----------------------------------------------}
procedure Infiltration;
```

```
  procedure Saturated_Flow;
  begin
    Drain:=Profile_SWCON*(WS[I]-soil.DUL[I].value)* Volume[I];
    sim.WN[I]:=WS[I]-Drain/ Volume[I] -
                  ((sim.WUptake[I]*time_step)/volume[I]);;
    Flux[I]:=Flux[I]-Hold+Drain;
  end; {Saturated_Flow}

  procedure UnSaturated_Flow;
  begin
    Drain:=Profile_SWCON*(sim.WN[I]-soil.DUL[I].value)*volume[I];
    sim.WN[I]:=sim.WN[I]-Drain/volume[I];
    Flux[I]:=Drain;
  end; {UnSaturatedFlow}

Begin {Infiltration}
  Hold:=(WS[I]-W[I])*volume[I];
  IF Flux[I] > Hold then
    Saturated_Flow
     else
      begin
        sim.WN[I]:=W[I]+Flux[I]/volume[I] -
                  ((sim.WUptake[I]*time_step)/volume[I]);;
        if (sim.WN[I] > soil.DUL[I].value+0.003) then
          UnSaturated_Flow
            else
             Flux[I]:=0;
      end;
end; {Infiltration}
{-----------------------------------------------}

Procedure Calculate_Fluxes;

    var
      Profile_WC_Chg  :  real;
      Node_WC_Chg     :  depth;
      I : integer;
    begin

      {calculate changes in water contents}
      Profile_WC_Chg:=0;
      For I:=2 to soil.LastLayer do
        begin
          Node_WC_Chg[I]:= Volume[I] * (sim.WN[I]-W[I]);
          Profile_WC_Chg:= Profile_WC_Chg + Node_WC_Chg[I];
          WC_Change:= (Profile_WC_Chg - Drain_Rate) / time_step ;
        end;

      {reset water contents for next time step}
      For I:= 2 to soil.LastLayer do
        W[I]:=sim.WN[I];
```

```
    end; {Calculate_Fluxes}
{-----------------------------------------------}

  Begin {tipping_bucket}
    Estimate_Parameters;
    Null_Setting;
    Flux[2]:= WInput[2] * time_step;
     for I:= 2 to soil.LastLayer do
       begin
         if Flux[I]> 0 then
          Infiltration
          else sim.WN[I]:=W[I]+Flux[I]/volume[I] -
                  ((sim.WUptake[I]*time_step)/volume[I]);;

         if I < soil.LastLayer  then Flux[I+1]:=Flux[I]
          else Drain_Rate:=Flux[I] / time_step; {in mm}
       end;  { For .. to soil.LastLayer}
    Soil_Evaporation;
    Calculate_Fluxes;
  end; {tipping_bucket}
```

List of Variables

Global Variables:

W	:	soil water content (m3/m3)
sim.WN	:	new soil water content (m3/m3)
Drain_Rate	:	drainage from bottom of profile (mm)
Volume	:	volume per unit surface area
WS	:	saturation water content
soil.bulk_density	:	soil bulk density
soil.part_density	:	soil particle density
soil.DUL	:	drained upper limit (field capacity)
soil.LL	:	lower limit (wilting point)

Local Variables:

J	:	counter variable
SWCON	:	layer drainage coefficient

HOLD	:	amount of water soil can hold above present level (mm)
Flux	:	flux of water into next layer (mm)
Profile_SWCON	:	profile drainage coefficient
Drain	:	drainage = flux (mm)
PO	:	soil porosity (cm3/cm3)
Profile_WC_Chg	:	change in water content in the soil profile over one time step
Node_WC_Chg	:	change in water content of one layer over one time step

3.2.14 Procedure Water_Budget

The procedure Water_Budget adds up rates of several variables related to the water budget of the soil-plant system during the day and converts rates expressed in kg m^{-2} s^{-1} at the time step level into units of mm/day. These variables are saved to the output file *.SUM if the option 'Out' is chosen in the simulator menu before starting a simulation.

The procedure Water_Budget is called automatically regardless of the model implemented by the user.

Computer Source Code

```
Procedure Water_Budget;

   var
        I : integer;
   begin
        ProfileWater:=0;
        ProfileAvail:=0;
```

```
        {sums up and converts to mm/day}
        SumPotTrans:=SumPotTrans + sim.PotTrans * time_step;
        SumPotEV:=SumPotEV + sim.PotEva * time_step;
        SumEV:=SumEv + sim.EV[1] * time_step;
        SumWCChange:=SumWCChange + WC_Change * time_step;
        SumDrain:=SumDrain + Drain_Rate * time_step;
        SumActTrans:=SumActTrans + ActTrans * time_step;
        SumWI:=SumWI+WInput[2] * time_step;
        sim.PotET:=sim.PotET + sim.ETP * time_step;
        NetHeatFlux:=NetHeatFlux + sim.HeatFlux/num_of_time_steps;

        For I:= 2 to soil.LastLayer do
             begin
               LayerWater[I]:= Volume[I] * sim.WN[I];
               LayerAvail[I]:= Volume[I] * (sim.WN[I] -
                       soil.LL[I].value);
                if LayerAvail[I] < 0 then LayerAvail[I]:= 0;
               ProfileWater := ProfileWater + LayerWater[I];
               ProfileAvail := ProfileAvail + LayerAvail[I];
             end;
    end;
```

List of Variables

Global Variables:

SumPotTrans	:	potential transpiration (mm/day)
SumPotEV	:	potential soil evaporation (mm/day)
SumEV	:	actual soil evaporation (mm/day)
SumWCChange	:	soil profile water content change (mm/day)
SumDrain	:	drainage from bottom of soil profile (mm/day)
SumActTrans	:	actual transpiration (mm/day)
SumWI	:	total water input (irrigation plus precipitation) (mm/day)
sim.PotET	:	potential evapotranspiration (mm/day)
NetHeatFlux	:	daily net heat flux accross soil surface (positive downwards) ($W\ m^{-2}$)
sim.HeatFlux	:	soil heat flux accross soil surface (positive downwards) ($W\ m^{-2}$)

LayerWater	:	amount of water contained in a layer (mm)
LayerAvail	:	amount of plant available water in a layer (mm)
ProfileWater	:	amount of water in profile (mm)
ProfileAvail	:	amount of plant available water in profile (mm)
Volume	:	Volume of soil per unit area (m)
soil.LL	:	wilting point soil water content (m3 /m^{-3})
sim.WN	:	current water content (m3 / m^{-3})

3.2.15 Procedure Water_Uptake

The amount of water flowing from soil to roots is directley dependent on how much more negative the root water potential (RootWP) is compared to the soil water potential (WP) (Gardner, 1960). Water flow into roots has also been considered inversely dependent on the resistance to water flow in the soil and in the root (Gardner and Ehlig, 1962). If we combine these two concepts with the assumption that there is steady state water flow through the plant (i.e. there is no change in the amount of water stored in the plant), then the following equation can be written:

$$(1)\quad sim.PotTrans = -\frac{(RootWP[I]-sim.WP[I]+soil.NodeDepth[I]*GR)}{Res[I]}$$

where:
sim.PotTrans is the water uptake by the plant (kg m^{-2} s^{-1})
I is the soil layer and node number
RootWP is the root water potential (J kg^{-1})
sim.WP[I] is the node soil water matric potential (J kg^{-1})
soil.NodeDepth[I] is the depth of node I from the soil surface (m)
GR is the acceleration of gravity (9.8 m s-2)
Res[I] is the root and soil resistance of layer I (kg s m^{-4})

The procedure first checks to determine if PotTrans is actually occuring (PotTrans >0) during any one time step. If not, it is assumed that water uptake for each soil layer is zero. When we enter the procedure WaterUptake the soil water potentials with depth (WP[I]) and the transpiration rate (PotTrans) are known. If the resistances to water flow with depth are known, we can then calculate a single root water potential that will result in the sum of water flowing from soil to roots at each soil depth exactly equal to PotTrans. This root water potential is calculated in the procedure RootWaterPotential. Contained within it is the procedure Resistances which calculates Res[I]. Once the root water potential is calculated, the amount of water flowing from the soil to the roots in each soil layer is calculated in the subprocedure RootWaterUptake.

In the procedure **RootWaterPotential** the root xylem resistance is assumed to be negligible and therefore the root water potential is the same at all soil depths. Rearranging the above equation to solve for RootWP gives (Childs, 1977; Riha, 1984):

(2) RootWP = [-sim.PotTrans+((sim.WP[I]-soil.NodeDepth[I]*GR)/Res[I]))
/ 1/Res[I]

In this program:

(2a) SSumRes = (sim.WP[I]-soil.NodeDepth[I]*GR)/Res[I]

(2b) PSumRes = 1/Res[I]

The most complex part of the entire water uptake procedure is the calculation of Res[I]. The equation used is ultimately based on that of Gardner (1960):

(3) q/A = -k * d WP/d r

where:
q is water flux (kg s^{-1})
A is the cross sectional area for flow per unit length of root (m2)
k is hydraulic conductivity (kg s m^{-3})
r is the radial distance for flow (m)
WP is soil water potential of soil or root (J kg^{-1})

The cross sectional area for flow per unit length of root (A) is represented by the following equation:

(4) A = 2 * pi * plant.RootRad

where plant.RootRad is the radius of the root (m). The hydraulic conductivity is calculated from an empirical equation (Campbell, 1974):

(5) K = soil.HydCond * (soil.AirEntryPot / sim.WP)^2+3*Soil.BValue

where:
soil.HydCond is the saturated hydraulic conductivity (kg s m^{-3})
soil.AirEntryPot is the air entry potential (J kg^{-1})
soil.BValue is the soil b-value

Substituting equations (4) and (5) into (3) gives:

(6) q/2*pi*plant.RootRad= -KS(soil.AirEntryPot/sim.WP)^N (d sim.WP/d r)

where N = 2+3*soil.BValue. Separating variables and integrating this equations results in:

(7) q/(2*pi) ln(Res4 /plant.RootRad) = -KS*soil.AirEntryPot^N
(1/(1-N)(sim.WP^1-N - RootWP^(1-N)

If this equation is put in resistance form:

(q*plant.RootDens = (sim.WP - RootWP)/Res) then:

$$(8)\ Res = \frac{(1-N)*\ln(Res4/plant.RootRad)}{2*\ pi*\ plant.RootDens * soil.HydCond * soil.AirEntryPot^N} * \frac{(sim.WP[I]-RootWP)}{(sim.WP^1-N - RootWP^1-N)} + plant.RootRes$$

The distance from the center of the root to the point where sim.WP is measured (RSoil) has been assumed to be (Gardner, 1960):

(9) Res4 = (pi * plant.RootDens)^ -0.5

where plant.RootDens is the length of root per unit volume of soil (m m-3).

Substituting eq. (9) into eq. (8) gives:

$$\text{(10) Res} = \frac{(1-N)*\ln\,(1/\text{RootRad}*(\text{pi}*\text{RootDens})^{0.5})*(\text{sim.WP[I]}-\text{RootWP})}{-2*\text{pi}*\text{RootDens}*\text{HydCond}*\text{AirEntryPot}^{N}*(\text{sim.WP}^{(1-NO)}-\text{RootWp}^{1-N})}$$

The calculation of Res[I] is straightforward for the soil resistance component of equation (10), when RootDens, RootRad, N, sim.WP, KS, and PE are specified with depth. In procedure Resistances, the calculation of RES1 through RES4 solves the soil resistance component of eq. (10) as a function of depth. Root resistance with depth knowing the total root resistance is calculated as follows (Campbell, 1986):

(11) RootRes[I] = RootRes/(RootDens[I]*LayThick[I])

where:
LayThick[I] = length of the layer I (m),
RootRes = Total plant root resistance (kg s m^{-4}).

Knowing the root water potential, RES[I] and sim.WP[I] the root water uptake in each layer is easily calculated from the equation:

(12) sim.WUptake[I] = -(RootWP-sim.WP[I]+soil.NodeDepth[I]*GR)/Res[I]

List of References

Campbell, G.S. 1985. Soil Physics with BASIC: Transport models for soil-plant systems. NY Elsevier. 149 pp.

Campbell, G.S. 1974. A simple method for determining unsaturated hydraulic conductivity from moisture retention data. Soil Sci. 117:311-314.

Gardner, W. R. 1960. Dynamic aspects of water availability to plants. Soil Sci. 89:63-73.

Gardner, W. R. and C. F. Ehlig. 1962. Some observtions on the movement of water to the plant. Agron. J. 54:453-456.

Childs, S. W., J. R. Gilley and W. E. Splinter. 1977. A simplified model of corn growth under moisture stress. Trans. ASAE 20:858-865.

Riha, S. J. 1985. Estimating water fluxes in Douglas-fir plantations. Can. J. of For. Res. 5:701-707.

Computer Source Code

```
Procedure Water_Uptake(var RootWP:real);

     const
          GR        = 9.8;          {Acceleration of gravity,m s-2}
          AddP      =-200;          {Constant to insure new root
                                     waterpotential is more negative than
                                     soil waterpotentials, J kg-1}
     var
          i,j       : integer;      {counters}
          Res       : depth;        {Array ofroot and soil resistances as
                                     a function of depth}
          Res1      : depth;        {Intermediate variable tocalculate
                                     Res}
          Res2      : depth;
          Res3      : depth;
          Res4      : depth;        {Array of soil resistances as a
                                     function of depth}
          PSumRes   : real;         {Summation of the root and soil
                                     conductances over all depths}
          SSumRes   : real;         {Summation of soil water potential
                                     divided
                                     by resistances over all depths}
```

```
procedure RootWaterPotential;

  procedure Conductances;
  begin
    Res1[j]:= -N1[j]*ln(1/(RootRad*sqrt(pi*RootDens[j])));
    Res2[j]:= Res1[j]/(2*pi*RootDens[j]*soil.conductivity[j].value
                 *POW(-soil.Air_entry_pot[j].value,N[j]));
    Res3[j]:=
         Res2[j]*(sim.WP[j]-soil.node_depth[j].value*GR-RootWP);
    Res4[j]:=
         Res3[j]/((POW((-sim.WP[j]+soil.node_depth[j].value*GR),
                       (-1-3/soil.B_value[j].value))
                -POW(-RootWP,(-1-3/soil.b_value[j].value))));
    Res[j] := Res4[j]+RootRes/(RootDens[j]*LayThick[j]);
    PSumRes:= 1/Res[j]+ PSumRes;
    SSumRes :=(sim.WP[j] - soil.node_depth[j].value*GR)/Res[j] +
              SSumRes;
  end;

Begin
  RootWP:=RootWP+AddP;
  For I:=1 to 3 do
    Begin
      PSumRes:=0;SSumRes:=0;

      For J:= FRoot to NRoot do
        Begin
          If RootWP < (sim.WP[J]-soil.node_depth[J].value*GR)
            then
              Conductances
            else
              Res[J]:=0;
        end;
    end;
  RootWP := (-sim.PotTrans + SSumRes)/PSumRes;
  if RootWP < -1500 then RootWP:=-1500;
end; {RootWaterPotential}


procedure RootWaterUptake;
  var
    i : integer;
  begin
    ActTrans:= 0;
    for i:= FRoot to NRoot do
      if (Res[i] > 0) and (sim.WP[I] > -1500.0) then
        begin
         sim.WUptake[i] := -(RootWP-sim.WP[i]+
                           soil.node_depth[i].value*GR)/Res[i];
         ActTrans:=sim.WUptake[i]+ActTrans;
        end
            else
```

```
                    sim.WUptake[i]:=0;
  end; {RootWaterUptake}


begin {WaterUptake}
  if sim.PotTrans <= 0
    then
      begin
        ActTrans:=0;
        for i:=2 to soil.last_layer do
          sim.WUptake[i]:=0;
      end
    else
      begin
        RootWaterPotential;
        RootWaterUptake;
      end;
end;{Water_Uptake}
```

List of Variables

Global Variables:

sim.WP	:	soil water potential (J kg^{-1})
sim.PotTrans	:	potential transpiration (kg m^{-2} s^{-1})
sim.WUptake	:	root water uptake (kg m^{-2} s^{-1})
ActTrans	:	actual transpiration (kg m^{-2} s^{-1})
plant.RootWP	:	minimum root water potential (J kg^{-1})

Local Variables:

I, J	:	counter variable
Res	:	Root plus soil resistance (kg s m^{-4})
Res1	:	intermediate variable for calculating Res
Res2	:	"
Res3	:	"
Res4	:	soil resistance (kg s m^{-4})

PSumRes : summation of root and soil conductances over all depths

SSumRes : Summation of soil water potentials divided by resistances over all depths (m6 kg s3)

Local Constants:

GR : acceleration of gravity (9.8 m s-2)

AddP : constant to assure root water potential is more negative than soil water potential (J kg^{-1})

3.2.16 Procedure Simple_Water_Uptake

Plant water uptake from any layer in the soil containing roots is allowed to proceed until a lower limit of plant-extractable water (permanent wilting point) is reached. The root density distribution in the soil profile is used to partition the transpirational demand between soil layers. Demand not met in any one layer is transferred to other layers as an additional demand. Root densities thus do not limit root water uptake in this simple representation, but serve solely to partition transpiration in the soil profile.

Computer Source Code

```
Procedure SimpleWaterUptake;

    var
      TotalRoots       : real;
      I                : integer;
      AdditionalDemand : depth;
      AvailableWater   : depth;
```

```
begin
  for I:= 2 to soil.LastLayer + 1 do
     AdditionalDemand[I]:=0;
  TotalRoots := 0;
  Acttrans:=0;
  if sim.PotTrans > 0 then
    begin
    For I:= plant.FRoot to plant.NRoot do
       TotalRoots:=TotalRoots + plant.RootDens[I]*LayThick[I];

    For I:= plant.FRoot to plant.NRoot do
     begin
      sim.WUptake[I] := (((plant.RootDens[I]*LayThick[I]) /
                         TotalRoots) * sim.PotTrans) +
                         AdditionalDemand[I] / time_step;
       AvailableWater[I] := (Volume[I] * (sim.WN[I] -
                              soil.DLL[I].value));

      if AvailableWAter[I] <=0 then AvailableWAter[I]:=0;
       if (sim.WUptake[I]*time_step) > AvailableWater[I] then
         begin
          AdditionalDemand[I+1]:= sim.WUptake[I]*time_step -
                                  AvailableWater[I];
          sim.WUptake[I]:=  AvailableWater[I] / time_step;
         end;

       ActTrans:=ActTrans + sim.WUptake[I];
     end;
   end
    else
      for I:= plant.FRoot to plant.NRoot do
        sim.WUptake[I]:=0;
end;  {SimpleWaterUptake}
```

List of Variables

Global Variables:

Local Variables:

TotalRoots	:	Total amount of roots in profile (m)
I	:	counter variable
AdditionalDemand	:	demand not met and transferred to next layer (mm);
AvailableWater	:	plant available water (mm);

3.2.17 Procedure Soil_Temperature

The change in soil temperature over time will depend on the ability of the soil to conduct heat and on the heat capacity of the soil. The thermal conductivity of the soil is to a large degree a function of its water content and bulk density.

In the procedure **Estimate_Parameters** four empirical coefficients used to estimate the thermal properties are estimated. Coeff4 is the thermal conductivity when soil.WN is zero and can be approximated by (Campbell, 1985):

(1) Coeff4[I]:=0.3+0.1 * soil.BulkDensity[I] * soil.BulkDensity[I];

where:
soil.BulkDensity is the bulk density (Mg m^{-3})

Coeff2 in part determines the differences in the thermal conductivity of saturated soils and is dependent on the total volume fraction of soils (Campbell, 1985):

(2) Coeff2[I]:=1.06 * soil.BulkDensity[I];

where 1.06 includes a correction for particle density, assuming a particle density of 2.65 Mg m^{-3}. Coeff1 also in pert determines the differences in thermal conductivity of saturated soils and is based on work by DeVries (1963). The volume fraction of quartz is assumed to be zero and the value for particle density is assumed as above:

(3) Coeff1[I]:=0.65-0.78*soil.BulkDensity[I] + 0.6* soil.BulkDensity[I] * soil.BulkDensity[I];

Coeff3 determines the water content at which thermal conductivity rapidly increases. This appears to be highly dependent on the clay content of the soil:

(4) Coeff3[I]:= 1.0+2.6 / (SQRT(soil.clayPercent / 100));

where:
soil.ClayPercent is percent clay of the soil

Once the coefficients are calculated in the procedure Estimate_Parameters, thermal conductance and heat capacitance is calculated for each layer in procedure **Capacitance_Conductance**. The heat capacitance (CP) is calculated multiplying the vulumetric specific heats of soil and water with the volume fraction of mineral soil and water, respectively:

```
(5)  CP[I]:= (SpecHeatSoil * soil.BulkDensity[I] / soil.PartDensity[I]
                + SpecHeatWater * sim.WN[I]) * (LayThick[I]/time_step);
```

where:
SpecHeatSoil is the volumetric specific heat of soil (2.4 MJ m^{-3} K^{-1})
SpecHeatWater is the volumetric specific heat of water (4.18 MJ m^{-3} K^{-1})
soil.BulkDensity is the bulk density (Mg m^{-3})
soil.PartDensity is the particle density (Mg m^{-3})
LayThick is the layer thickness (m)
time_step is the time step (sec)
sim.WN is the water content (m3 m^{-3})

The equation used to estimate the soil thermal conductance (K) for any soil layer is taken from McInnes (1981):

```
(6)  K[I]:=    (Coeff1[I]+Coeff2[I]*sim.WN[I]-(Coeff1[I]-Coeff4[I]) *
               EXP(-(POW((Coeff3[I]*sim.WN[I]),4)))) /
               (soil.NodeDepth[I+1]-soil.NodeDepth[I]);
```

where:
Coeff1 - 4 are empirical coefficients related to soil water content and bulk density
sim.WN is the soil water content (m3 m^{-3})
soil.NodeDepth is the soil node depth (m)

Since this equation is divided by the length of the soil layer to which it applies, the conductivity becomes the conductance in this one-dimensional flow problem.

The procedure **Boundary_Conditions** specifies the upper and lower boundary conditions used in the soolution to the heat flow problem. Heat transfer from the surface of the soil to the air is assumed to be directly dependent on the difference between air temperature and surface soil temperature times a surface boundary conductance provided as input (loca.BLC). The temperature at the bottom of the profile is kept constant at the initial soil temperature for the last soil layer (soil.InitSoilTemp[LastLayer]) specified in the soil input file.

Heat fluxes are calculated by applying the equation of continuity to the Fourier law:

$$(7)\quad CP * \frac{d\ SoilTemp}{d\ time} = d\left(K \frac{d\ SoilTemp}{d\ NodeDepth} \right) / d\ NodeDepth$$

The numerical solution to this equation is similiar to the solution of the water flow problem. First a Jacobian matric is formed in the procedure **Jacobian** and then the procedure **Thomas_Algorithm** uses the Thomas Algorithm to solve a series of equations using Gauss elimination. Since the conductances and capacitances are not a function of the driving force as is the case in the water flow problem, no itterations are needed to find the correct solution for the new soil temperatures. After a new set of soil temperatures is calculated, procedure **Calc_Fluxes** calculates the heat flux (sim.HeatFlux) accross the soil surface (positive downwards):

```
(8):  sim.HeatFlux:=loca.BLC*(G*(sim.SoilTemp[1]-sim.SoilTemp[2]) +
                    loca.F*(TN[1]-TN[2]));
```

where:
sim.SoilTemp[1] is the air temperature (°C) at last timestep

sim.SoilTemp[2] is the surface node soil temperature (°C) at the last timestep
TN[1] is the air temperature (°C) at the next timestep
TN[2] is the surface node soil temperature (°C) at the next timestep
loca.F is the weighing factor for the finite difference solution
G is (1-loca.F)
loca.BLC is the boundary layer conductance

List of References

Campbell, G.S. 1985. Soil Physics with BASIC. Elsevier, New York. 149 pp.

DeVries, D.A. 1963. Thermal properties of soils. p.210-235. In: vanWijk, W.R.(ed) Physics of Plant Environment. North-Holland Publishing Co., Amsterdam.

McInnes, K.J. 1981. Thermal conductivities of soils from dryland wheat regions of Eastern Washington. M.S. thesis, Washington State University, Pullman.

Computer Source Code

```
Procedure Soil_Temperature;
     const
          SpecHeatSoil   =    2400000.0;
          SpecHeatWater  =    4180000.0;
     var
          I           :     integer;
          G           :     real;       {1-F}
          Coeff1      :     depth;      {coefficients to estimate
                                         thermal Cond}
          Coeff2      :     depth;
          Coeff3      :     depth;
          Coeff4      :     depth;
          K           :     depth;      {soil thermal conductance}
          CP          :     depth;      {soil thermal capacity}
          TN          :     depth;      {soil temperatures at new time
                                         step}
          BGauss,CGauss,
          AGauss,DGauss:    depth;      {partials in Jacobian matric}

    procedure Capacitance_Conductance;
       begin
         for I:= 2 to soil.LastLayer do
           begin
           CP[I]:= (SpecHeatSoil * soil.BulkDensity[I].value/
```

```
                    soil.PartDensity[I].value + SpecHeatWater *
                    sim.WN[I]) * (LayThick[I]/time_step);
          K[I] := (Coeff1[I]+Coeff2[I]*sim.WN[I]-(Coeff1[I]-Coeff4[I])
                  *EXP(-(POW((Coeff3[I]*sim.WN[I]),4))))/
                  (soil.NodeDepth[I+1].value-soil.NodeDepth[I].value);
          end;
      end; {Capacitance_Conductance}

    procedure Boundary_Conditions;

      begin
        G:=1-loca.F;
        K[1]:=loca.BLC;
        sim.SoilTemp[1]:=AirTemp;
        sim.SoilTemp[soil.LastLayer+1]:=
              soil.InitSoilTemp[soil.LastLayer].value;
        TN[soil.LastLayer+1]:=sim.SoilTemp[soil.LastLayer+1];
      end;

    procedure Estimate_Parameters;
       begin
         for I:=2 to soil.LastLayer do
           begin
           Coeff1[I]:=0.65-0.78*soil.BulkDensity[I].value+0.6 *
                    soil.BulkDensity[I].value*soil.BulkDensity[I].value;
           Coeff2[I]:=1.06*soil.BulkDensity[I].value;
           Coeff3[I]:=1.0+2.6/(SQRT(soil.clayPercent));
           Coeff4[I]:=0.3+0.1*soil.BulkDensity[I].value *
                              soil.BulkDensity[I].value
           end;
       end;

    procedure Jacobian;
       begin
         TN[1]:=AirTemp;
         For I:=2 to soil.LastLayer do
           begin
             CGauss[I]:=-K[I]*loca.F;
             AGauss[I+1]:=CGauss[I];
             BGauss[I]:=loca.F*(K[I]+k[I-1])+CP[I];
                        DGauss[I]:=G*K[I-1]*sim.SoilTemp[I-1]+(CP[I]-
                        -G*(K[I]+k[I-1]))
                        *sim.SoilTemp[I]+ G*K[I]*sim.SoilTemp[I+1];
           end;
         DGauss[2]:=DGauss[2]+K[1]*TN[1]*loca.F;

DGauss[soil.LastLayer]:=DGauss[soil.LastLayer]+K[soil.LastLayer]*
                loca.F*TN[soil.LastLayer+1];
       end;

   procedure Thomas_Algorithm;
      begin
```

```
        For I:=2 to soil.LastLayer-1 do
          begin
            CGauss[I]:=CGauss[I]/BGauss[I];
            DGauss[I]:=DGauss[I]/BGauss[I];
            BGauss[I+1]:=BGauss[I+1]-AGauss[I+1]*CGauss[I];
            DGauss[I+1]:=DGauss[I+1]-AGauss[I+1]*DGauss[I];
          end;

TN[soil.LastLayer]:=DGauss[soil.LastLayer]/BGauss[soil.LastLayer];
        {Back substitution}
        For I:=soil.LastLayer-1 downto 2 do
          TN[I]:=DGauss[I]-CGauss[I]*TN[I+1];
      end; {Thomas_Algorithm}

   procedure Calc_Fluxes;
     begin
       sim.HeatFlux:=K[1]*(G*(sim.SoilTemp[1]-sim.SoilTemp[2])
                     +loca.F*(TN[1]-TN[2]));
       For I:=2 to soil.LastLayer+1 do
         sim.SoilTemp[I]:=TN[I];
       sim.SoilTemp[1]:=TN[1];
     end;

   begin {SoilTemperature}
     Boundary_Conditions;
     Estimate_Parameters;
     Capacitance_Conductance;
     Jacobian;
     Thomas_Algorithm;
     Calc_Fluxes;
   end;  {SoilTemperature}
```

List of Variables

Global Variables:

sim.SoilTemp	:	soil temperature (°C)
sim.HeatFlux	:	surface heat flux (W m^{-2})
soil.BulkDensity	:	soil bulk density (Mg m^{-3})
soil.PartDensity	:	soil particle density (Mg m^{-3})
soil.LastLayer	:	last soil layer number
soil.NodeDepth	:	depth of soil layers (m)
soil.ClayPercent	:	percent clay fraction (%)

soil.InitSoilTemp	:	initial soil temperature (°C)
loca.BLC	:	boundary layer conductance (20)
loca.F	:	weighing factor, finite difference method (0 - 1)
AirTemp	:	air temperature (°C)
sim.WN	:	soil water content (m3 m^{-3})
LayThick	:	layer thickness (m)

Local Variables:

I	:	counter variable
G	:	(1-loca.F)
Coeff1	:	coefficients to estimate thermal properties of soil
Coeff2	:	"
Coeff3	:	"
Coeff4	:	"
K	:	soil thermal conductance
CP	:	soil thermal capacity
TN	:	soil temperatures at new time step (°C)
BGauss,CGauss, AGauss,DGauss:	:	coefficients in Jacobian matric

Local Constants:

SpecHeatSoil	:	volumetric specific heat of soil (2.4 MJ m^{-3} K^{-1})

SpecHeatWater : volumetric specific heat of water (4.18 MJ m^{-3} K^{-1}).

3.2.18. Const_Soil_Temperature

This procedure maintains the soil temperatures of each layer at the initial value specified in the soil input file (soilInitSoilTemp[I]).

3.3 Linking modules

The attempt was made to design the procedures in a modular fashion in order to exchange them as freely as possible and to keep them compatible. Nevertheless, it is important to be aware of the input and output requirements of the different procedures. Some require input that necessitates implementing another procedure. To use the potential driven Water_Uptake procedure to calculate plant water uptake, for example, the Richards_Flow water flow procedure has to be selected, since Tipping_Bucket_Flow does not produce soil water potentials as output.

3.4 Run Time Plotting

A selected number of variables (up to four at a time) can be plotted during the execution of a simulation run. To choose the variables to be plotted, select option 'Procedures' from the GAPS Simulator menu, then select 'View'. A list of variable names will appear from which either one, two, or four can be selected to be plotted

on the screen. Simply scroll up and down the list and select by hitting the 'Activate' key. 'Deactivate' disables a particular variable. After a simulation comes to an end, the program will pause to give you a chance to look at the finished plot or to screen dump it to the printer. Hit <enter> to return to the GAPS Simulator menu.

3.5 Saving Output to Files

If desired, output data can be send to files on disk for later use. At this time, GAPS does not allow you to specify which variables to save. It will optionally create a summary output file, that will write daily summary variables to disk, and also save information on the particular implementation of a simulation run, such as input and output file names and simulation procedures used. This file always carries the extension *.SUM . Two other files will be created when data is to be saved at the time step level. One file (*.EX1) contains the values of variables that are a function of time and depth in the soil profile, such as water content and water potential, water uptake from each soil layer, soil water fluxes between each of the layers and soil temperatures. Another file (*.EX2) contains only time dependent information, such as current rates of evapotranspiration, drainage (from the bottom of the profile), soil heat flux, and others. All three files will be placed in the directory \GAPS\DATA. All three files will have the same file name, but different extensions. These files can be used in conjunction with plotting routines to obtain further output from the model or they can be read into spreadsheets for further manipulation.

To save output data, select option 'Out' from the GAPS Simulator menu. This will take you through a series of three menus. In the first menu ('Hourly') you can select an already existing file from the displayed list and overwrite it ('Load')or create a new file by specifying a name (without file extension) and choosing 'Make'. Choose 'quit' if you don't want to save hourly data. The next window lets you do the same for a daily output file, which will also contain information on the simulation run configuration. The third window will allow you to select a format for saving output, that you must have created previously with the GAPS Editor (see Chp. 2.1.5). Output can be saved on selected days and at selected hours during the day.

To get hard copies of the output files, access them via the GAPS Plotter (Chpt. 4.3) or simply print them from DOS.